Battelle
The Business of Innovation

Final Interim Report – Task 1.4

Battelle's Experience with ERW and Flash Weld Seam Failures: Causes and Implications

By

B. N. Leis
and
J. B. Nestleroth

Battelle Memorial Institute
505 King Avenue
Columbus, OH 43201

Prepared for

U.S. Department of Transportation
Pipeline and Hazardous Materials
Safety Administration
1200 New Jersey Ave., SE
Washington DC 20590

Contract No. DTPH56-11-T-000003
Battelle Project No. G006084

September 20, 2012

Battelle does not engage in research for advertising, sales promotion, or endorsement of our clients' interests including raising investment capital or recommending investments decisions, or other publicity purposes, or for any use in litigation.

Battelle endeavors at all times to produce work of the highest quality, consistent with our contract commitments. However, because of the research and/or experimental nature of this work the client undertakes the sole responsibility for the consequence of any use or misuse of, or inability to use, any information, apparatus, process or result obtained from Battelle, and Battelle, its employees, officers, or Directors have no legal liability for the accuracy, adequacy, or efficacy thereof.

ACKNOWLEDGMENTS

Useful discussions with current and former Battelle staff members while preparing this report – most notably among those Messrs Ted Clark and Robert Eiber, respectively – are gratefully acknowledged, as are the contributions of approximately 25 current and former Battelle staff members whose work led to the archived reporting that underlies this work.

EXECUTIVE SUMMARY

This report presents an evaluation of the database dealing with failures originating in electric resistance welds (ERW) and flash weld (FW) seam defects as quantified by Battelle's archives and the related literature. Thereafter, the database was analyzed and trended as the basis to determine the utility and effectiveness of hydrotesting and in-line inspection (ILI) to assess pipeline condition. Finally, those outcomes were used to evaluate the viability of the predictive tools that couple with defect sizes and the seams properties to implement an operator's integrity management (IM) plan, noting the gaps and related implications as part of that evaluation.

Many conclusions relative to the details have been noted throughout the reporting, with some of the key ones noted in closing the section on traits, trends, and observations. The higher-level conclusions from that section, evaluated in light of the prior section that considered the full scope of the report in light of the integrity management process, include:

1. Higher-pressure hydrotesting coupled with ILI and related in-the-ditch-methods (ITDM) provide the only practical basis to assess pipeline condition, with a well designed hydrotest capable of exposing the pipeline condition during the course of the test.
2. In-line inspection tools can find seam weld anomalies, however some anomalies that lead to failure have gone undetected. With better definition the seam defect parameters that need to be quantified by inspection methods, objective data on the current state of the art of inspection technology, improvements in sensing technology, and the combination of inspection methodologies, an adequate in-line inspection approach to detect all critical seam weld anomalies appears possible.
3. While both hydrotesting and ILI are in need of refinement and development, respectively, the current uncertainty in regard to the effectiveness of ILI in contrast to the better understood circumstances for hydrotesting suggests a primary role for hydrotesting in condition assessment, serving as a short term stopgap while certainty builds in regard to ILI for detection and sizing, supported by ITDMs.
4. Seam properties vary greatly from the center of the bondline out into the upset/heat-affected-zone, which are direct metrics of the underlying microstructural differences and also indicative of seam quality. However, in general, the underlying details and their implications may not be broadly understood in the ILI and its supporting nondestructive inspection community. It is plausible that sensor and signal conditioning/analysis algorithms have been developed in other applications that could enhance detection and sizing via ILI and ITDM.
5. Condition assessment is only one part of the IM Plan – which involves a range of decisions such as when to re-inspect and what to rehab and when, that depend on predictive models that in turn rely on defect sizes and related properties. Clear gaps have been identified in practices used to size features, which have a first-order effect on the utility of an IM Plan. Gaps in approaches to quantify the needed properties have been identified, as have first-order differences in such properties in or across the seam relative to the pipe body. Clearly, work is needed in regard to both quantifying inputs to the

predictive models, with related errors forced by idealizations necessitated by fundamental gaps in those models.

6. While work remains as part of this project that begins to address some of the many gaps identified, because this is the first project to consider the integrity of ERW/FW seams in an integrated fashion one can anticipate such work will define the path forward, more so than close the issues along that path. Details are presented in this context in the Recommendations section of the report.

Finally, while potentially useful guidance might be gleaned from the details of the database and the trending reported in Figures 11 through 16, and in Figures 27 through 35, the interdependent complexity evident in the five factors found to control defect response to pressure suggests such generalizations might be dangerous. For example, the nature of the short and blunt oxide-filled penetrator suggests that it poses little threat to integrity. In contrast, inclusion of a pinhole in the API list of defects – which can result from the breakdown of the oxide in a penetrator – warns against that generalization, because a pinhole is a leak path. This coupled with fact that all other defect types considered have failed at in-service pressure levels, and so can pose an integrity threat to an operating pipeline, precludes listing generalizations regarding aspects like: a) the range of SMYS causing failure, b) the nature of pressure reversals, c) defect shapes, d) local properties, and e) predictive models.

The only clear factor that emerges from Battelle's database over that more than 50-year period it has been developing is that the frequency of seam-related failures is generally decreasing since the 1970s – as the trending demonstrates. Because this decrease appears to reflect improved controls in production and the use of better in-mill inspection technology, consistency in their use and diligence in applying this technology is critical. Otherwise problems will recur, such as emerged in regard to pipe expansion, which became an issue circa 2007. Of concern in this context is also evident in the modest upturn evident in seam issues that also was evident in the trending. Many useful conclusions are detailed as a result of the trending, being listed in the summary sections throughout report.

TABLE OF CONTENTS

Page

LIST OF FIGURES

Page

LIST OF TABLES

Page

LIST OF ACRONYMS AND SYMBOLS

CFR	Code Federal Regulations (United States)
CP	cathodic protection
DA	direct assessment
DF	design factor
DNV	Det Norske Veritas
e	strain
EA	environmental assessment
EMAT	electromagnetic acoustic transducer
ERW	electric resistance weld
FW	flash weld
HAZ	heat affected zone
HCS	high consequence area
HFERW	high frequency electric resistance weld
HFI	high frequency induction
HSC	hydrogen-stress cracking
HSLA	high-strength low-alloy
ID	inside diameter
ILI	in-line inspection
IM	integrity management
INGAA	Interstate Natural Gas Association of America
ITDM	in-the-ditch-methods
KAI	Kiefner and Associates
LFERW	low frequency electric resistance weld
LOF	lack of fusion
MAOP	maximum allowable operating pressure
MAS	maximum design stress
MFL	magnetic flux leakage
NTSB	National Transportation Safety Board
OD	outside diameter
O&M	operations and maintenance
PHMSA	Pipeline and Hazardous Material Safety Administration
PRCI	Pipeline Research Council International
PSL2	Product Specification Level 2
PTW	part-through-wall
PWHT	post-weld heat treatment
QA	quality assurance

QC	quality control
RA	Research Announcement
S	stress
SCC	stress corrosion cracking
SEM	scanning electron microscope
SMYS	specified minimum yield stress
SSC	selective seam corrosion
t	time at aging temperature
t_r	equivalent aging time at lower temperature
T	aging temperature
T_r	lower or room temperature
TW	through-wall
UT	ultrasonic testing
WSD	working stress design

BATTELLE'S EXPERIENCE WITH ERW AND FLASH WELD SEAM FAILURES: CAUSES AND IMPLICATIONS

Introduction

On 1 November 2007, a 12-inch diameter pipeline operated by Dixie Pipeline Company (DPC) was transporting liquid propane when it ruptured in a rural area near Carmichael, Mississippi. Upon its release to the lower pressure of the atmosphere, the liquid propane expanded to gas, with the resulting cloud eventually igniting. Although this rupture did not occur in a high consequence area (HCA), the cost of this incident including the loss of product was reported by DPC at more than three million dollars; more importantly, it resulted in the death of 2 people, with 7 others suffering minor injuries. The National Transportation Safety Board (NTSB) determined that the extent of the rupture, a factor which contributes to the size of the release, was due to fracture running axially along the pipe in the longitudinal electric resistance weld (ERW) seam.[(1)*] Based on analysis of the details presented in the NTSB's Factual Report[(2)], the likely fracture origin was identified by others[(3)] as a defect in the seam weld, contradicting the opinion held by the NTSB that the origin was in a girth weld, which turned to propagate in the longitudinal seam.

Following analysis of the Carmichael incident, the NTSB issued Recommendation P-09-1 on the Safety and Performance of ERW Pipe. In related comments[(4)], the NTSB cited concern for the reliance of the Pipeline and Hazardous Material Safety Administration (PHMSA) on the use of in-line inspection (ILI) and hydrotesting as the basis to assess the integrity of upset seam welds, and called into question the viability of these practices for that application.

The recommendation issued by the NTSB called on the PHMSA to conduct a comprehensive study to identify actions that can be implemented by pipeline operators to eliminate catastrophic longitudinal seam failures in ERW pipe. Subsequently, the PHMSA published a Research Announcement (RA) that outlined a work scope to address the NTSB's Recommendation. The RA led to a contract with Battelle, working with Kiefner and Associates (KAI) and Det Norske Veritas (DNV) as subcontractors, to deliver to that work scope. At a minimum, the RA required a project that assessed the effectiveness and effects of ILI tools, hydrostatic pressure tests, spike pressure tests; pipe and seam material strength characteristics, defects, and failure mechanisms; the effects of aging on ERW pipelines; operational factors; and data collection and predictive analysis. Of these, this report considers pipe and seam material strength characteristics and failure mechanisms, and the effects of aging on ERW and flash weld (FW) pipe, and considers their implications in the context of ILI tools, hydrostatic pressure tests, and spike pressure tests.

Background

Companies engaged in root and direct cause analysis that includes tasks like failure analysis, operate under contractual terms and conditions that not only differ from company to company, but also can be client-specific. For the three entities involved in this project, the contractual

* Superscript numbers refer to the list of references compiled at the end of this report

provisions that governed DNV's work allow KAI to work directly with DNV's archives, whereas Battelle's contractual constraints limit outside access to reporting relevant to this project.

Given the different contractual circumstances, it was possible for KAI to access and review DNV's related archive. On that basis, KAI reported(5) a synopsis of the failures archived by KAI and DNV, and commented briefly on their implications relative to integrity management. As part of that reporting they also developed an Excel database that summarized the details of the joint archive relevant to the purposes of this project. Independently, Battelle evaluated its archives subject to the further constraint that precluded release of circumstances/details that identified the operator, or associated the cause and effects/consequences of a failure to a date or specific incident. Accordingly, the circumstances and outcomes of Battelle's archives are presented in a "sanitized" framework, as the basis for evaluating and trending to understand cause – effect relationships in regard to the failure and the associated operating/service conditions. Those outcomes were then integrated as the basis of an assessment of the viability of hydrotesting and in-line inspection (ILI) to manage pipeline system integrity.

Like the KAI report, this report is specific to pipeline systems constructed of pipe made using upset autogenous weld seams, specifically ERW and FW seams. The data were collected in an Excel database developed in parallel to that generated by KAI. It becomes apparent when comparing the two databases that Battelle's archives are dominated by ruptures, while the joint DVN/KAI archive[1] (hereafter termed the "aggregate database") covers a broader mix of leaks and ruptures. It is also apparent that both databases show a balance between liquid versus natural gas as the transported product. Thus, the scope of this report and its database is complementary to the aggregate database presented in Reference 5.

Considerably more than 100 reports from Battelle's archives were reviewed as candidate resources for ERW and FW seam-related failures. The criteria for consideration beyond that initial review and potential inclusion in this report, which were developed in view of the above-noted focus, included:

a) failure originating in a ERW or FW seam;
b) reliable identification of the type of defect;
c) information on the pipe that included size and grade; and
d) details of the failure including the failure pressure relative to service conditions.

For most of the reports that satisfied these criteria, the data also included the seam producer and year of production or pipeline construction, the date of the failure, the date of the initial mill or field pressure test (if any, which for some early construction involved gas tests), and photographs of the fracture surface(s) and related cross sections. Many reports also listed properties data for the pipe, and some even included seam data. Reports that failed to meet the above listed criteria were excluded, which unfortunately culled some comprehensive studies that focused on the metallurgical aspects to resolve issues that arose in commercial production, or in trial production as the process evolved as stronger grades emerged.

[1] Reference 5 covers 226 failures known to KAI and 70 known to DNV.

While some excellent studies were excluded, more than 80 reports met the criteria listed, several of which covering multiple retest failures. These reflect analysis done largely by metallurgists and mechanical and/or civil engineers, all of whom were highly experienced regarding pipelines, pipe production, and failure analysis. In addition, one report was written by a welding engineer, with a second written by a specialist in nondestructive inspection. In total, approximately 25 individuals contributed to this archive of seam failures considered, which was derived from files that could be located with reasonable ease that spanned decades of study, changes in archival technology, and the evolution of Battelle's processes over time. Recognizing that access to high-quality photographs is necessary to satisfy the second of the criteria listed, files that had been reduced to microfiche or were available only as photocopies were not considered.

Reports that were evaluated covered pre-service pressure testing, hydro-retesting, and in-service failures. For the 289 failures reported, a "sanitized" spreadsheet was developed that documents the relevant data (see Annex A). While these results represent the work of many contributors, the work of six primary authors forms the bulk of this archive, which listed alphabetically included: E. B. Clark, R. J. Eiber, T. P. Groeneveld, J. F. Kiefner, B. N. Leis, and W. A. Maxey. In addition to the work done under contract with Battelle, the results of two reports made available to Battelle for comment and analysis through related contracting also were considered.

UPSET AUTOGENOUS SEAM-WELD PROCESS AND IMPLICATIONS

Upset Autogenous Weld Processes

An autogenous weld is one produced without deposited weld metal. Autogenous welds can be used to make pipe by joining the adjacent faces of the skelp under the effects of heat and pressure applied normal to the wall of the pipe, which for line-pipe produces a diagonal bond line, or lap weld. In contrast, an upset autogenous weld is made by joining the adjacent edges of the skelp under the coupled effects of heat and pressure, which for upset welds is applied in the circumferential plane of the pipe to form a butt weld. Thus, at a minimum, making a quality upset autogenous weld requires the consistent application of adequate pressure and heat. But, as for any other welding process, it also requires suitable quality steel and appropriate preparation and fit-up between the abutting edges.

Today, upset autogenous welds are made continuously, with pipe joints cut sequentially from that production, whereas over a period of several decades such welds also were made over the length of a joint of pipe. The first of these processes is used to today to produce ERW pipe, whereas early ERW pipe was produced joint-by-joint, as was FW pipe (produced exclusively by A. O. Smith Corporation). The essential difference between ERW and FW production was that the seam in a FW joint closed over the full length of joint, while for ERW the seam was closed from one end to the other. Continuous production has the advantage that once a steady-state is achieved, so long as process-upsets are avoided, pipe can be produced free of the issues often associated with the startup or shutdown of a process, as occurred in the early production for both ERW and FW processes.

The heat necessary to the upset autogenous processes of interest today can be developed by resistance or by induction, whereas the earlier autogenous welds made on smaller diameter pipe used heat from a fire source directed at the seam to develop what was termed a fire weld[(6)]. For resistance welds, contact between the butted edges causes a rapid rise in temperature local to the contact, whereas for induction welds the temperature rise is comparably rapid, but slightly more of the circumference of the pipe is heated adjacent to the weld zone. For the FW process, a direct current (DC) source was used[(7)], with contact / closure / welding occurring over the length of the joint. DC also was used by one ERW producer (Youngstown Sheet and Tube [YS&T]). Initially, current was typically delivered to the skelp in the ERW process through wheel type electrodes, which was supplied via DC as noted above, or from a low frequency (LF) alternating current (AC) source. Such seams (including those made using a DC source) have been termed LF electric resistance welds (LFERW). Frequencies for such welds are often cited at up to 360 Hz, although values as high as 900 Hz also have been reported[(8)]. Because of the low frequency and the wheel contact scheme adopted, the resulting ERW seam had a comparatively wide heat-affected zone (HAZ).

For ERW pipe, the edges are brought together through a stand of rolls wherein the last "fin" pass(es) create a V shape, and force that V closed. Pressure between the abutting faces develops due to the encircling stand of rolls that reacts against the mechanical mismatch caused by skelp that is slit slightly wider than needed, and the thermal mismatch due to heat-induced expansion, with the butting edges forged together in a plastically upset zone. If the upset pressure due to mismatch is adequate, the force created is sufficient to expel virtually all of the molten steel from the interface, which in concept carries the oxides and impurities with it out of the bondline.

Regardless of the process used to develop the heat and pressure, asperities on the butted faces heat and melt first, with such melting spreading over and along while these edges are forced into contact. In many ways this momentarily liquid interface serves to flux the faying surfaces, while forging due to the upset force caused by the thermal and mechanical mismatch creates the bond. As the liquid serves to flux the faying surfaces, whereas forging produces the weld with virtually all of the liquid that is essential to other fusion-based welding processes being expelled, it has been noted that FW and ERW processes could be considered non-fusion pressure welds.[(9)]

As the abutting edges compress and virtually all of the liquid is expelled, adequate mismatch in a well-made seam causes the remaining hot metal to plastically upset and become forged together. At the same time, the excess upset metal and the once momentarily molten film flows out to the ID and OD surfaces of the pipe under mismatch-induced pressure, which creates what is termed "flash". Thus, as noted above, the forged bond does not rely on fusion, but rather heat and mismatch-induced pressure that must be adequate to forge the bond, and create sufficient upset metal to expel the liquid and impurities. Because the bondline forms due to forging rather than fusion, terms like lack of fusion (LOF) can in this context be considered inappropriate in regard to forged autogenous welds[(9)]. It follows from a production perspective that a viable autogenous weld requires 1) a steady adequate supply of heat as the V closes and 2) adequate mismatch to create the pressure that causes the upset to forge the bond and in turn expel the molten steel and the oxides and impurities out of the interface/bondline. Process upsets in either aspect can lead to defects, as discussed later.

Schematics of an Upset Autogenous Weld versus Reality

Figure 1a shows schematic view of the pipe in transverse cross section local to the seam as the weld is completed. The untrimmed flash, which is contained within the dashed ellipse shown in this figure on the upper side of seam, involves an axial V-groove with oxidized out-bent fibers lying to either side, all of which are local stress raisers. For this reason, at least the exterior portion of the flash must be removed. For that to occur, sufficient upset must develop and the seam must be reasonably symmetric to ensure that the usual setup to trim the flash effectively removes such stress raisers. Accordingly, sometime after the pipe exits the welding station, the flash is scarf'd off by cutters set up to trim the flash on the inside diameter (ID) and the outside diameter (OD) of the pipe.

While in typical production varying amounts of the upset removed in this step, this process must function within nominal bounds set by specification. On occasion process upsets cause too much metal to be removed, which when it occurs cuts into the pipe body can leave the wall thin relative to the wall tolerance. In contrast, insufficient upset or significant seam asymmetry can cause too little flash-trim, which leaves potentially significant stress raisers to be identified and dealt with later in the production process. Figure 1b shows a schematic view of a transverse cross section local to the seam after it has been scarf'd at the ID and OD neat to the full wall of the pipe. Not all seam producers used a scheme that trimmed neat to the pipe wall, with the welds of some producers, such as flash welds, showing a characteristic trim appearance, as Figure 2a illustrates.

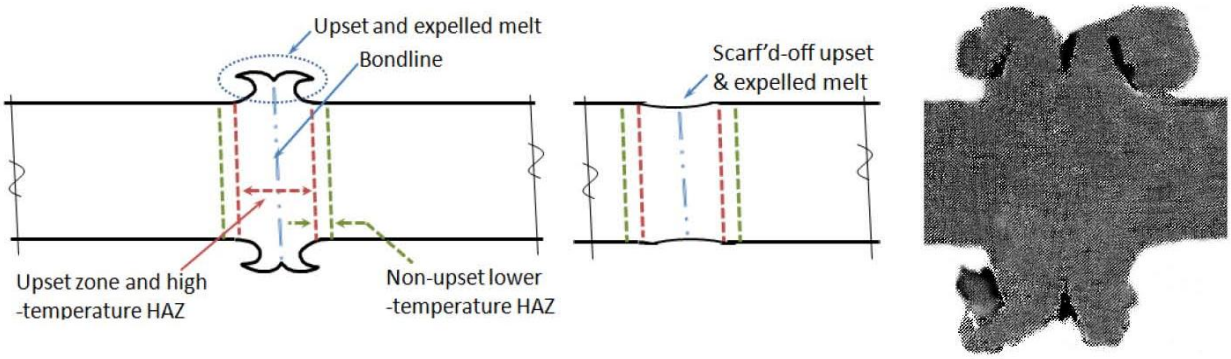

a) schematic of an as produced seam, viewed prior to ID/OD trimming

b) schematic after a near flush ID/OD trim

c) FW process prior to ID/OD trimming

Figure 1. Views of transverse cross sections through an upset autogenous seam weld

Cross Sections of Some Upset Autogenous Seam Welds Removed from Service

The photographs in Figure 2 show cross sections of pipe from a few of the early producers after the seam has been scarf'd to illustrate what can be found relative to the schematic view in Figure 1b. All views are shown with the pipe ID oriented to the bottom of the image, at roughly the same magnification, with the nominal wall thickness (in inches) included for reference in the captions. All, except one, represent intact seams. The captions also indicate the producers when known, and include A O Smith FW, DC-LFERW produced by YS&T, and seams from two other AC-LFERW producers. It is apparent that quite differing trim practices have been followed,

with the production process for two cases leading to rather skewed seams, and misalignment evident along with other anomalous outcomes.

While the images in Figure 2 are from pipe that has been removed from service generally because of a seam-related issue, it is apparent that some cross sections appear as expected, while from an alignment perspective alone others do not. In regard to macroscopic shape, Figures 2a, and 2c have symmetric seams, although that in Figure2c shows ID flash that comes close to today's maximum trim requirement, but this was not in place when this seam was made. These symmetric seams are in contrast to those shown in Figures 2b, 2d, and 2e, where misalignment due to vertical-edge offset, or poor edge shearing, or both, have caused a skewed bondline. For the just noted sequence, these seams are skewed from vertical by 8°, 25°, and 5°, respectively. It is evident that just a 8° skew can cause an unusual and possibly problematic ID-trim configuration, with a similar feature formed for the seam skewed by 25°. Misalignment also can cause a locally under-thin wall, and can also reduce the upset force, which based on prior discussion can lead to a low-quality bondline.

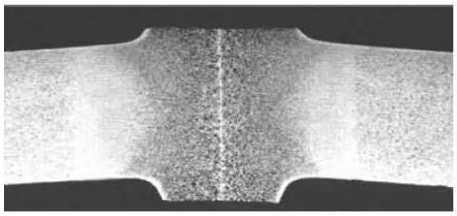

a) FW with t = 0.250"

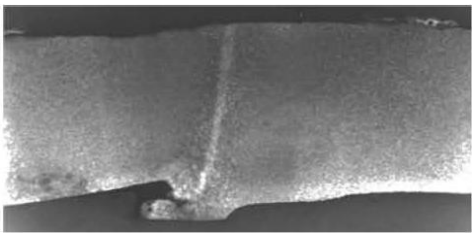

b) YS&T with t = 0.312"

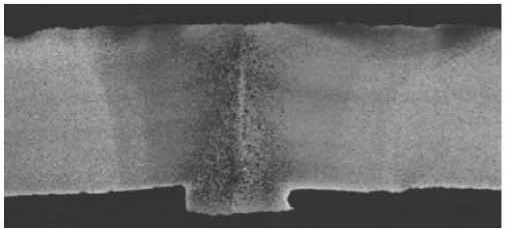

c) unspecified with t = 0.312"

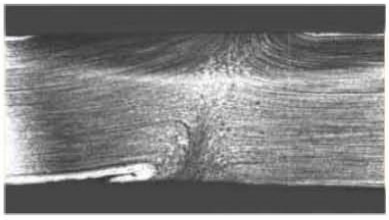

d) YS&T with t = 0.250"

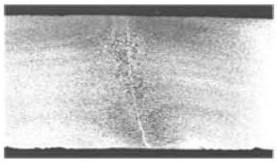

e) Republic with t = 0.250"

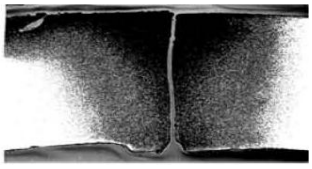

f) YS&T with t = 0.250"

Figure 2. Views of cross-sections through intact seams, after the flash was trimmed

As for the skewed seams, the report associated with the cause of the ID groove shown in Figure 2f did not directly address its cause. However, the report notes the pipeline was transporting gas that was not indicated to be sour or wet, and the report stated that the failure initiated in the bondline from the ID. The images indicated that failure was due to cracking that developed and grew in service along the bondline. While it remained inconclusive, the report suggested that untempered martensite found in the seam combined with atomic hydrogen formed in relation to the cathodic protection (CP), leading to hydrogen-stress cracking (HSC). Significantly, such a mechanism would focus at the root of the ID groove. In turn, based on the prior section

wherein failures in the bondline form due to inadequate upset, the circumstances of this failure are not inconsistent with this ID groove lying in untrimmed flash, which remained untrimmed because of inadequate upset.

Evolution of Upset Autogenous Welding over Time

As time passed, the ERW process was better understood relative to defects that became evident over time, and technology evolved. The LFERW process gave way to a much higher frequency AC source that used KHz frequencies and higher power levels (high frequency electric resistance welds [HFERW]). Sliding contact was introduced, which when coupled with the higher frequency produced a narrow HAZ and a more controlled and efficient process that was capable of high production speeds. Induction welders also evolved, which were capable of producing a narrow HAZ, leading to what is termed a high frequency induction (HFI) weld. Finally, a post-weld heat treatment (PWHT) was added to the process, to normalize/anneal the HAZ, with a view to avoid concerns like that noted in reference to Figure 2f. For some producers, like Stupp, the transition to HFERW was made in the early 1960s, while others like US Steel, made this transition before or in the mid-1960s. The PWHT was broadly incorporated into the process beginning roughly the same time, which like the transition to HF differed in time from mill to mill. In regard to so-called domestic production, the transition to HFERW is often cited as complete circa the early 1970s for the major producers, and certainly was completed later in that decade. It should be noted that such dates are specific to (most) domestic production, whereas for some foreign producers this transition came somewhat later. A final point to note in this context is that so-called vintage (pre-1970) ERW pipe includes both LFERW and HFERW, with both contributing to the failure experience of ERW line pipe.

The evolution of technology facilitated the design of sliding contact ERW and HFI welders to direct the current into and along the skelp edges in the V formed by the fin pass(es) and the welding roll, with an impeder employed as needed for the HFI process. While these autogenous seam processes have evolved with a design that better focuses heat at the abutting edges creating a narrow momentary molten state at the apex of the V, they are otherwise largely comparable to the vintage processes with the exception of the PWHT. The major changes over time in addition to the process involve its control[(e.g.,10,11)], and subsequent seam inspection[(e.g.,12)]. When coupled with the ongoing improvements in testing and inspection of the inbound skelp typical of any pipe making process, these changes ensure better quality for modern upset autogenous welds. But, as for pipe produced using other seam-welding practices, source steel and pipe quality can vary across pipe mills, depending on their experience and quality control and assurance, and that of their skelp suppliers, which today can be sourced worldwide. Recent work illustrates the sensitivity of HFERW and HFI seam quality to process parameters[(e.g.,13)], including a study of the heat/melt zone in V as the seam is completed that shows periodicity remains in the melt[(14)].

As indicated above, the abutting edges to be bonded are brought together through a series of forming rolls. According to Reference 8, three roll-forming schemes are or have been used to produce ERW pipe, with similar concepts adopted for HFI pipe. The original and still popular concave-convex roll system consists of pairs of rolls mounted horizontally with a convex roll forming the ID and a concave roll supporting the OD of the pipe, with this shape maintained

through the fin pass(es). Forming also is done using flanged-vertical rolls, which is done entirely from the OD surface after first using a convex-concave stand to start the process. The final scheme is cage roll-forming, which makes use of a modified convex-concave process. Regardless of how the pipe is formed, all roll-forming ends with a fin pass(es), which serves to a) prepare/shape the skelp edges, b) precisely align the edges, and c) maintain the V angle.

The forming scheme and weld setup for single-pipe processes differs necessarily from that for continuous production. For example, FW pipe made from the late 1920s through 1970 formed a can, and introduced the DC current, joint by joint, rather in than continuous production.[7] This seam developed as the abutting edges were forced together over the full length of the joint. As is logical, single-pipe production made use of steel preparation and forming schemes common to the joint-by-joint production of pipe of that era, which were used to make pipe by other welding practices. What is known about this process is best documented through related patents and the literature developed and distributed by the A O Smith Corporation[7]. This is much the same today as technology is disseminated via publically available company reports[e.g., 13,15], through company presentations in other industry venues[e.g10,11] and conferences[e.g.,16], and occasionally in technical journals[e.g.,14,17]. The internet also is an effective tool in presenting details of related developments and company-specific processes[e.g.,12,18-22]. Aside from the patents and limited corporate documentation, little else is readily available that is specific to the details the FW process, which ended production circa 1970 (anecdotally because of difficulties in producing the higher-strength grades that were emerging at the time).

In summary, either resistance or induction can be used to heat the abutting edges of the skelp as the basis for welding, with the pipe roll-formed in a manner that develops a V between the edges, after which they are forced together to create an upset autogenous weld. Details of the HFI versus ERW process and the perceived benefits of each can be found in several references[e.g.,18-21], including some that delve into the technical details[13,14,17]. While the above cited literature is broadly useful, care must be taken to separate the marketing motivation from the technology aspects, as much of this work has been done by pipe makers and equipment suppliers and lacks peer review.

Potential Process Upsets and Sources of Defects Prior to Welding

Pipes made with an upset autogenous seam undergo a similar sequence of steps prior to welding, which where applicable parallels that for the other types of seamed pipe. For some ERW seams, this begins with the cross-skelp weld that joins sequential coils to keep the process continuous over more than a single coil. The websites of various producers invariably show coil rather than plate joined by a cross-skelp weld as feed for production, which implies that the maximum wall thickness available is limited by steel available in coil format. Use of coiled skelp might also reflect the observation that the upset force increases in proportion to wall thickness, whereas skelp quality might diminish, which can also limit the use of plate as feed to the process. Regardless of the reasons, the skelp next moves through steps that include leveling / aligning, slitting / edge trimming, (roll) forming, and final edge preparation / fin pass(es), with the specific steps and sequence being mill-specific. Slack also is provided in some mills, to maintain process continuity prior to the forming step, with other steps that are/can be common to all seam types

also involved, the details of which can be easily found via keyword-driven web searches. Of these steps, process upsets in leveling / aligning, slitting / edge trimming, final edge preparation / fin-related pass(es) are potential sources of defects, which could eventually pose an integrity threat. For processes that produced pipe joint by joint, or from a single coil, while the cross-seam step was not needed, the steps that followed to complete the weld were comparable, whereas the production setup and equipment differed, as outlined later.

Leveling/aligning is a potential source of many defects, because twisted or cambered skelp can cause an offset in the edges at the apex of the V, which lead to an asymmetric weld and a skewed bondline that in turn can cause a significant reduction in the local wall thickness. The images in Figure 2 show a few examples of the consequences of misalignment as the abutting edges in the V converge at the apex; much worse examples are evident in Battelle's archives. While the fin-related pass(es) are designed to manage such concerns, their design and function anticipates skelp that has been leveled/aligned within reasonable limits. Process changes and controls were introduced over time to better address this aspect, but it remains a concern for early production for several reasons that all make it difficult to identify misaligned edges. These include: a) high production speeds that limit the utility of visual inspection, b) evidence on the OD mismatch is removed with the flash trim, and c) the ID was not visually accessible.

Slitting / trimming to the correct width, regardless of when this is done in the process, and the effects of twisted/cambered skelp can be a concern because both lead to locally under-width feed into the fin pass(es). Slit skelp can become an issue if the thickness of the skelp varied significantly from edge to edge, being thicker at the center, which can lead to unequal wall thickness at the bondline. In turn, this means the displacement mismatch essential to forge the pressure weld can be locally absent. Offset thickness leads to the issues evident in Figure 2, whereas decreased displacement mismatch causes inadequate upset that in extreme cases means the abutting edges do not arc/heat adequately, nor does sufficient pressure exist to develop the forged bond. Gross issues in the width of the skelp also could cause issues in proper aligning PWHT once it became common practice. Thus, one consequence of inadequate pressure is variable forging conditions leading to variable to no bondline strength, with variable to no fluxing of the abutting edges, so the oxide and other contaminates are not fully expelled from the bondline, with neither outcome being desirable. A second consequence is poor/inadequate PWHT.

The process used to trim to width and the final edge preparation also can be sources of concern, with their significance evident in papers by producers and those supporting this industry[(e.g.,22)]. Poor trimming and edge preparation can tear-out or displace metal that is essential to develop the displacement mismatch needed to forge the pressure weld, such that upset the force and thus the upset developed can be locally limited, potentially leaving the molten steel that contained the oxides and other contaminants in the bondline. Dirt, grease, scale, or other oxide films if still present on the skelp when it reaches the apex of the V also are a concern because they effect bondline quality, and could reduce its local strength and/or toughness.

In addition to the above process concerns, skelp quality relative to microstructure and chemistry can be factors for upset autogenous welds. Because of the metal upset that develops, as was

illustrated in Figures 1 and 2, any microstructural banding that involves local through-thickness weakness, for example oxides and sulfides that are strung-out and flattened in rolling, creates a potential crack path. Such cracking does not propagate in the bondline, but rather develops in the upset metal, from the ID and/or the OD. Steel cleanliness also can be a concern because chemistries that lead to local corrosion cells can focus corrosion in the vicinity of the seam, which can lead to cracking into the bondline.

In summary, potential process upsets prior to welding set up circumstances that can open to a range of defects that can form in the bondline or the upset/HAZ during or after welding, as outlined next.

Potential Process Upsets and Sources of Defects Due to Welding

The rapid rise time for temperature due to resistance and induction heating coupled with high speed of production requires good continuous interface contact as the V closes to produce a quality weld, the significance of which is evident in papers by producers[13,14]. With current contact designed to focus heating as the V closes, a reduction in the current flowing into the V (aside from that due to the AC waveform) can cause locally reduced temperatures, which affect the melt zone and the extent of heat-induced expansion that further affects the pressure leading to the forged weld. It follows that momentary reductions in the current level or, even worse, the loss of current can cause a major reduction in the strength of the bondline. The historic use of lower-frequency AC sources coupled with wheel contact that transferred current over a relatively short distance along the edge of the V further contribute to this concern. Consequently, defects due to lower bondline strength can be anticipated if that short contact zone was upset by the presence of debris or contaminants, or by upsets in the current supply. As noted earlier, over time, process improvements were introduced through the use of sliding contact and much higher frequencies, both of which work to offset such concerns.

Following welding, the ID and OD flash gets trimmed, after which pipe joints are cut to length. As issues emerged with brittle seams, modifications have been made to the initial ERW process to include a PWHT to normalize/anneal the HAZ; this step is also common to the HFI process. The PWHT step is critical, because the heat due to resistance or induction is removed quickly by the large heat sink created by the pipe body, which can lead to hard microstructures that lack toughness and are prone to embrittlement. Accordingly, upsets in the PWHT can render much of the seam brittle, such that defects initiated for other reasons encounter little resistance to crack growth and failure, with failure due to hydrogen-related processes also plausible. Such circumstances underlie the in-service rupture associated with Figure 2f. Accordingly, inadequate PWHT is by itself a cause for concern, and it can couple with other causative factors.

The step that involves flash removal can be complicated by alignment issues such as asymmetric seams, with some distorted well beyond that shown in Figure 2b, 2d, and 2e evident in Battelle's archives. In such cases, the process designed to remove the flash and the inherent V-groove it contains can miss the upset region to a varying extent, and thus leave such features to potentially develop due to in-service loadings. Proper alignment of the internal trim tool was a particular problem in the earlier days of ERW production, which traced often to setup and skelp-width control, among other factors. Figure 2b illustrates this situation wherein the flash to the left side

of the seam remains at the ID. As implied earlier, inadequate leveling or camber also can become an issue in post-weld processing that leads to locally reduced wall thickness as steel is scarf'd from the body or the seam due to locally out-of-round pipe. By itself, locally reduced wall simply increases the stress in proportion to the net section lost; this by itself is not a concern unless the loss is extreme or occurs in conjunction with other causative factors.

In summary, process and other upsets during and after welding open to a range of defects that can lie in the bondline or in the upset/HAZ of the weld, whose size, shape, and axial continuity coupled with the local mechanical and fracture properties control the stability over time, and the integrity as a function of pressure, pressure cycles, and other such factors.

Defects and Potential Failure Mechanisms in the Bondline

As evident from the prior section, the nature of the upset autogenous weld leads to circumstances that can form defects in the bondline or the upset/HAZ of the seam. Regardless of the cause, it was evident that breakdowns in current flow into the V can lead to inadequate heating and limited melting. In addition, breakdowns that lead to inadequate upset can decrease the quality of the forged pressure-weld, and/or leave a solidified melt zone that includes oxides and other contaminants in the bondline. Each of these process breakdowns leads to reduced or possibly no bond strength, and in some scenarios also a brittle bondline, which depending on the circumstances lead to defects known as cold welds, black-oxide defects (including penetrators), and stitched welds.

As occurs for most failure analyses, the cause of failure and whether other aspects are contributory is based on knowledge of the circumstances, the macroscopic appearance in the vicinity of the origin, cross sections reconstructed through the failure (with insight available from cross sections made at either end or both ends of the failure that generally are viewed as-polished and after an etch), and from the appearance of the fracture surface. When a leak is evaluated, the origin can be simply identified and opened in a manner that preserves the features and demarks the secondary fractures, whereas when a rupture occurs some skill may be required to locate the origin, depending on the nature of the origin and the extent of the rupture.

Photographs of the typical fracture features associated with cold welds, penetrators, and stitched welds are included in Figures 3, 4, and 5, to document the typical appearance of such defects. Because operators that experience failures and others evaluating EWR failures can use such images as a guide to understand their circumstances, a range of images is presented as parts to each of these figures. Because the focus here is on seam defects in pre-1970s ERW and FW pipes, the images and discussion that follow next are specific to such pipe. But as defects continue to occur in more recent pipe made using the HFI and HFERW processes, such defects will be considered later in a section that contrasts HFERW pipe to its LFERW predecessor.

Cold Welds. As defined by the American Petroleum Industry (API)[23], the term cold weld is "metallurgically inexact, generally indicating a lack of weld bonding strength of the abutting edges due to inadequate heat and/or pressure." The term cold weld applies to a failure origin that shows some axial continuity and does not exhibit axially periodic changes in seam strength. The API notes that "a cold weld may or may not have separation in the weld line" and indicates that

"more definitive terms should be used whenever possible." In this context, cold welds can run from a featureless fracture surface, where little bond strength develops, through one that is patchy or blotchy in the areas where some load transfer occurred across the seam prior to failure (sometimes termed paste welds). Finally, cold welds can occupy part to all of the wall thickness. Figure 3 shows several images that are characteristic of cold welds.

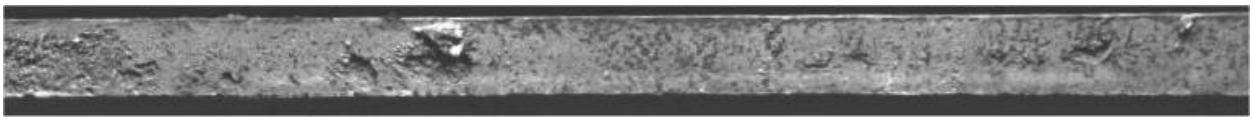

a) fracture surface from a very long lower-strength defect that continued to the right

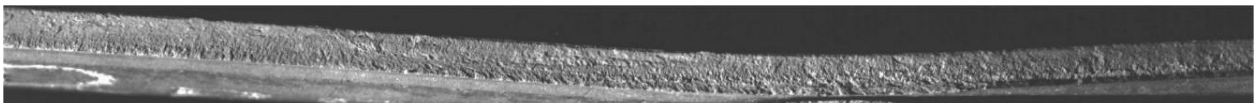

b) fracture surface from a slightly stronger, quite long defect that continued out both sides

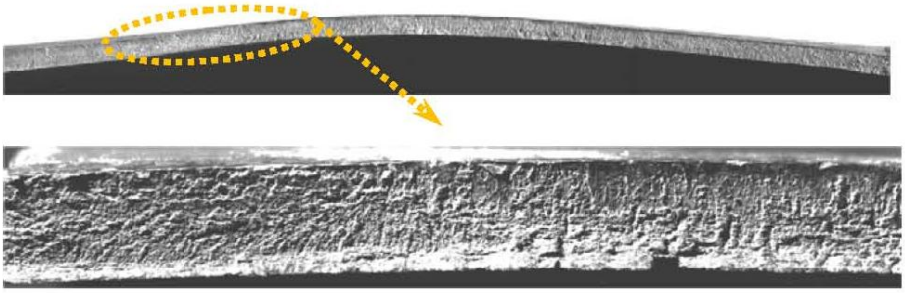

c) similar to b): the detail below shows patchy and narrow vertical features that (prior to cleaning) are separated by "black oxide"

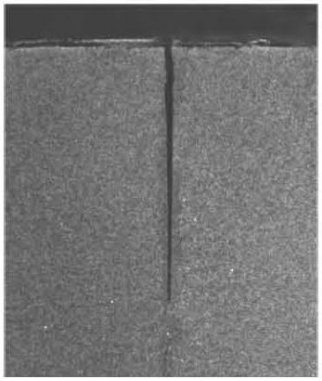

d) cross-section through a PTW defect =~0.5 t

Figure 3. Views of LFERW cold weld features: wall t = 0.312" except for c) t = 0.344"

Figure 3a shows an example of a cold weld that developed little strength, as its fracture surface is close to featureless, with just the vicinity of its mid-length shown in this figure. This view is cut from a longer feature that continued to the right of the image. The view in Figure 3b shows another cold weld that has developed some strength in contrast to the view in Figure 3a, which is apparent in this image in its slightly rougher sometimes patchy appearance. Figure 3c,which macroscopically similar to Figure 3b, is included as the background for the inset below that illustrates some of the details of this type of defect. The image below derives from the area outlined by the dashed ellipse, where patchy and narrow vertical features are evident. When such surfaces are viewed prior to cleaning, "black oxide" lies compacted between them. Finally, the view in Figure 3d shows the upper portion of a cross section across a part-through-wall (PTW) separation in a cold seam, which absent the coating would be visually apparent under close examination, whereas such separations whereas contained subsurface would not. Note from this section that the faces of the separation are virtually smooth – indicating what was a very low strength interface – effectively an unforged or cold bondline.

Because the abutting edges oxidize due to heating as they move toward the V, if there is inadequate metal upset and/or inadequate heating then some to all of that oxide is not expelled

from the interface between them. In such cases the bondline shows evidence of this in the form of a black oxide that is clearly apparent if the defect is viewed prior to cleaning. Periodic current upsets lead to corresponding momentary swings in heat input to the V, which could contribute to the vertical features apparent in Figure 3c, toward the right-hand side of this image, whereas other types of process upset can cause patchy areas of oxide.

Occasionally the ERW/FW process developed features that in some reporting were termed "fingers" of oxide, which when they penetrate through-wall (TW) are one form or class of defects unique to upset autogenous welds. While initially such features are adherent and fill the bondline, due to the effects of pressure cycling, or periodic larger pressure swings as occur with hydrotesting, this oxide can breakup, leading to short TW leak paths. Such leaking seam features are termed pinholes by the API[23] in reference to ERW seams, which the API defines as "a short unwelded area in the weld line extending through the entire pipe (wall) thickness."

Figure 4a shows a view that includes voids left behind by oxide fingers that remained on the opposing fracture surface. This image fits the written definition, but is rather different from the illustration used by the API. Figure4b shows a much different view of oxide formation and disposition, as in this case the oxide formed along the edge of the bondline, and runs along and into the wall over a rather large patch, and remains intact as this is an as-opened view of the fracture surface.

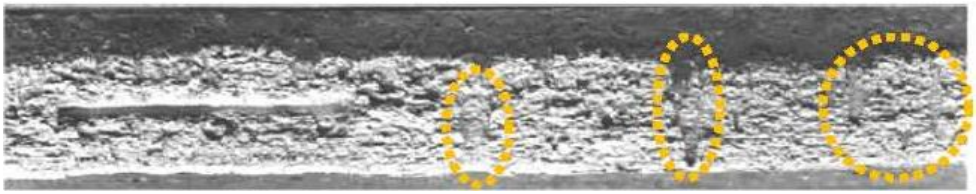

a) showing oxide fingers from OD patch, with one small TW feature: DC-ERW seam; t = 0.219"

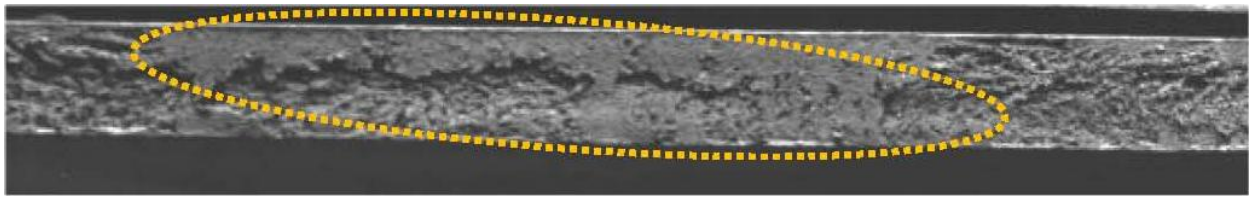

b) showing oxide in an LFERW seam running at the surface and well into the wall: t = 0.375"

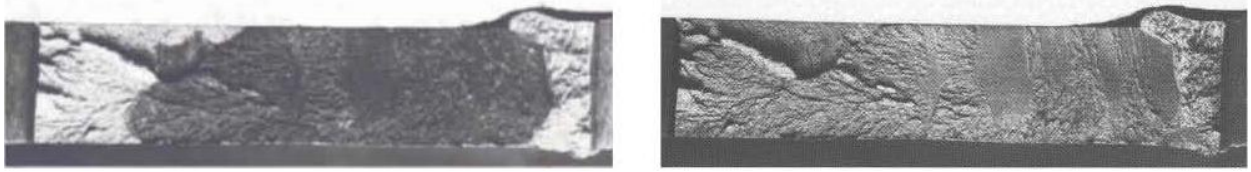

c) showing a TW defect at the pipe's end in a FW seam: left as-opened, right as-cleaned; t = 0.344"

Figure 4. Views showing black-oxide features in ERW and FW seams (OD surface is up)

Penetrators. The API, in Standard 5T1[23], defines a unique feature in regard to FW seams, which it terms a penetrator. The API defines a penetrator rather generically as "a localized spot of incomplete fusion" – with the implication by way of its name that such defects penetrate TW. The photo used by the API to illustrate a penetrator looks rather like the oxide finger shown in Figure 4a, which, as is evident from the caption for that figure, can be found in ERW seams as

well as the FW seam which API 5T1 identifies with it. Confusion arises relative to API 5T1 in this context, because the photo of the feature noted in 5T1 as a penetrator, is defined there specifically for FW seams, but has been historically labeled as "penetrator (ERW)" in 5T1. Reality in this context is that oxide fingers can form in an upset seam produced using either the FW or ERW process. On that basis, the term penetrator and its definition as written by the API appear generic to both of these autogenous weld processes.

Weld-Area Cracks. While the term penetrator is not unique to a FW seam as implied by API 5T1[(23)], seams made using the FW process did develop a unique defect that is consistent with the written API definition of a penetrator, which also was not prevalent in ERW pipes. But, whereas this PTW bondline defect fits that written definition, its appearance is inconsistent with that of the related photo API 5T1[(23)]. Instead, this planar PTW defect, which on occasion did develop TW, is a much better match to the API photo of a weld area crack, which 5T1generically defines as "a crack in the weld line or weld upset zone". This defect also is broadly consistent with the continuing description that notes it is "insufficient to cause complete rupture of the material" and other caveats. This bondline defect was formed at or very near the ends of the pipe, which possibly explains why they managed to pass the mill hydrotest even though being TW or nearly TW.

Figure 4c shows an example of this FW defect, with the adjacent girth weld evident on the right side of these images. As evident from the images, this leak path through the wall was excised by saw-cuts from wither end of a coupon cut from the pipe, which then was opened after chilling in liquid nitrogen (LN_2). The image to the left side in Figure 4c is a view of this TW feature as-opened, while that to the right is after cleaning. The differing appearance between these images reflects the presence of oxide and other impurities that remained trapped in the seam. Because the finer features in both images are comparable, it is apparent that this oxide was rather thin, and uniform in thickness, and so likely reflects locally inadequate upset (which could be traced to several causes). Because these short potential leak paths tended to form at/near the ends of the pipe joints, it is conceivable that they formed due to issues unique to the aligning and clamping of the formed can, or due to related setup controls. For this reason, images of transverse cross sections through this unique cold-weld feature often also show the girth weld adjacent to the defect, as is the case for Figure 4.

Because the features shown in Figure 4 develop under process upset conditions that affect the bondline, they are variations of the circumstances that lead to the broad family of features that fall into the type of defect termed cold weld. All form because inadequate metal upset leads to inadequate forging, and/or a physically cold weld forms due to inadequate heat, both of which could leave process oxide and other impurities in the bondline. In this context black oxide features can be found with a wider range of shapes, and sizes, running along seam edges, and/or into the thickness, over quite short to much longer distances – with variations in location, length, and depth that depend on the skelp and the processing parameters in the V at time the skelp feeds their formation. Figure 4 illustrates three such variations, ranging from the short cylindrical TW features shown in part a), to the thicker compacted broad blotchy layers that lay along and through the seam apparent in part b), to the very thin and uniform layer evident in part c) of the figure.

Stitched Welds. Finally in regard to process upsets that affect the bondline, process upsets can cause periodic momentary variations in the heat input to the V that in the presence of adequate metal upset lead to periodic variations in the strength across the forged weld. While not documented in print to the authors' knowledge, one plausible source of such periodic variation in heating is an excessive rate of production. If sufficient weakness develops over the length of the feature subject to the pressure carried by the pipe, the weaker areas fail first, followed by the stronger areas. This situation leads to fracture features that appear axially discontinuous with periodic TW bonding, which have been termed stitched welds – as illustrated in Figure 5.

The API 5T1[(23)] defines a stitched weld in specific reference to ERW seams as "variation in the properties of the weld occurring at short regular (periodic) intervals along the weld line". 5T1 goes on to indicate that stitching forms due "to repetitive variation in welding heat" that leads to "a regular pattern of light and dark areas" that develop due to relative differences in the strength across the forged bondline. When the periodic strength across the bondline is high, the steel in this interface stretches further prior to failing than where it is less strong, which leads to a strong contrast between areas along the seam that are periodically much weaker that the adjacent areas along the seam. This differential strength leads to the "the light and dark areas" noted in the API's definition. In such cases the stitched appearance is clear, as is the case in Figure 5a.

Examination of Figure 5a shows that the stitched appearance becomes stronger moving from the left edge to the right edge in this image, which shows only a portion of this feature that continued beyond the right margin of this figure. The difference in the clarity in the stitching in Figure 5a moving along the image from left to right is due to increasing differential strength between the weaker and stronger areas as the image tracks the bondline. Where the periodic variation in bond strength is not greatly different, there is less difference in the stretch across the forged weld prior to failing between the adjacent areas, so the contrast between the periodically weak and still weaker areas diminishes. Eventually this differential strength is lost, as is the stitched appearance as the process tends to what was noted above as a cold weld or a sound weld. This is illustrated in Figure 5b that shows weak stitching that ran for only a few inches within an otherwise cold weld, in contrast to that shown in Figure 5a, which represents a portion of a feature that showed strong stitching that ran axially the order of one foot.

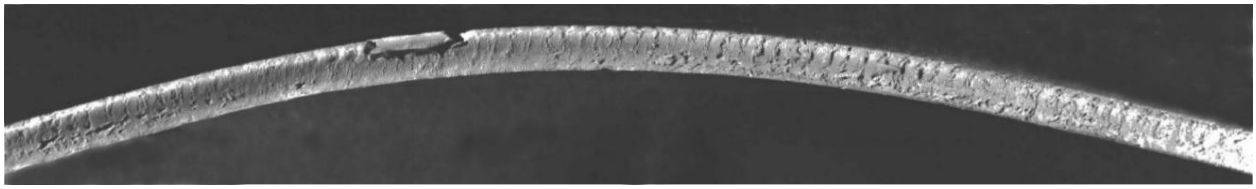

a) strong stitching in DC-ERW: t = 0.312" – OD surfaces mated

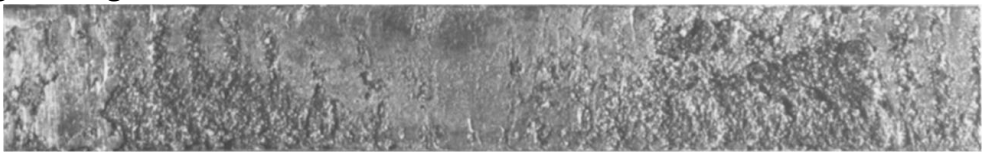

b) hints of stitching in LFERW: t = 0.250" – OD surfaces is topside

c) the feature in Figure 5b shown at a scale comparable to that in Figure 5a

Figure 5. Macro views of stitched welds

In regard to Figure 5b, note that hints of weak stitching lie to either side of a short area that shows the traits of a cold weld. In regard to the indicated actual wall thickness shown in the captions and the sizes of the images, the feature in Figure 5b ran for roughly one-tenth of the length of the feature shown in Figure 5a. When the image in Figure 5b is viewed at comparable magnification as in Figure 5c, it is difficult to identify the hints of stitching evident at higher magnification. This observation makes clear the need to use appropriately prepared samples, and adequate magnification to identify periodicity in differential strength along the seam when evaluating a possibly stitched weld.

Cold welds can be found adjacent to stitching or in combination with a penetrator or oxide finger on a longer fracture that runs down the bondline, because such features reflect varying degrees of inadequate metal upset, and/or inadequate heating along the seam. Accordingly, these features can form in isolated patches, or run axially in combination with each other seam defects, depending on the causative circumstances. Consistent with the flexibility available under the API definition of a cold weld, some bondline features have been termed LOF defects. However, as noted earlier some texts on welding[(e.g.,9)] make clear that the upset autogenous seam is a result of heat and pressure – the basis for forging – rather than fusion, which occurs for other welding processes. To avoid controversy in this context, the few such cases termed LOF defects in Battelle's reporting have been relabeled as cold welds. Battelle's reporting has on occasion also labeled bondline features by more definitive terms, which again is consistent with API's suggestion for cold welds. When terms such as weak plane, bondline inclusions, etc., were used, they were retained, but are reported secondary to the term cold weld – with a view to establish a broader basis for data trending and integration. When secondary terminology is found, it tends to be used to elaborate on features that formed due to breakdowns in process due to inadequate metal upset, which failed to expel oxides, inclusions, and such from the bondline.

Logically, bondline defects tend to be axial, planar, and normal to the pipe wall, and thus tend to fail due to pressure-induced loads across the seam; however, seams also have failed due to ovalization that focused bending in and across plane of the seam. Regardless of the source of the tension across the seam, the failure of bondline features will depend on the length, depth, and continuity of the defect; the properties of the bondline/interphase; and the magnitude of the load across the seam. Either fracture or plastic-collapse can controls this failure, with the failure mode being brittle versus ductile versus mixed depending on the transition versus service temperature. The consequence as a leak versus a rupture, and the axial extent of axial propagation, also depend on the properties, and can depend on the transported product. It is noteworthy that not all cold welds pose an immediate integrity threat, as the high temperature oxide present in such seams is adherent, and can block the leak-path for through-wall cold welds. However, as time passes, and pressure cycling or other step pressure changes occur, such as due to a hydrotest, what was adherent to the interface, and intact, can break up and separate from the interface, leading to a leak or possibly a rupture in the event the defect extends in length.

Selective Seam Corrosion. A fourth common bondline defect develops in service that traces to the quality of the steel. This type of defect forms where a breakdown in the coating occurs along

with inadequate CP (if any) in the presence of dirty steel, which promotes selective corrosion in the bondline. Because this occurs in the bondline, this defect type has been termed selective seam corrosion (SSC). Even moderate SSC can be visually identified from the OD, as it causes grooving that often is associated with corrosion either side of the seam upset. Figure 6a shows an OD view of SSC, while Figure 6b shows a cross section view, and Figure 6c documents the appearance of this defect on the fracture surface. As becomes evident later, depending on the involvement of associated corrosion, sections along and through SSC features can vary greatly.

Because SSC is a bondline defect, once the defect reaches a critical size occurs, as noted above for the previously discussed bondline features, failure often occurs under fracture control rather than plastic-collapse. Where OD corrosion also develops, related wall thinning also can be a contributing factor.

Work done as a part of this project, reported by Det Norske Veritas[24] (DNV), notes that several mechanisms that have been proposed to explain how and/or why SSC occurs, including:

- galvanic interactions between the weldment and the base metal;
- differences in dissolution/corrosion rates for different steel phases;
- inclusions and chemistry segregation in the weldment; and
- crevices that form between inclusions and the steel or are present due to LOF.

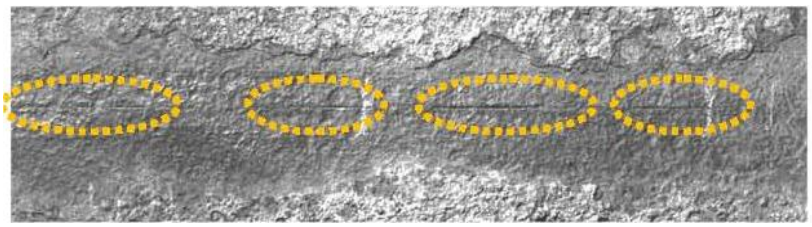

a) strip a few inches wide viewed from the OD surface

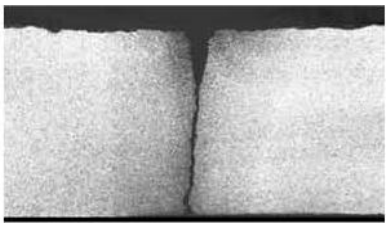

b) LFERW: wall t = 0.250”

c) as-opened fracture surface: LFERW; t = 0 322” – OD surfaces is topside with the upper ~20% of the image is SSC grooving and shallow more localized crack-like growth

Figure 6. Macro views of some selective seam corrosion features

Of the mechanisms identified, DNV notes sulfur enrichment and sulfide inclusions that lead to localized corrosion seem to have the greatest merit and the largest body of supporting evidence. This view is consistent with other reviews of this defect’s occurrence[25]. In addition to controlling the level of sulfur and inclusion shape and composition, they note the overall steel composition and microstructure, weld heat input, and post-weld seam or full pipe body heat treatment are important considerations to minimizing SSC susceptibility. Others[e.g.,26] that have reviewed this type of defect, whose work was cited by DNV, report a clear propensity for SSC absent local evidence of sulfides. As such, one can infer that the underlying mechanism remains ill-defined, with the possibility being that more than one mechanism is responsible, depending on the local circumstances.

Defect Origins and Potential Failure Mechanisms in the Upset/HAZ

Discussion in the section on process upsets and sources of defects during and after welding also indicates that the autogenous weld process opens to defects that can form in the upset/HAZ region of the seam. Such defects can be traced to either the quality of the steel or to process upsets involving alignment/fit-up across what becomes the bondline. Of these, the primary integrity threat that forms in the upset/HAZ of the seam is termed a hook-crack.

Hook Cracks. The API defines hook cracks (or upturned fiber imperfections) identically for the FW and ERW processes as "separations resulting from imperfections at the edge of the skelp, parallel to the surface, which turn toward the ID or OD pipe surface when the edges are upset during welding." Such imperfections develop due to through-thickness weakness that can exist in the microstructures of "dirty steel" that posed a concern until steel cleanliness was recognized as critical for higher toughness at lower transition temperatures in the 1960s. The dirtier chemistry of the earlier steels meant there could be a significant amount of inclusions or other impurities, which during rolling becomes flattened and elongated (pan-caked/strung-out). Hook cracks can form in the layered structures associated with the flattened and elongated inclusions from along the bondline, but more typically developed out further in the upset region.

Hook cracks are so named because their hook-like shape because the upset leads to an out-bent shape. Figure 7a illustrates such cracking, against the background of a macro-etched cross section through the defect. Such cracking can initiate from one side of the pipe, either the ID or

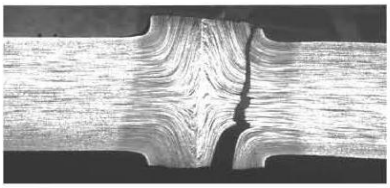

a) ID origin: simple crack path tracking macro-flow lines FW with t = 0.281"

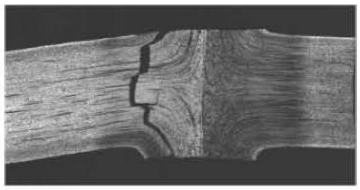

b) ID/OD origins: simple macro-flow cracking FW with t = 0.281"

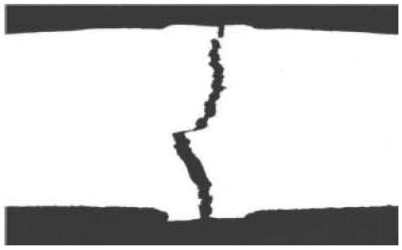

c) OD Origin: complex crack path tracking planes of inclusions LFERW with t = 0.375"

d) fracture surface for a hook crack originating in and running along a dominant macro flow plane the defect exposed in a hydrotests of LFERW pipe with t = o.344" is clearly evident

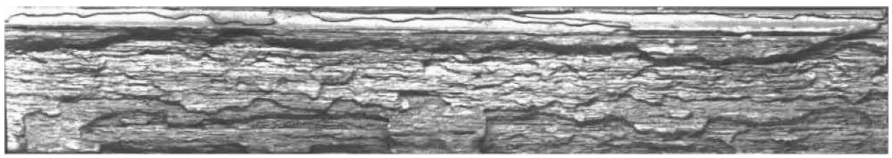

e) portion along the facture surface of more complex hook crack failure – the origin is about the same depth as in part d) above, but uneven in depth, being somewhat deeper than apparent in the section shown in part c) above – exposed in hydrotesting of LFERW pipe with t = 0.375"

Figure 7. Macro views typical of hook cracking – OD is shown topside

the OD, but on occasion cracking initiates more or less at the same location from both sides, and depending on the circumstances and grow more or less symmetrically as evident in Figure 7b.

Depending on the number of sites that initiate such cracking over the length of the hook crack, and the number of near-parallel planes of inclusions that are sufficiently weak to participate in the failure, cross sections made through hook cracks can vary greatly in complexity. Logically, where the cross section is simple the fracture surface is equally simple, whereas complex cross sections involve equally complex fracture features. Figure 7a reflects a situation where a single dominant origin formed and grew until the feature reached a critical size and ruptured while in service operating under Title 49 of the US Code of Federal Regulations (CFR) Part 195. In this case, the origin tracks the flow line and then turns as expected to a plane perpendicular to the hoop stress. In contrast, the path for the feature shown in Figure 7c is quite complex, with an unetched section used to clearly illustrate this path. Related microscopy shows this hook crack's origin lies to the right of the bondline, and that after briefly tracking the flow line of its origin the crack path jumps onto and/or across other planes of inclusion stringers, eventually crossing the bondline and then tracking back to it to fail in the bondline. As becomes evident shortly, the fracture features that develop under comparable circumstances are equally complex.

The hook cracks and their fracture surfaces in Battelle's archives run from the simple views in Figures 7a, 7b, and 7d, to more complex than evident in Figures 7c and 7e. While sizing the origin in Figure 7d poses little problem, sizing origins like that in Figure 7e that vary in depth is less simple. In addition to the term hook crack, features such as these are termed as out-bent fiber cracks, and woody fractures in Battelle's reporting. All cases where the term woody fracture has been used involve hook crack origins, and reference is made to dirty steel. For the sake of broadening the utility of the database in trending and data integration, such features are listed as hook cracks.

As for bondline defects, hook cracks tend to be axial, and can have planar components that can lie near normal to the pipe wall, with segments of the crack's surface also tracking the flow lines. Such was the case for Figures 7a, 7b, and 7d. However, as shown above, cracking that originates in a hook crack can be complex, as was the case in regard to Figures 7c and 7e. As evident in Figure 7b, cracking with a hook crack origin can initiate from both the ID and the OD at the same axial location, and grow along the flow line that originates in prior to turning onto a plane perpendicular to the hoop stress. As evident in Figure 7b, both ID and OD origins turned and grew to almost the same depth, after which the both tracked along a flow plane before turning again onto a plane perpendicular to the hoop stress, where the coalesced causing a rupture. In scenarios where such growth is stable TW, hook cracks can develop to a depth equal to the full thickness of the pipe, rather than just 50% of the wall as some report.

Hook cracks initiate, and grow in depth and length, and fail due to pressure-induced loads across the seam, just as was detailed earlier for bondline defects, and like those defects could also fail due to ovalization if it was focused in the vicinity of the seam. Failure for a hook crack depends on the length, depth, and the axial and TW continuity of the defect, the properties of the interphase and HAZ, and the magnitude of the load across the seam. Either fracture or plastic-collapse can controls this failure, with the failure mode as brittle versus ductile versus mixed

depending on the transition versus service temperature, and both the consequences as leak versus rupture, and the axial extent of axial propagation depending on the properties (and also the transported product).

Occasionally, because of process problems during the PWHT smaller hook-crack origins and origins in other seam defects fail in a brittle manner, whereas they might have remained stable if the steel was more fracture resistant. Where the origin is due to mill process issues such as alignment or edge defects, such origins are identified by those terms, often in conjunction with a generic label like mill defect. As illustrated in Figure 2, poor vertical alignment of the edges (offset edges) can cause asymmetric skewed welds, the degree to which varies with the offset and the amount of upset mismatch (force). Larger offsets coupled with higher upset forces reflect the worst case scenario, which when coupled with scaring can cause thinning of the wall along the weld – which is in some cases already the weakest link for a joint of pipe.

The cross section in Figure 8a shows etched views of LFERW that had a nominally 0.250-inch thick wall, where the effects of offset edges combined with the upset force to produce a skewed weld where the ID scarf caused wall-thickness reduction adjacent to the seam over most of the length of the joint that initiated rupture in a hydrotest. The seam is skewed the order of 12° from perpendicular, and is associated with ~11% reduction in the pipe wall due to the ID scarf, which was trimmed neat to the wall on the right side of the seam, but cut well into the offset wall on the other side of this seam, and into the OD surface. The extent of the over-scarf in this case was compounded by an in-tolerance but less than nominal thickness pipe wall.

a) slight ID/OD over-scarf in a seam skewed due to edge offset **b) detail in a)**

Figure 8. Views of unique upset folds formed due offset: LFERW with t = 0.250”

Figure 8b shows a magnified view through this seam to illustrate the local flow patterns in the upset at the interface with the mating edge. Toward the OD in the upper third of the thickness there is evidence of strong uniform upset flow to the OD surface of the pipe, with clear evidence in this cross section of the strength that developed across the bondline in the upper-third of the wall thickness. The effects of the offset and resulting skewed bondline and the related weakness of the forged weld are clearly evident along the lower two-thirds of the thickness. Early in the upset process, when the abutting edges and developing bondline were still normal to the pipe wall, upset flow began as it should – uniformly toward the ID and OD – more or less from the mid-thickness. However, as the upset continues, what began as compression across the abutting edges, couples with shear, due to the offset edges and being driven by upset force. Due to by the

shear, a portion of the upset flow must reverse directions, which is most evident near the mid-thickness – particularly on the left side, as shown in the figure. The resulting weakness is most evident throughout the lower half of this bondline. Given these features, the images in Figure 8 represent a hook crack origin along the bondline, with continued growth into the wall involving flow line separations – much like that for origins located further out into the upset/HAZ. While this failure occurs as a hook origin, it is due to a mill-process issue, with this and other defects due to alignment and other setup aspects grouped into the generic category termed mill defects.

Other Defects and Hook Origins. Much less frequent failures also occur that originate in the upset/HAZ portion of the seam. API 5T1[23] identifies several types of defect in this context that are specific to upset autogenous welds. These include: a) contact marks and related arc burns "resulting from the electrical contact between the electrode ….. and the pipe surface," and b) inclusions that are "foreign material or non-metallic material entrapped in the metal during solidification". In addition to these pipe-making issues, other types of defect form where environmentally assisted (EA) processes are active, which typically focus in a locally "hard" microstructure. The locally hard/brittle microstructures develop because a PWHT was not initially part of the autogenous process, or because of an upset in the PWHT, making it ineffective. In general, such failures trace to the presence of hydrogen, due to upsets in the corrosion protection system, or its availability from the transported product. These defects have been variously named, tending to reflect the nature of the indicated cause of the embrittlement or other EA process involved.

In summary, there are several general classes of defect that can form in the autogenous weld process, which include cold welds, penetrators, stitched welds, SSC, hook cracks, and mill defects. Other less frequently occurring defects often involve EA processes.

High Frequency versus Low Frequency ERW and Implications

As discussed above, a major change in the ERW process involved the shift to HFERW and the use of sliding contact, which many consider to be completed for domestic production by the early 1970s. As such, some use the term pre-1970s ERW as a catchall for LFERW; however, because this transition started in the early 1960s for some producers, this descriptor may be inappropriate for some pre-1970s ERW. That said, it also should be noted that there were growing pains with this transition; some HFERW experienced multiple pre-service hydrotest failures, with similar issues plausible in the context of HFI welded pipe. Reporting on metallurgical studies that were reviewed but not tabulated as part of this document showed these often traced to microstructural issues due to source steel, as well as process issues. Thus, the use of pre-1970s ERW might be more relevant to discriminate pipe quality rather than the seam process.

While changes affected via the HFERW/HFI processes can limit the frequency and extent of bondline defects, they do not ensure a quality seam unless clean quality skelp is used, to avoid the same concerns that occurred in the LFERW/FW seams. Accordingly, HFERW/HFI seams can be prone to many of the same issues that occurred for LFERW, particularly where dirty steel opens to hook cracks and SSC. Several papers address defect types that can occur in seams made using HFI/HFERW processes[e.g.,27,28], including susceptibility to selective attack in the

seam, which in such cases tends to be termed grooving corrosion[25,29]. Regarding weld-process defects, one paper by an welding equipment producer[27] discusses the "most common defects" and lists nine in total for just the bondline, whereas as noted above process defects also can occur in the upset/HAZ, as well as via grooving corrosion in the bondline depending on the steel used. To be fair, many of the nine seam defects reflect the same concerns as noted for LFERW in regard to cold welds, stitched welds, and penetrators. In fairness it is noted that much has been done in the context detailed research into the HFI/HFERW to understand causes of such defects[e.g.,14,17], and to adapt these processes to limit their formation in production.

Regardless of the improvements affected by the use of high (lower range AM radio / KHz) frequencies and the manner it is introduced into the pipe, there is always a chance for process upsets to cause defects. Thus, avoiding issues in-service is dependent on quality control (QC) and quality assurance (QA), and the use of appropriate pre-service testing in the mill, and then again post-construction. But even with such controls, failures have continued, albeit at reduced rates. In addition to the occurrence of cold welds, hook cracks, and SSC (or grooving corrosion), there are some defect types that are appear unique to the high frequency process[27].

In summary, good steel and a good seam give rise to good pipe – so it takes QC and QA in the steel mill in order to ensure a good seam results from the same QC/QA in pipe-making to produce PSL2 line pipe.

Potential Mechanisms for Defect Growth

Pipelines operate in groundwater and even though coated at some point in their life and nominally subject to CP do experience corrosion (due to holidays in conjunction with upsets in CP), and also are subject to EA processes if the local conditions drive such mechanisms, as for example hydrogen embrittlement. The transported product can also carry constituents that pose a concern from the ID. The following paragraphs illustrate defect growth in regard to both fatigue and stable tearing.

Wherever planar and crack-like defects are present, fatigue due to repeated pressure cycling is a potential mechanism for their growth, as would be hold-times at higher pressure, which motivate growth by stable tearing, sometimes termed stress-activated creep. Certain mill process issues can lead to long axial PTW defects, such as inadequate metal upset and some edge defects can grow by fatigue, as can hook cracks. Figure 9a shows an overview of a secondary crack found nearby an in-service rupture, which was opened in after chilling in liquid nitrogen (LN_2) to reveal the fracture features. Related metallographic cross sections made clear that this was a hook crack, with the initial PTW origin having a depth of roughly half the wall thickness, which runs along almost the full length of this image. Figure 9b shows a slightly magnified view of the fracture surface wherein sequential crack advance is evident, which scanning electron microscopy (SEM) after cleaning indicated was due to fatigue due to pressure cycling of this pipeline that operated under Part 195.

The V-groove formed by SSC, as shown for example in Figure 6, can lead to failure through the net-section by collapse- or fracture-controlled failure, depending on the properties of the seam, the hoop stress relative to the specified minimum yield stress (SMYS), and the length and depth,

and the axial continuity of adjacent grooving, but it also can fail by continued SSC and/or corrosion causing a perforation. Cracking initiated along the root of the V-groove could grow by fatigue due to repeated pressure cycling, or by sustained high pressure that motivates growth by stable tearing, or by some other EA process, but generally these features develop by continued SSC.

a) uncleaned overview of cracking from a hook crack origin in LFERW pipe with t = 0.250”

b) detail illustrating in-service crack growth mid-length along the view above

Figure 9. A hook crack and its fatigue growth – liquid operation, in-service rupture

Figure 10 shows a view of continued SSC growth that is scaled proportional to the wall thickness roughly the same as Figure 9a. In contrast to failure that might develop through the root of the V-groove, or through the axial coalescence of adjacent V-grooves, this form of SSC leads to very localized narrow attack than can develop deep into the pipe wall from the root of the V-groove, resulting in crack-like features that pose a much greater integrity threat than the V-groove alone.

Figure 10. View of SSC and its continued growth as narrow crack-like features along the root of the V-groove: LFERW with t = 0.322”

The fracture surface in Figure 10 is illustrative of such localized attack into the pipe wall. The image, which is a portion of a much longer run of SSC, lies along a fracture surface that has been cleaned to remove the rust from what is otherwise fast-fracture associated with a rupture. The OD of the pipe runs across the upper edge of the image below which is shallow axial V-groove, with segments of localized deeper but narrow attack growing in crack-like segments from the root of the V-groove. Because it continues to grow by the same mechanism that nucleated it, this image does not show a demarcation along its surface due to a change in the defect growth mechanism, as can be seen for example in Figure 9a. SEM of this feature after cleaning did not indicate major differences in the fracture surface morphology. More on stress corrosion cracking (SCC) growth follows later in this report.

In summary, defects that develop due to process and other upsets that lie in the bondline or in the upset/HAZ of the weld can grow by several mechanisms, depending on the nature of the defect, and the operational scenario in regard to pressure level relative to SMYS, pressure cycling, and so on, and the pipeline’s environment. Subject to those parameters, the extent of the growth will,

as usual for any defect, depend on the size, shape, and axial continuity of the defect, and the mechanical and fracture properties local to the defect.

FAILURE DATABASE: CHARACTERISTICS, OBSERVATIONS, TRENDS, AND IMPLICATIONS

Battelle's Archives

As noted in the Background section, this report is based on Battelle's archives[2] concerned with ERW and FW seams. That readily accessible print-format archive involved well more than 100 reports that in total involved contributions from about 25 individuals, which were written over a period of more than 55 years running from the late 1950s, with the last finished as recently as a few months ago.

This report presents the results of an evaluation and trending of the circumstances and outcomes for these failure analyses as the basis to understand causes of failure for such welds. To be useful to this process, the candidate reports had to provide sufficient data to assess the viability of hydrotesting and ILI in managing pipeline system integrity. On that basis, the minimum requirements for inclusion of a failure in this evaluation and trending included: a) origin of failure at an ERW or FW seam defect; b) characterization of the defect; c) pipe data (at least grade and geometry; and d) details of the failure – with more detail presented in this context earlier in the Background section.

These requirements were met in more than 80 reports that considered pre-service, hydro-retest, and in-service failures, and which in many cases provided details on multiple failures within a single report. The resulting database documents 289 seam failures, with the "sanitized" details summarized for trending in digital format as a spreadsheet, and the tabulation in Annex A. For most of the reports evaluated and trended, the available information also included the seam producer and production year, the date of the failure, the hydrotest history, and good quality photographs of the fracture surface and related cross sections, with aspects of some of the images shown in color where it adds value in interpretation. About half of the reports included properties data, with a few also having information concerning related ILI.

Because the more than 80 reports present analyses done by authors whose training involved quite different disciplines typically involving metallurgy, and mechanical and/or civil engineering, and made use tools and technology that have changed significantly over time, the chance exists that terminology and the perspective of the authors differs. However, because Battelle has been among the foremost involved since the early days of pipeline failure analysis and related research, it is not a surprise that a report by report review of the photographic record and other details shows that the interpretation has remained very consistent. Although some of the terminology and the emphasis given to differing aspects of these analyses is occasionally unique depending on the authors perspective and his interests, terms like cold weld, stitched weld, penetrator, hook crack, selective seam corrosion, and so on, were found to be largely consistent

[2] The reports considered work done by Battelle under contract or related directly to such work.

over the decades. Of the terms employed and discussed herein, the descriptors reported hereafter are as presented in the original reporting, save for the few exceptions noted earlier in discussing the various types of defects. The occasionally used term "woody fracture" has been substituted for by hook crack, because based on cross sections it occurred consistently with hook cracks (and included the notation dirty steel). Single-use terms including weak plane, lack of fusion, and inclusions in weld have been substituted for by the generic term cold weld. This was done because cross sections indicated these failures occurred in the seam, and such features form due to inadequate metal upset that fails to develop strength in the forged weld and fully expel oxides and/or other contaminants from the seam.

Database Traits

Pipe Service and Failure Consequences

Battelle's database contains information on a mix of failures that represent service under CFR Title 49 Part 192 or Part 195, which cover natural gas transmission and transmission of hazardous liquids, respectively. Service under Part 192 in Battelle's reporting involves both gas or sour gas, while for Part 195 both liquid/crude and products pipelines are involved, which occasionally includes details of the transported fluid. Failures for gas transmission service outnumber those for service under Part 195 by a ratio of about two to one.

For reporting by authors known to recognize rupture defined relative to the potential for dynamic (running) axial fracture involving fluids/conditions that can support this process, whether a leak or a rupture occurred was determined based on the outcome as reported. Rupture in this context occurred if the defect extended axially beyond its initial length; otherwise a leak occurred. If uncertainty existed relative to the author's understanding of this definition, or there were other plausible concerns, rupture was evaluated based on photographic details when available (which was generally the case); however, where sufficient detail was absent, the reported outcome was accepted. On the whole, what was termed rupture was eventually reported as such, with virtually no changes made regarding this parameter. It is noted that there is little question as to the occurrence of rupture for in-service failures involving transported fluids and circumstances that can support this process, and for gas pressure testing. The fact that about two-thirds of the failures represented service under Part 192 whereas many of the outcomes for service under Part 195 involved axial splits perhaps contributes to this consistency past versus present.

Battelle's database is dominated by ruptures, by a ratio of about eight to one. It is noteworthy that some of these ruptures have occurred at quite low pressures, with such ruptures confirmed by reference to the photographic evidence. It is also noteworthy that the leak population for the Battelle database reflects almost the same proportion of pipelines in liquid/products service as compared to gas service as does the total database; consequently, service does not appear to influence the ratio of ruptures to leaks.

Figure 11 contrasts the just noted traits for Battelle's database to the database developed by KAI, which was alluded to in the background. As noted earlier, that complementary database includes 297 failures, which is almost identical in size to that of Battelle, with 70 of those failures documented from the archives of DNV. Based on the data reported, it appears that the database

developed between KAI and DNV also reflects a set of minimum selection requirements like that listed above for Battelle, such that this complementary database is robust. Accordingly, the combination of Battelle's archives with the joint archives of KAI/DNV roughly doubles the size of the database that underlies this report. As circumstances permit, the ensuing analysis presents the outcome of Battelle's archives relative to the combined databases, which in this comparison is termed the aggregate database. If desired, the outcome for the joint KAI/DNV archive can be determined by inspection as the difference between Battelle's database, and the aggregate result.

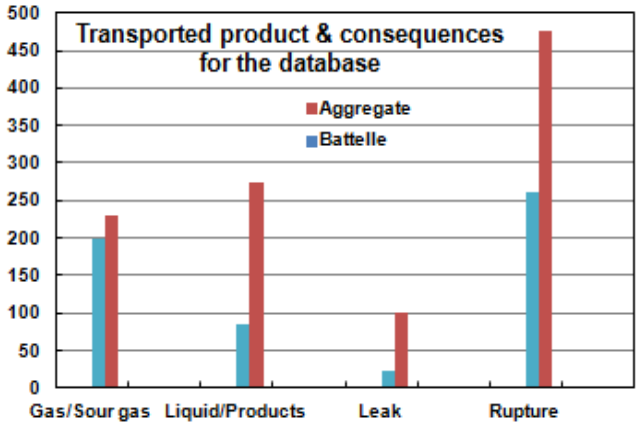

Figure 11. Comparing datasets relative to service conditions and failure consequences

It is apparent from Figure 11 that the KAI/DNV archive[3] includes a larger proportion of pipe in service under Part 195 than 192, leading to an aggregate ratio of roughly 1.2 to 1. As both KAI and DNV are known to recognize rupture defined relative to the potential for dynamic axial fracture, it is anticipated that whether a leak or a rupture occurred as they report it is compatible with the outcomes in the Battelle database. While Battelle's database was dominated by ruptures in the ratio of about eight to one, the results for the KAI/DNV database shows a larger proportion of leaks, leading to an aggregate ratio of rupture to leak of about 4.7 to 1. In this context the individual databases complement one another, and lead to a more balanced database. Insights into such differences become evident as further details of these datasets are introduced.

Pipe Diameter and Wall Thickness

Consider next the range of pipe diameter and wall thickness involved, which is summarized for Battelle's database and the aggregate dataset in Figure 12. Figure 12a shows that diameters ranged from nominally 5 inches up through 34 inches, whereas Figure 12b shows that wall thickness ranged from 0.125-inch up through 0.438-inch. Where nominal diameters were cited in Battelle's reporting (i.e., cases for pipe 12 inches and smaller), the actual fractional size was confirmed. It is evident from Figure 12a that Battelle's database is dominated by pipe with diameters larger than 14 inches, whereas that for KAI/DNV is dominated by the smaller diameters. While these trends on diameter do show quite different populations are represented by these two datasets, given that almost 600 results are represented by the aggregate database it

[3] While Battelle's archives considered for present purposes involve reporting developed through contracts with Battelle, the basis of the subcontractor's archives is uncertain, as to whether the work was done under contract to those entities, as compared to work known to those participating in this project on behalf of those entities.

is anticipated this aggregate population is reasonably representative for pipe that has been produced using an upset autogenous process.

As larger diameters tend to be associated with service under Part 192, a dominance of gas service for Battelle's database could rationalize this trend, yet Figure 11 shows only a two to one ratio in this context, which does not adequately explain this outcome. Figure 12b does not show any clear preference for heavier or lighter wall pipe, except for one of the heavier thickness intervals, so it is not obvious what drives this trend to larger pipe diameters – aside from the observation that this wall thickness / pipe diameter combination is commonly used in ERW/FW systems.

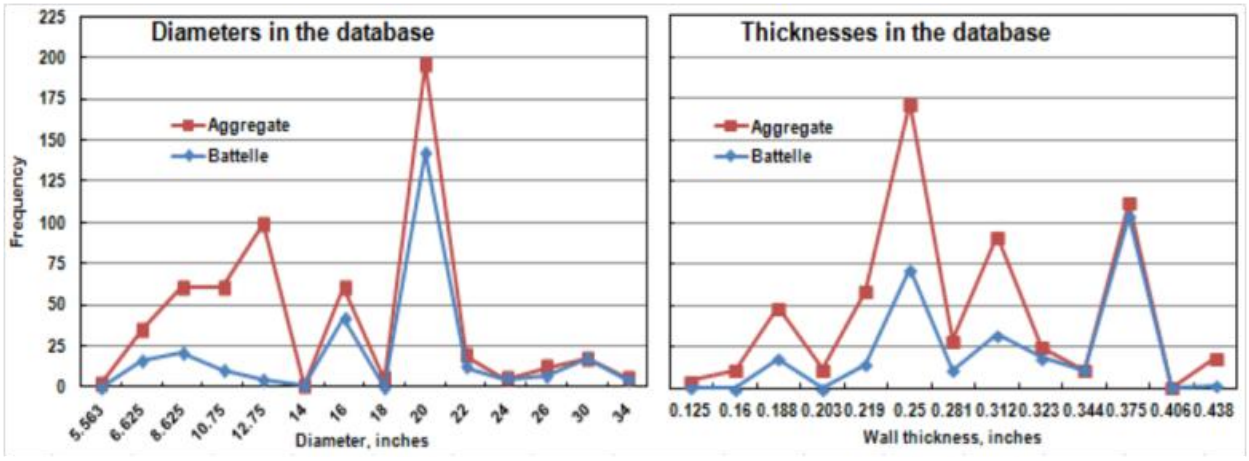

a) diameter **b) wall thickness**

Figure 12. Comparing the datasets relative to pipe geometry

The dominance of the larger diameters does help explain the high occurrence of ruptures for Battelle's database, because increased diameter is a higher-order driver for axial instability – such that any hint of axial extension gives rise to a clearer indication of rupture for any defect at or longer than its critical length.

Pipe Vintage, Suppliers, and Time to Failure

Consider next the vintages and suppliers involved, and the time history that underlies the failures covered by the available database. Figure 13a indicates pipe that has had seams fail represents production from in the 1920s up through the present, with the trends shown indicating that little difference of consequence exists between the two datasets involved. Battelle's database includes pipe produced by (names in contracted form): A.O. Smith; Bethlehem; Canadian Phoenix; Jones and Laughlin; Kaiser; LTVCopperweld; Republic; Stelco; Stupp; Tubacero; and YS&T. The KAI/DNV database expands this to include pipe produced by (again in contracted form): ACME; Cal-Metal Pipe; Huludao City; Lone Star; Maverick Tube, Newport Steel, Page-Hersey; Tenaris Prudential; TexTube Pipe; and US Steel. As such, the list of producers is comprehensive, as is the interval of production.

Considering the evolution of the upset autogenous process and the periods when significant portions of the pipeline infrastructure have been constructed it appears that the trends in Figure 13a are indicative of the proportion of the mileage built using such pipe, and the evolution of both the steel used and the seam processes. Realizing, as made clear earlier, that the steel

used underlies two of the most common causes of failure in upset autogenous welds, advances in steel quality can greatly influence trends in such failures. In this context, the significant improvements that began with the introduction and evolution of the continuous casting process and continued in the mid 1960s as the high-strength low-alloy (HSLA) grades saw broader use are evident in the sharp decline in frequency over that interval.

Overlaid on the benefits from such improvements was work dome to improve the ERW processes, through use of the HFERW and HFI processes, and related developments in sliding contact, and PWHT. The learning curve associated with that could rationalize the spike evident in both datasets circa the 1960s. Another factor that could contribute to that spike are failures in seams due to efforts to ensure pipeline safety as hydrostatic testing and retesting became popular about the same time. The reduced threat level achieved since the efforts circa the 1960s has been maintained since by continued use of these practices, and developments that followed in steel and pipe making since the 1970s. While this includes the evolution of higher-strength grades through use of thermal-mechanical controlled processing (and related variations), it is only recently that X80 grade pipe is becoming available with an upset autogenous seam[15].

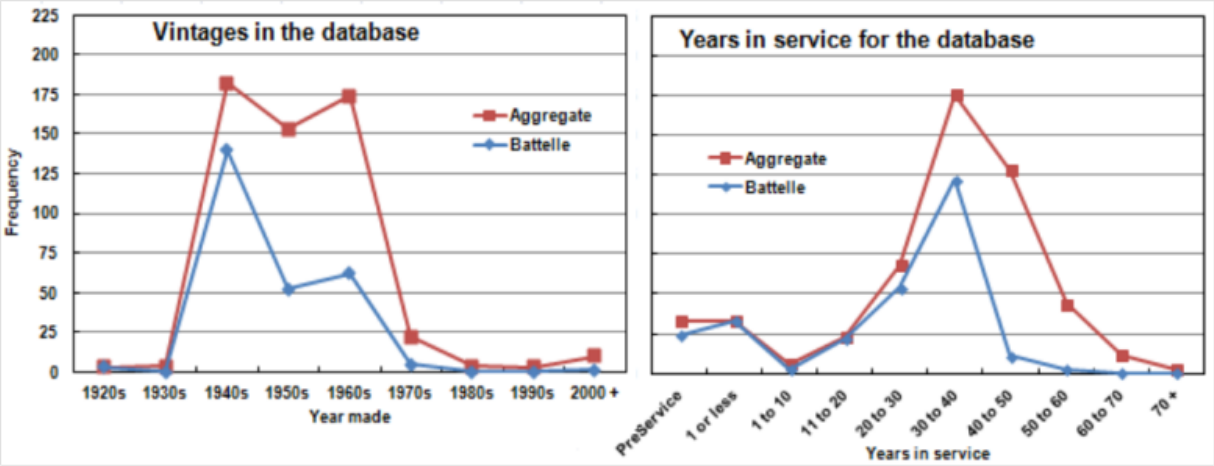

a) year produced for the pipes involved **b) years in service prior to failure**

Figure 13. Comparing trends for the vintages and years in service for the pipes considered

While the trends for production since the 1970s remain low, it should be noted that several failures have occurred in the 1990s and since that are known to Battelle, most of which are not considered herein due to contractual constraints. The point in this context is that while the frequency of failures has declined significantly, vigilance and quality remain essential elements in making quality steel and in producing quality line-pipe.

Figure 13b shows trends for the time in service prior to failure for the available data. As for part a) of this figure, the trends between the two data sets are comparable. Failures in pre-service hydrotesting, which became by an ASME Code requirement that was subsequently mandated by the CFR, as they adopted that code circa the late 1960s, are evident as is what might be termed infant mortality or burn-in. Thereafter, both populations show periods of increasing time in service prior to failing, which for both peaks (after different periods), and then declines. Such trends are common to any failure process, with the eventual decline controlled by the age of the

oldest pipe with upset autogenous welds that remains in-service, and its usage. As is logical, seams that fail early reflect the combination of larger defects that have the poorest properties local to the defects, which are subject to sufficient pressure to activate the defect and promote its growth to a leak or a rupture.

Grade and Failure Pressure

Figure 14a characterizes the available failure data in terms of the grades covered, while Figure 14b presents the range of failure pressures that led to the mix of leaks or ruptures noted above in Figure 11.

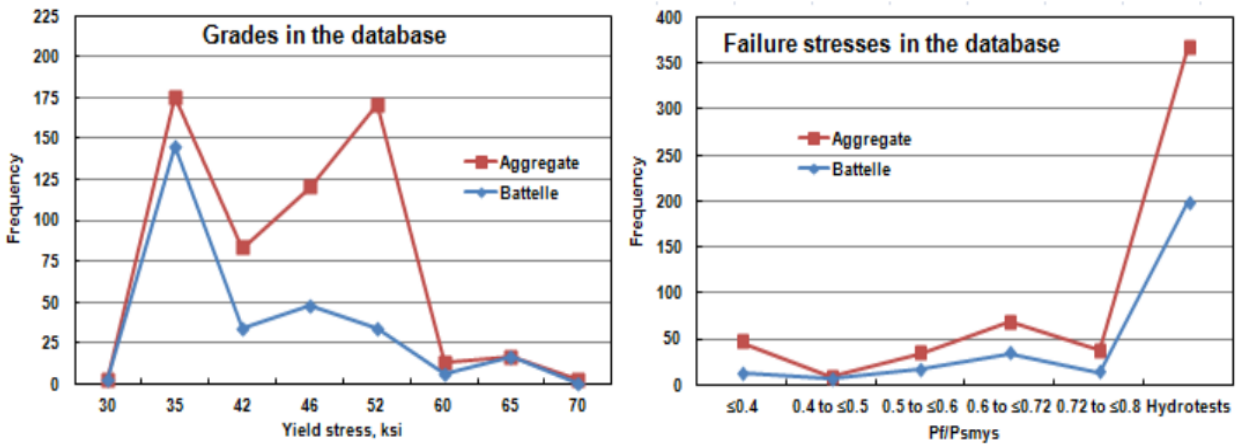

a) grade (as nominal yield stress) **b) failure pressure relative to SMYS**

Figure 14. Comparing databases relative to grade and failure pressure

Figure 14a indicates that failures are available to characterize the response of defects in Gr B up through X70, although the data for grades above X52 are relatively sparse[4]. Battelle's database dominates the results for the Gr B, and with the exception of X52 is in balance with the aggregate trend. The results in Figure 14b show that in-service failures occur from relatively low levels of SMYS, up through the limits of the maximum allowable operating pressure (MAOP), without any clear tendency to increase with increasing operating pressure. However, the pressure dependence of failures becomes clear at pressures associated with hydrostatic testing, as is evident in Figure 14.

Trends and Observations Relative to Battelle's Database

The results in Figures 11 to 14 illustrate the traits of Battelle's database relative to the aggregate database, which reflects results from the Battelle archives coupled with the archives of DNV and KAI. As noted in the section titled Battelle's Archives, those archives reflect reporting that has developed over more than 55 years, spanning from the late 50s through a few months ago. In contrast, the work done by the entities that underlie the joint archives of KAI and DNV reflect

[4] Some sources indicate that X60 skelp became broadly available in the very early 1960s whereas that for X70 dates to the very early 1970s. On this basis, ERW pipe would not be broadly available in Grade X60 until the mid to late 1960s, while that in Grade X70 would not be broadly available until the mid to late 1970s. The earliest evidence of ERW failures in X60 in pipe in Battelle's archives reflects 1967 production, with none evident for X70. That said, other factors related to ERW production of microalloyed steels affect its availability, and likely also its acceptance.

reporting from roughly the mid to late 1980s, and as such could represent a somewhat different cross section of the issues that might develop for vintage ERW/FW seams. In addition, because the issues that can develop with upset autogenous pipe seams differ from operator to operator depending on the pipe's service and operational environment, differences can develop in the trends between archives, such that the trending that follows, and the results and observations that drive the conclusions, are specific to the archive being considered.

Trends in Normalized Failure Pressure

Figure 15 presents results for normalized failure pressure based on the same information shown in Figure 14b in terms of the normalized cumulative frequency of occurrence. The cumulative frequency used in Figure 15 is the sum of all failures up to the indicated pressure, whereas the x-axis in Figure 14b simply groups the data within a pressure interval. Clear trends develop when the data are shown in this cumulative format. Whereas Figure 14b does not indicate a trend up through about 80% of SMYS, Figure 15 shows three distinct trends. The first clear transition in response begins at ~40% of SMYS, at about the 5th percentile. Thus, a relatively small fraction of the failures occurs at or below 40% of SMYS, which remains the case up through beyond 50% of SMYS. While the vintage ERW/FW seam poses a smaller chance for failure at lower pressures, just one incident under such circumstances can open to significant consequences depending on the transported product. Logically, failures that underlie this initial trend, shown as the dotted line in the figure, tend to reflect the larger defects, and can be anticipated to reflect the poorest of properties. Because, as becomes evident later, such features can be exposed effectively by higher-pressure hydrotesting, it is possible to manage this threat.

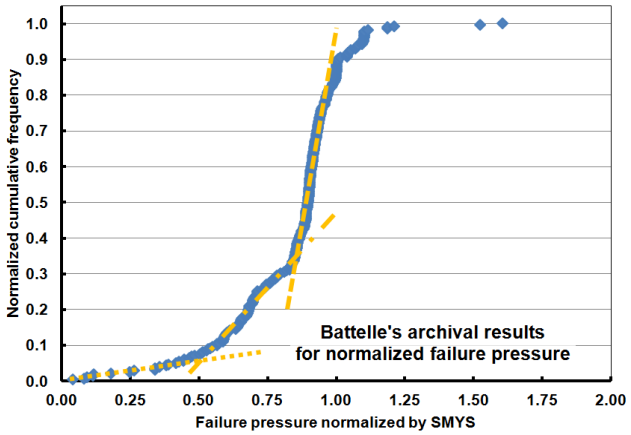

Figure 15. Normalized failure pressure versus normalized frequency (Battelle's dataset)

Beyond the initial trend just discussed there is a second clear trend. This trend is shown in Figure 15 as the dash-dot line. This trend reflects data that cover normalized failure pressures in the interval from about 50% of SMYS up through about 80% of SMYS, which involves roughly 30% of the failures. Inspection of the database indicates that the majority of these failures occurred due to hydrotesting, gas-pressure testing, or hydrostatic retesting. The third trend in Figure 15 (shown as the dashed line) represents about 70% of the failures all of which occur at pressure levels associated with hydrotesting or hydro-retesting, and reflects the clear dominance of the higher pressure bins for the data as grouped in Figure 14b. Thus, the common practice

binning of data in pressure intervals, as was done for Figure 14b, masks the clear failure-pressure dependence of defects formed in autogenous welds, which becomes apparent in Figure 15. On this basis, hydrotests to a sufficiently high pressure can effectively expose the types of defects that are found in ERW/FW seams. This is clearly demonstrated later in analysis that parses the results in Figure 15 by defect type, which quantifies effectiveness as a function of pressure for each of the most common defect types.

Pressure Reversals and In-Service Growth at Defects

While the several trends evident in the Battelle dataset make clear that hydrotesting can be effective in exposing defects in upset autogenous seams, this same database makes clear that this practice can lead to pressure reversals. The term pressure reversal is used to indicate that failure of the pipeline occurs at a pressure less than that achieved in a prior hydrotests of that segment.

Figure 16 presents results from Battelle's database covering a major fraction of the available results for which the circumstances are well characterized and typical of such response. The y-axis in this figure is normalized cumulative frequency which, is shown as a function of the ratio of the magnitude of the pressure reversal normalized by MAOP that typically was close to the maximum operating pressure (MOP).

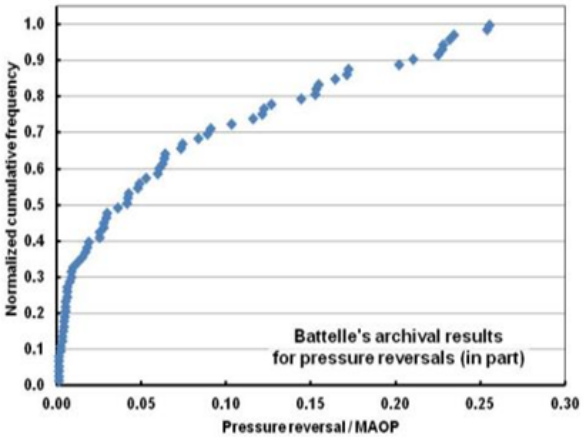

Figure 16. Traits of the pressure reversals in Battelle's database

Pressure reversals can occur upon re-pressuring following repairs made due to a hydrotest failure that occurs en route to achieving the target test pressure in a given test section of a pipeline. They also can occur as the pipeline is pressurized as it reenters service following the pre-service pressure/leak test, or upon the return to service following a pressure retest. The magnitude of the reversal is equal to the difference between the prior maximum test pressure and the pressure achieved with the reversal. As such, the prior hydrotest pressure history for the pipeline section considered, or for some early construction where a gas test was used the prior gas-test pressure history, is essential to quantify the frequency of pressure reversals and their magnitude.

Figure 16 indicates that the majority of the reversals are relatively small, with roughly half of the population considered in this analysis causing a decrease in test pressure less that 5% of MAOP. Realizing that smaller pressure reversals can occur due to subtle differences in test practice and related explanations, and that local properties uncertainty and/or differences are not causative in

regard to reversals, the occurrence of larger pressure reversals the order of several percent and more indicates that the defect population is growing, either in depth, or length, or both. For failures that occur during the pressure test, the growth involves stable tearing, with axial coalescence between adjacent defects likely accounting for the larger reversals. However, the first failure that occurs in a pressure re-test at a pressure below that of a prior pressure test for the test-section, and in-service failures that occur at pressures below that of a prior pressure test, both indicate that some in-service growth mechanism has been active, such as fatigue. Battelle's database includes many of both scenarios, which for the in-service failures particularly in the pipe in service under Part 195 provide clear evidence that a mechanism such as fatigue is active. It follows that while few present SEM images or macroscopic evidence of such growth like that in Figure 9b, such a mechanism must be active.

Defect Size and Shape, and Fracture Behavior

The overall size and shape of defects have been considered in assessing the defect type based on photographic images for the more than 80 reports that comprise Battelle's database. That process indicates such features often are discontinuous both TW and along the pipe. Because they are discontinuous, and realizing the uncertainty in determining the portion(s) of the feature that underlie the reported failure pressure, no attempt has been made as yet to characterize this population in regard to length, depth, or net-section area for present purposes. Suffice for present purposes to outline the complexity and uncertainty in quantifying size and shape. Beyond that complexity, and uncertainty, it must be emphasized that the dimensional metric to quantify defect severity for collapse controlled failure is net-section area. In contrast, when fracture controls failure measures of both length and depth are required to quantify defect severity in what can be a quite nonlinear framework – which renders net-area inadequate.

Issues when Quantifying Size and Shape Based on "As-Opened" Fracture Appearance

The feature shown in Figure 17 is useful to illustrate some of the issues that can arise in sizing what appears to be a rather simple feature when evaluated "as opened". This feature was identified early in a pre-service pressure/leak test of recently produced HFERW pipe. The segment involved was part of a pipe-string that was in pre-test prior to being pulled-in as part of a directional drill. As the pipe was still above ground, the leak became obvious early in the test, at quite low pressure (~30% of SMYS). After receipt at Battelle, the extent of the leak path was identified using nondestructive techniques, after which a coupon that contained the leak path was removed. Saw-cuts were then made into the coupon along the plane of the seam, to near the limits of the feature, which after soaking in LN_2 was wedged opened to expose the leak path. While the saw-cut came very tight to the defect on the left side, as evident in Figure 17, the feature was uncut, whereas an ample margin was present on the right side. While not evident in Figure 17, this defect was found coincidentally within inches of a girth weld (end of the pipe joint), which helped to rationalize its surviving a 10-second mill hydrotest to 90% of SMYS.

The image in Figure 17 shows the fracture as opened, with the OD surface up. Given this defect was found during a pre-service hydrotest, the size of the feature is as it developed during the welding process, but also could include some amount of growth due to the 90% mill test, and/or

the pre-service test. Overall it appears as a single defect, with a length of ~2⅜ inches, while its maximum depth appears to run through the full wall. Characterizing this from a fracture mechanics perspective might idealize it as a TW defect coupled with a rectangular area-based equivalent length somewhat under 2 inches, while for plastic collapse analysis it could be represented in terms of its net-section area. However, whether either is relevant can depend on details hidden by the oxide, and as well as the ability of existing models to quantify such response absent knowledge of the strength across the interface and its toughness.

Figure 17. Fracture surface, as opened: HFERW with t = 0.219" and OD surface up

Cross sections made through the reconstructed fracture after capturing all needed images of the intact surface show that the failure occurred fully within the bondline of the weld. Transverse cross sections made through rings of pipe that lay just beyond the ends of the excised coupon showed that the bondline was free of through or part-through thickness defects, and otherwise sound. Etched views of those sections were typical of modern HFERW – although the HAZ appeared rather broad. These views showed scattered ferrite in the bondline, and the presence of some center-line segregation that did not contribute directly to this failure. While the weld was slightly over-scarf'd, this was minor and well within the wall tolerance.

Examination of the as-opened fracture surface (Figure 17) showed Fe_2O_3 (rust) that over a portion of this fracture surface was overlaid on Fe_3O_4 (magnetite). The rust likely formed during the water pressure test, while the magnetite likely formed as a high-temperature oxide during pipe making. The short length of the feature and the sound welds either side of it suggest the possibility of significant load transfer of the hoop stress around this defect, yet a leak was clearly evident at quite low pressure. The inference is limited strength developed in what is a cold weld (weld-area crack), with a weak bond (if any) forming across this interface.

Figure 18a is a photograph of the mating face of the surface shown in Figure 17 but with the OD surface oriented down, which was taken after cleaning that removed both oxides. Cleaning as done at Battelle includes a polished face on the sample being processed, which provides the means to monitor the process to avoid altering any fine features over the course of the cleaning. From a macroscopic view, the features after cleaning lead to conclusions on defect cause and size and shape comparable to those based on Figure 17. The largely featureless fracture surface appears typical of a cold weld, with small blotchy areas indicating patches where the bond was somewhat stronger than for the surrounding area. While more detailed examination of the features as shown in Figure 18a supports this view over much of the surface of the leak path, small planar features that show clear evidence of failure in response to increasing hoop stress also can be identified, which can be seen in the image shown in Figure 18a, as follows.

Study of Figure 18a in the boxed area toward the right end of the image shows a nearly semicircular thumbnail feature that emanates from the OD, which Figure 18b shows at higher magnification. This area was covered by Fe_2O_3 but did not show evidence of magnetite. SEM indicated a clear difference in the surface morphology between areas that had been overlaid by magnetite as compared to the thumbnail. The fine features indicated ductile tearing within this thumbnail, indicating that it formed due to a process other than that causing the cold weld.

The outer boundary of thumbnail has a length of a little more than ½ inch. While small in absolute terms, this does represent ~20% of the overall feature length measured at ~2⅜ inches during the related failure analysis. In addition to the large thumbnail, SEM showed the presence of a few other smaller thumbnails along the OD. Figure 18b includes three nested indicators that mark the bounds of three crack fronts: the deepest is TW, and the other two mark shallower features. Guided by Figure 18b these fronts can be identified in Figure 18a. SEM study indicated that the smallest of the fronts noted in the image contained other nested but smaller features that like those shown had experienced self-similar advance, such as can be seen for cracking in some steels. If the deepest thumbnail is considered along with its length and overall shape, then this thumbnail feature is responsible for much of the right end of what was characterized based on Figure 17 as a cold weld.

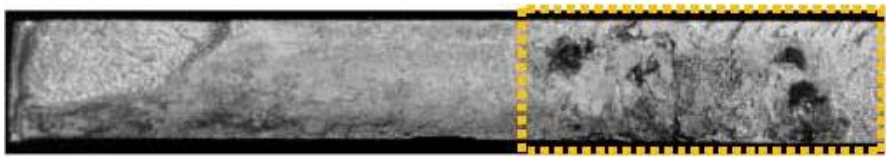

a) view as-cleaned – boxed area is shown below

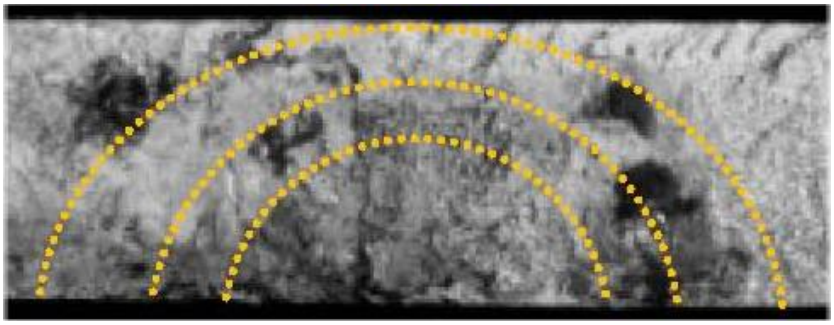

b) boxed area in a) slightly magnified, showing thumbnail shaped crack fronts also evident in a)

Figure 18. View of fracture surfaces, after cleaning (mating face, OD now shown down)

Because this large thumbnail shows evidence of self-similar step growth beyond its initial boundary, this portion of the interface carried load at least early in the mill pressure test, and apparently grew incrementally in size. SEM indicated its origin developed from several smaller adjacent thumbnail features that apparently nucleated due to the stress raiser caused by the cold weld that adjacent to this thumbnail traverses the full thickness. In contrast, the left end of the cold weld transitions gradually into a sound bondline, with the stress local to that gradual transition less than at the near step change in depth to TW at its right (relative to the image as shown in Figure 18. Regardless of the cause of the compound nature of the defect pictured in

Figure 17, the results discussed above indicate that sizing cold welds can be uncertain, not to mention complicated, when based on macrofractographs of dirty and/or oxide-masked fractures.

Practical Significance of Errors Made in Assessing Defect Size and Shape

The key question relative to complications in quantifying defect size, shape, and continuity is: what is their practical significance regarding a) integrity management, and b) the related issues raised in Recommendation P-09-1[(1)] and related commentary and critique[(4)]. Concern was expressed regarding the adequacy of hydrotesting and ILI in support of condition assessment as inputs to determine safe pressure capacity and re-inspection interval. Quantifying safe pressure capacity and re-inspection interval requires predicting the failure pressure as a function of defect size and properties. So the role of defect size is clear – it is a key metric defining condition, along with others like coating quality, adequacy of CP, and so on. It remains to quantify the practical significance of defect size relative to integrity management and P-09-1.

Whether or not inputs to integrity management are adequately quantified depends on the errors they cause in quantifying safe pressure capacity and re-inspection interval. For present purposes, error can be adequately quantified in terms of simple quantitative order-of-magnitude analysis for collapse- and fracture-controlled failure.

For collapse-controlled failures, integrity the predicted failure pressure is proportional to the remaining net-section, which for a TW defect is proportional to the relative defect length. Thus, a 20% error in defect length causes a 20% error in predicted pressure, while a 40% error in length causes a 40% error, and so on. Similar simple analysis for fracture controlled failure requires considering both defect length and depth, and defect shape. For a TW defect in a test section that is wide compared to the dimensions of the defect, the failure pressure is proportional to $[(\text{overall length} / 2)^{1/2}]$. On that basis, and dimensions like those shown in Figures 17 and 18, a 20% overestimate of defect length causes a 44% error in predicted pressure, while a corresponding error of 40% in length causes a 35% error in pressure, with a 60% error in length causes a 26% error, and so on. While this error in failure pressure diminishes as the error in defect length increases, the error remains larger than that for collapse at reasonable error levels.

Whether comparable order-of-magnitude outcomes develop for PTW features can also be quantified. While "simple" analysis in that context becomes much less simple, the outcomes are comparable – even modest errors in length, depth, and net-section area lead to quantitatively significant errors in failure pressure from a practical safety perspective. Errors in defect sizes, shapes, and continuity lead to corresponding significant potential errors affecting re-inspection intervals and the period for safe-service in the event in-service growth is plausible.

It follows that what is often viewed as an estimating exercise to scope defect length, depth, and net-section area can lead to practically significant errors, which in view of the usual process that relies on as-opened fracture features as in Figure 17 can range from misleading to quite unsafe, depending on the purposes of the analysis. In regard to Figure 18, the net-section associated with the cold weld is about 55%; the remainder of this feature apparently nucleated and grew in the mill hydrotest, and caused a reversal when the field hydrotests was initiated. Correspondingly large errors result in the context of predicted response for collapse as well as fracture controlled

failure. Confusion as to the cause of the pressure reversal in the associated pre-service test, and the viability of the pipe and its pressure capacity, gets compounded based on the circumstances (cf. Figure 17), and become clear only after the fracture surfaces are cleaned. While this clearly is a unique scenario, it does serve to illustrate the need to understand what portions of the as-opened fracture features and the related defect(s) control their growth, and failure pressure. Without such, correct failure predictions reflect good fortune much more than good technology.

In summary, errors in predicted length can cause significant errors in predicted failure pressure, which ripples through other aspects of integrity assessment, including analysis of remaining life and the re-inspection interval. These size-characterization errors become even larger when considered in light of other plausible error sources, like seam properties.

Size, Shape, and Fracture Features Typical of the SSC

In the same way that the hook cracking shown earlier in Figure 7d had a uniform consistent depth, if the vee-groove formed by SSC has a uniform appearance on a largely uncorroded OD pipe surface, then its transverse cross section often involves a near constant depth profile. That said, one anticipates a V-groove much like that shown in Figure 19a to exist in relation to the uniform OD surface groove shown in Figure 19b. As for Figure 7d, such SSC features could be easily quantified by length and depth, and characterized using an idealized geometry.

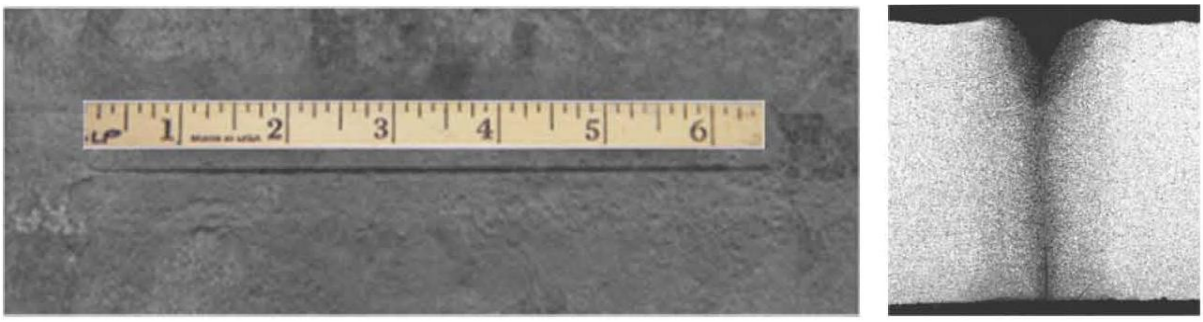

a) OD surface view of uniform SSC x-section: t = 0.312”

b) typical transverse

Figure 19. SCC that reflect uniform seam attack absent significant surface corrosion

While SSC that develops free of significant related corrosion can appear as a longer continuous groove, as in Figure 19, SSC also can be axially discontinuous and show significantly varying groove depths along the V-groove. Such features can occur without corrosion adjacent to the selective attack as shown in Figure 19, but equally can occur with corrosion local to the flanks of the V-groove, creating a much broader groove, and also can involve corrosion on the adjacent pipe surfaces, which for both the groove and the OD surface can be quite asymmetric. Figure 20 presents four views of cross sections made through SSC in pipe recovered from the field that reflect much of what can be found for SSC – with asymmetry between the corrosion on the flanks of the V-groove and the OD surface possible beyond the combinations shown.

The formation of a V-groove due to SSC can trigger failure through the net-section, either by continued corrosion, or collapse- or fracture-controlled failure, depending on the properties of the seam, the hoop stress relative to SMYS, and the length and depth, and the axial continuity of

adjacent grooving, as evident for example in Figure 6a versus Figure 19a. In addition to failure through the root of the V-groove, or through the axial coalescence of adjacent V-grooves, SSC can lead to very localized narrow attack than can develop deep into the pipe wall from the root of the V-groove, creating crack-like features that pose a much greater integrity threat than the V-groove alone. Figure 10 showed a fracture surface that was illustrative of such localized attack into the pipe wall, which is further discussed next in regard to Figure 21.

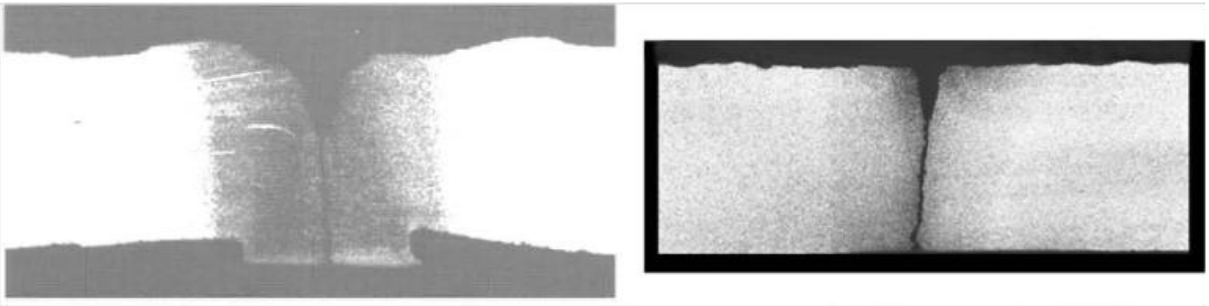

a) broad symmetric V-groove: t = 0.344” **b) narrow symmetric V-groove: t = 0.312”**

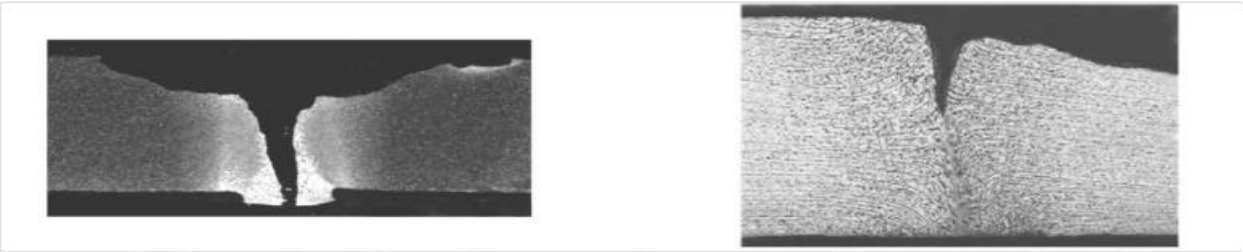

c) symmetric OD corrosion adjacent V-groove full wall at edges of the image is 0.250” **d) asymmetric OD corrosion adjacent V-groove full wall at left edge of the image is 0.375”**

Figure 20. Four variations on the appearance of SSC in LFERW seams in cross-section

a) view as it appears to the unaided eye, with localized attack below a shallow V-groove: t = 0.322”
b) detail along the image in a) showing the full wall

Figure 21. Fracture surface illustrate crack-like features formed via SSC: LFERW

The image in Figure 21a lies along a fracture surface cleaned to remove the rust from what is otherwise fast-fracture associated with a rupture. This feature involves a shallow axial V-groove with segments of localized deeper but narrow attack that create crack-like segments along the root of the V-groove. For the segment of Figure 21a illustrated in Figure 21b at about three times the magnification for the base image, the attack shows a scalloped appearance, suggesting that the growth into the wall occurs locally along the front of the feature. But such behavior is

not always observed, which could reflect a growth stage wherein the attack works to broaden along the leading edge, which fills in between the scalloped attack.

In addition to the SSC as illustrated above, it is plausible for this form of selective attack to occur where strong microstructural gradients develop. While no photographs are available anecdotal evidence indicates that another form of SSC has been observed in YS&T pipe, which has gone through a PWHT. Some cases are noted where a longitudinal groove was reported along the intersection of the PWHT zone and the pipe surface, away from the bondline.

Implications for the Predictive Analysis of SSC

While the discussion of SSC thus far has focused on the complexity that can occur with various types of defect, this section began with discussion that noted some forms of SSC can be easily sized and represented by simple idealized geometries. Reality involved with ERW/FW seams is that some forms of SSC are the easiest to characterize among the defect types that develop in upset autogenous seams. For example, the axial length of the SSC shown in Figure 19a is easy to quantify, while the depth profile for such features is easy to measure via cross sections, as in Figure 19b or Figure 20b, taken sequentially along its length. Depth can be nondestructively sized, provided that crack-like selective attack as evident in Figure 10 or in Figure 21 has not occurred. For features that show a uniform in appearance overall, as for Figure 19a, the depth of the attack is more or less uniform, as is the flank angle of the V-groove. In regard to these dimensionally simple features a net-section can be easily quantified as the basis to predict failure by plastic collapse. While such features appear as rectangles in axial profile, fracture mechanics typically does not deal with defects whose depth is constant, but rather tends to idealize axial profile as semielliptical. However, where the defect is long compared to its depth, other idealizations such as plane strain are possible within the scope of available fracture theory.

For purposes of collapse and fracture analysis, the interface strength across the SSC defect can be taken as zero. Fracture resistance local to such features tends to be determined by that of the pipe below the defect. Accordingly, the choice of properties for purposes of integrity assessment and analysis is relatively straightforward for uniform SSC defects, except in regard to growth rate.

The circumstances for the SCC shown in Figure 6a appear simple, although a number of axially adjacent co-linear features are apparent. Unfortunately, depending on the lengths, depths, and the spacing of such co-linear features, the available technology for collapse and fracture analysis becomes stretched – as solutions applicable to such scenarios[e.g.,30] are limited. Because the extent of solution is limited, assessing integrity can be a challenge.

In summary, the range of SSC features encountered runs from simple through quite complex. While technology to deal with the simpler geometries exists, it does not for the more complex features. As such, implementing hydrotesting and ILI as the basis to assess the integrity of such features can require technology beyond that in hand today. But in that context aspects of the critique noted in regard to P-09-1 could be simply resolved by developing a library of collapse and fracture solutions for the practical range of such features – thereby facilitating viable integrity analysis. Equally, the complexity noted above in regard to the cross sections shown in

Figure 20 also involves a limited practical range of features, such that a library of collapse and fracture solutions also could be developed to facilitate their analysis. As ILI evolves to better detect and characterize all types of seam anomalies, the need for such tools will broaden significantly with the demand to include prioritizing features, and choosing which to dig and when.

Size, Shape, and Fracture Features Typical of the Cold Welds, Hook Cracks, and Related Features

The above discussion regarding sizing complexity, analytical/predictive modeling, and the properties required to support such analysis reflects generic concerns and needs, with these same aspects considered next for the generic grouping of the more common defects that involve cold welds and hook crack origins.

Prior discussion regarding cross sections and photographs of fracture features dealing with cold welds and hook crack origins indicates a similar range of complexity comparable to that evident for SSC. While the scope of the images considered earlier could be expanded significantly to more broadly illustrate the range of circumstances found in service, only a few additional images need be considered to adequately cover what has been observed relative to the usual idealizations involved in fracture and collapse analysis.

As for SSC, for the simplest cases the defects are planar, and can be uniform in depth over their length. For example, Figure 7d showed a simple PTW hook crack origin that appears continuous and smooth both axially and into the thickness. The profile of this hook crack is consistent with the usual rectangular PTW idealization adopted for the analysis of collapse-controlled failure. The shape shown in Figure 7d also is close to the idealization of a PTW defect used in fracture mechanics, although fracture theory idealizes the axial profile of such PTW features as semielliptical, rather than a constant depth (to avoid computational issues). However, where such defects are long compared to their depth, other idealizations exist within the scope of available fracture theory that could approximate the failure response of this defect. While none of the images shown to this point reflect the usual TW idealized profile adopted for both fracture and collapse analysis, they are planar. This is apparent from the image of the largely rectangular featureless cold weld bounded either side by a somewhat stronger bondline shown in Figure 22.

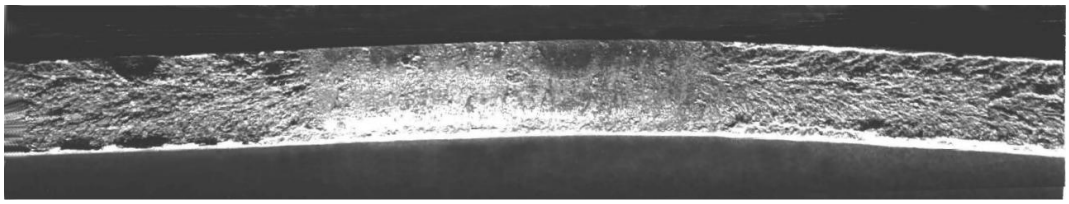

Figure 22. View of a TW, nearly rectangular cold weld: t = 0.312, shown surface OD up

Segments representing a combination of inadequate upset and inadequate heating can appear along a longitudinal FW/ERW seam in a variety of shapes, which can range from a shallow PTW feature to a TW defect. While planar if the defect lies in and along the bondline, such features are anything but rectangular at either end, or nearly constant in depth. Examples of fracture surfaces illustrating this can be found in Figures 3 through 5, 7, 9, and 17.

It follows that the SSC features illustrated and discussed in regard to Figures 6b, 10, and 21a have analogs for both hook cracks and cold welds. But as outlined in regard to SSC, the nature of their complexity is limited in practice by the range of inadequate upset and heating that causes them. So, as for SSC, while the available technology for collapse and fracture analysis falls short of addressing this range of complexity, the critique noted in regard to P-09-1 can be simply resolved by developing a library of collapse and fracture solutions to bridge this gap. As the ranges of generic shapes and sizes needed in regard for SSC parallels many of those needed for hook cracks and cold welds, work done to address SSC needs to broaden marginally to address the threat posed by these types of defects. Finally, as for SSC, as ILI evolves to better detect and characterize all types of seam anomalies, the need for such analytical tools will broaden significantly with the demand to include prioritizing features, and choosing which of them to dig, and when.

The fracture surfaces just noted, coupled with the related cross sections and those shown in Figures 2 and 8 provide insight into the strength and toughness of hook cracks and cold welds. From a regulatory perspective, the longitudinal joint factor for electric resistance and electric flash welded pipe made according to API 5L[31] is one. On that basis, the upper-bound strength across a well made forge-welded seam should be equal (or could exceed) that of the pipe body. In contrast, the views in Figure 3 suggest that the lower-bound strength across a cold weld is near zero, particularly for those that run TW and are featureless over their full length. Other cold welds, like that shown in Figure 3c, are featureless over their full thickness, but only over a fraction of their length. In regard to Figure 3c, it is featureless and so with near-zero strength over only about 30% of its length, and is short enough that the surrounding intact seam will tend to offset this local weakness. Such results suggest that the strength of cold welds per unit area runs from zero, up through near the ultimate tensile strength (UTS) of the steel in the pipe body.

In this context, the strength across a bondline defect reflects the area that is bonded coupled with the quality of the bond – which is expected based on the mechanics of failure. As such, where penetrators like those evident in the oxide fingers shown in Figure 4a are involved, little loss in strength is anticipated unless many such features form in very close proximity. This observation suggests that in an otherwise sound cold weld the presence of an occasional penetrator will become evident only at higher pressures, and so would be found as the cause of a failure much less frequently than a featureless cold weld. Table 1, which documents the types of defects causing failure in Battelle's database and their frequency of occurrence relative to the other major types of defect, supports this expectation.

Table 1. Types of defect in Battelle's database and related details

Origin Type	Cold	Penetrator	Stitched	Hook	SSC	Mill	Total
Occurences	183	4	5	77	16	4	289
Relative %	63.3%	1.4%	1.7%	26.6%	5.5%	1.4%	

Relative Frequency of Occurrence by Defect Type and Implications

Before continuing the above discussion, it is appropriate to indicate how defects were binned in Table 1 for cases where the features considered had the traits of more than one of the defect

types listed, as noted earlier and in regard to API 5T1[(23)]. Determining control of a failure by SSC is clear in regard to the existence of a well formed groove, when no other causative factors are involved. Where other factors such as a cold weld were involved, dominance of SSC was established relative to the severity of the SSC based on the so-called grooving factor[(32)5]. As a value of two or larger is often taken to indicate a threat of SSC (and to indicate susceptibility to this localized attack), cases where this factor exceeded two were taken as SSC – otherwise the other causative factor was taken as dominant. As Table 1 shows, SSC is the controlling cause of failure for about six percent of these failures, but appeared as a factor in several other failures – either alone or in combination with corrosion.

Where SSC was not a consideration, the next clear discriminator used to bin the features was the location of the defect in the seam. This was based on cross sections through the failure, but occasionally cross sections made those through the sound seam at either end of the failure also were considered. Features evident in the sections were evaluated relative to the apparent role of adequate upset and heating, and other potential contributory factors such as alignment, or other mill process aspects. As a PWHT was not part of the process until about the mid-1960s, issues due to inadequate normalizing, or the presence of untempered martensite and high hardness were noted but generally not considered causative – although they would be for HFERW failures.

After considering the features in the cross sections, views of the fracture surfaces were assessed. Fracture surfaces that appeared largely featureless and/or were flat to nearly flat in the cross sections were taken as cold welds – regardless of other potentially causative aspects – because the strength across the bond was dictated by the cold weld. In cases where other factors were noted as causative in the original reporting, these were retained in related commentary. The key to distinguishing a stitched weld from a cold weld was the expectation that a good bond would be periodically separated by a poor bond. Thus, where stitched features could be discerned, but the weld developed little strength primarily because it was in combination with a cold weld, the weld was considered cold. The image in Figure 5b illustrated such a case, for which hints of stitching are apparent but failure is dictated more by inadequate strength more than intermittent strength (i.e., stitching). Battelle's database shows only a few failures where clear evidence of intermittent strength controlled the failure – as illustrated for example by Figure 5a. Because stitched welds show a mix of a strong bond with a periodically poor bond, such features are anticipated to develop reasonable strength across the interface. If the poor bond had zero strength, and the good bond had full strength, then such features would be anticipated to fail at a hoop stress on the order of one-half the UTS for the pipe body. This coupled with the unique electrical upset understood to cause stitching suggests they should occur rather infrequently, which is consistent with the results shown in Table 1.

Cases were noted where material was present in the bondline, such as oxides or inclusions, as illustrated for example in Figure 23. When such features were localized along an otherwise featureless or nearly featureless fracture surface, they were considered secondary as failure was controlled by the cold weld. In contrast, where the bondline was strong in the presence of TW

[5] The grooving factor is the ratio of the (localized corrosion plus the OD general corrosion) to the (the OD general corrosion), and provides a metric of the severity of the depth of the groove.

localized oxide fingers, the failure was noted as a penetrator. Battelle's database shows only a few failures where penetrators affected the bondline strength sufficiently to cause failure in-service or at hydrotests pressure levels – as illustrated for example in Figure 4a. While this database did not show the feature termed a pinhole in API 5T1, their definition involves a shape and size that is analogous to a penetrator such that their failure behavior is likely similar.

a) overview (ID distortion occurred when opening the defect) **b) detail in a)**
Figure 23. Cross-section through a large particle trapped in the bondline: t = 0.219"

To be considered in this report, defects indicated by cross sections to lie outside the bondline had to lie within the upset/HAZ of the weld. While arc burns were evident in several cases, some with cracking, failures were not identified as other more dominant features controlled such cases. Accordingly, all failures that occurred outside the bondline developed in due to weakness caused by pancaked inclusions and/or other impurities in the steel, or the exposure of end-grain that generally also involved pancaked inclusions and/or other impurities – with all initiated within the trimmed portion of the upset. As noted earlier, flow due to the upset turns these areas of weakness perpendicular to the hoop stress. Where EA processes are active, end-grain in the presence of pancaked inclusions and/or other impurities can lead to EA cracking due for example to hydrogen stress cracking. Because the upset responsible for such origins ties to cracking that develops at least initially in the manner of a hook crack, all cases with this origin have been labeled as hook origins. Where EA processes or other factors have contributed, or continued its growth, those factors were noted as secondary. As Table 1 indicates, hook origins were the second most prevalent cause of failure in Battelle's database.

Variations in the strength across hook-crack origins can be anticipated by contrasting the images shown for this type of defect in Figure 7d, which such they can be short and shallow, with that in Figure 24a that has been included to illustrate that hook-crack origins also can be quite long. Figure 24b provides further scope to the appearance of hook cracking, and illustrates complexity in identifying the portion of the crack that is the origin and shows a rather brittle-like appearance.

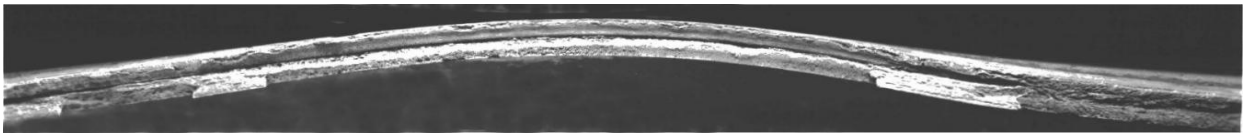

a) longer, rather deep hook crack: DC-ERW with t = 0.312"

b) shorter origin: FW with t = 0.281" – magnified ~x2 relative to part a)

Figure 24. Views illustrating variability in hook cracking

The strength developed across the interface between the pancaked inclusions and/or other impurity varies with the nature of the impurity and its continuity in that interface. This variation in strength coupled with the range of sizes shown indicates failure pressures will run from near zero, thought that associated with failure in the pipe body. Thus, as for cold welds properties

relevant to this type of defect are needed to make viable predictions of failure pressure and remaining life. Growth rates relevant to fatigue clearly are of value, as fatigue is cited in regard to many of the field failures involving hook cracking in Battelle's database – particularly in regard to liquid/products pipelines. As for cold welds, the length of the origin also is a factor, as for shorter features are reinforced by the surrounding intact seam – although this aspect should be embedded in the collapse or fracture solution used in the integrity assessment.

Cases Involving Environmental Assisted Processes

As has been noted in regard to hook cracks, the end-grain exposed in the upset steel when the flash is trimmed has been a source of cracking in association with the environment on the OD of the pipe, or the transported product on the ID. The cross section in Figure 2f shows one illustration associated with what was noted as hydrogen stress cracking. In addition, so-called slot-corrosion has developed within the upset – which as for the other EA-related cases noted in the reporting has been listed as secondary to the upset features that act as origins for hook cracking.

The image in Figure 25a illustrates slot-corrosion as it appeared on the ID, while Figure 25b shows this in cross section that was cut at the location identified by the notation shown in Figure 25a after this image was taken. The view of the ID surface indicates slight corrosion occurred local to the flanks of the slot-corrosion, which has its origins within the upset of the seam. The cross section In Figure 25b includes both faces of this failure, the study of which determined that the origin of the failure lay along the ID of this seam, and developed from this corrosion. Other instances exist similar to this, but because the origin of the failure was not coupled to the corrosion, the presence of this slot-corrosion has not been cited as a factor.

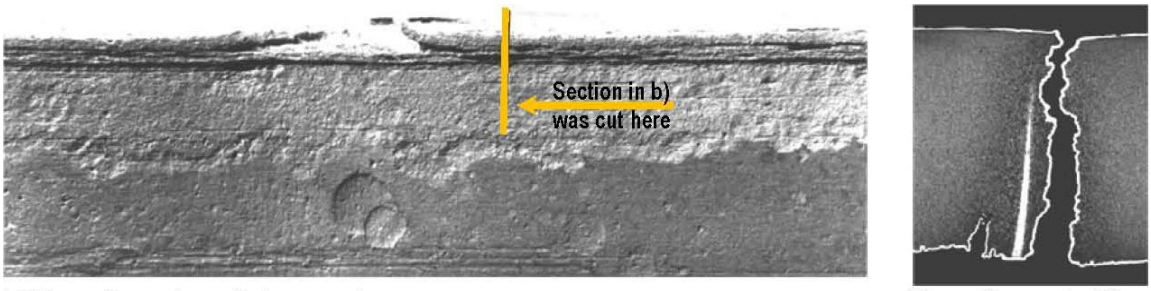

a) ID surface view slot-corrosion **b) section noted in a)**

Figure 25. Slot-corrosion in association with the ID upset: DC-ERW with t = 0.250"

In addition, Battelle has seen SCC in the vicinity of the bondline and upset which occurs along with cracking in the body of the pipe. Figure 26 illustrates this using a cross section through a shallow short crack that lies in the upset to the right of the bondline. The section shown was cut adjacent to the SCC in the upset that triggered this hydrotests failure. As for the other cases where the failure involved an EA process developing from a hook origin, such have been noted as secondary to that defect type.

Failures due to environmental effects either ID or OD were clearly involved in four of the 71 hook cracks involved in Battelle's database. This outcome reflects the sample of failures examined over the decades at Battelle rather than some unique aspect of the FW/ERW processes.

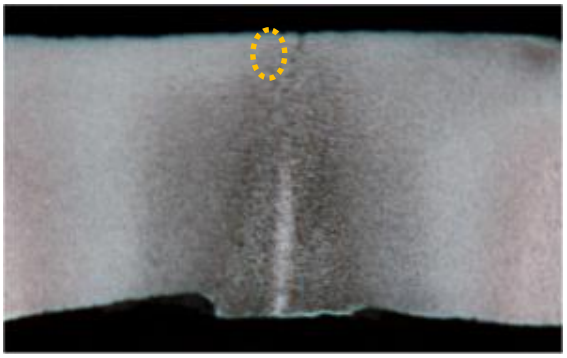

Figure 26. Shallow SCC origin in the upset of a DC-EWR seam: t = 0.250"

Implications for the Predictive Analysis of Cold Welds, Hook Origins, and Related Features

As for SSC, it is apparent that the shapes of cold welds, hook origins, and the other features considered can range from complex through simple, running from PTW to TW. For some of the cases considered, it was clear that identifying the location and extent of the origin can be difficult, as can determining the portion of the defect that was activated to cause the failure. Characterizing the defect's size, and representing the feature's shape using the idealized formats for which solutions currently exist, can likewise be problematic, except for the simplest of PTW and TW defect geometries. For example, the axial length and PTW depth of the hook crack origin shown in Figure 7d is easy to quantify and can be reasonably represented by idealizations for which fracture and collapse solutions exist today. Likewise, the TW nearly rectangular cold weld origin in Figure 22 is easy to quantify and can be reasonably represented by idealizations for which fracture and collapse solutions exist today.

In contrast to the simple cases just noted, the hook origins in Figure 7e and Figure 24b are more difficult to identify and much harder to size; both lack reasonable idealizations for use in predictive analysis. The same can be said in regard to some cold welds and stitched welds. For example, it is not clear where toward the left side of Figure 5a this stitched origin begins, and what idealization is available to represent its response for fracture-controlled failure. Likewise, for cold welds like that shown in Figures 17 and 18 that involve a long run along one of the surfaces, it is not clear how much of this length is relevant to the failure behavior of the defect, and what the best approach is to idealize such features in predicting fracture-controlled failure response. Parametric analyses are needed to identify the best idealizations for such features and establish a library of solutions to facilitate the analysis of such seam defects. Once those aspects are better quantified, the interpretation algorithms and reporting schemes for ILI seam tools should be undated to embed such insights. While it generally suffices to deal with a net-section area for purposes of collapse analysis, the effective width over which to quantify net-section can be a concern for axially oriented features, with the situation being more difficult in regard to fracture-controlled failure, where depth profile also must be addressed.

Review of available collapse and fracture solutions for pipelines shows that solutions do exist for the simpler circumstances. However, most practical cases are anything but simple. In such cases the available technology for collapse and fracture analysis becomes stretched – as solutions applicable to such scenarios[e.g.,30] are limited or do not exist. Because the extent of solutions are limited, assessing integrity in regard to most seam defects can be challenging.

While for SSC the interface strength across the defect can be taken as zero, it is evident from the above discussion that the strength across this interface ranges from near zero for truly cold welds, up through strength of the pipe body for sound welds. For purposes of collapse, this range of strengths can be addressed using concepts like effective area coupled with measures of strength that reflect the type of defect. With that approach, the metric used for seam strength would increase moving from cold welds, up through paste-welds and stitched bondlines, and on to hook origins. Approaches to quantify toughness for use in fracture analysis could use the outcomes of testing focused in the bondline for samples cut from cold welds, or stitched welds, while a measure that reflects testing of sections located off the bondline might be taken as representative for failure through the upset/HAZ of the seam. Where vintage welds are involved absent the PWHT, samples cut from such welds could be indicative of their resistance, provided the correct area of the seam is interrogated in the testing. Further discussion of this practice follows in the next section, where aspects of defect growth rates also are explored.

In summary, the range of bondline and upset/HAZ defects ranges from simple through quite complex. While technology exists to deal with the simpler geometries exists, it does not for the more complex features. Thus, implementing hydrotesting and ILI as the basis to assess the integrity of such defects can require technology beyond that currently available. That said, this limitation could be simply removed by developing a library of collapse and fracture solutions for the practical range of such features – thereby facilitating viable integrity analysis and closing one aspect of the critique noted in regard to P-09-1. As noted in regard to SSC, as ILI evolves to better detect and characterize all types of seam anomalies, the need for such tools will broaden significantly with the demand to include prioritizing features, and choosing which to dig and when. While in the ditch tools can be useful in validating the outcomes of an ILI, they are not relevant to practical detection, and so considered less important to ILI in managing the integrity of ERW/FW seams.

Seam Properties – Strength versus Toughness

Analysis of integrity done relative to collapse controlled failure makes use of strength properties, such as quantified for the pipe body by a transverse flatted strap or round bar, or a cross weld strap in regard to the longitudinal seam weld[31]. In contrast, the fracture theory that underlies predictions of fracture controlled failure relies on measures of fracture resistance. Such metrics typically reflect a measure of the resistance to initiation of cracking, and a measure of the resistance to continued cracking, which are determined from tests of coupons that contain crack-like defects.[e.g.,32] While fracture theory involves properties determined in rather involved experiments[33,34], the pipeline industry has relied historically on testing consistent with the pipe mill to quantify fracture resistance, through use of a Charpy-vee Notch (CVN) specimen and test practice[35].

The microstructure in an ERW/FW seam reflects the base structure of the incoming skelp and its modification by the thermal-mechanical cycle of the forged-weld. It is evident from the various cross sections shown through seams that many different microstructures can form, and that these can depend on the varying thermal-mechanical history experienced throughout the seam. Thus, the properties of the seam needed as inputs to predictive integrity analysis are a composite of the microstructures involved in the vicinity of the origin, which depends on the type of defect, and that encountered along the path taken as propagation continues through the pipe wall, and/or along it. Most critically, it is clear that there can be significant changes in microstructure over quite short distances, such that it is not possible to sample a reasonable volume of material in this microstructural gradient to quantify the highly localized properties.

Currently, there are no standard practices to sample for the strength or fracture resistance of an upset seam, or to quantify rates of in-service growth, for example due to fatigue. However, some exploratory work has been done to assess alternative approaches. One scheme considered to quantify the tensile response across the seam made use of a double-notched tensile strap centered axially about the seam[36], which given its design also provided insight into fracture resistance. Work using cross-weld tensile testing indicates that the mechanical properties for vintage welds show a range of strengths, which run from the rated capacity of the pipe body through quite low levels, depending on the defect type and its relative size[37].

Attempts also have been made to quantify the composite toughness within the seam, through testing that centered the CVN notch in the bondline, or placed it in the upset/HAZ, and/or in the of pipe body[38]. As evident in Figure 27, this CVN practice indicates that the properties in the ERW/FW seam can fall well below typical body data, in regard to both the plateau and shear-area transition temperature (SATT).

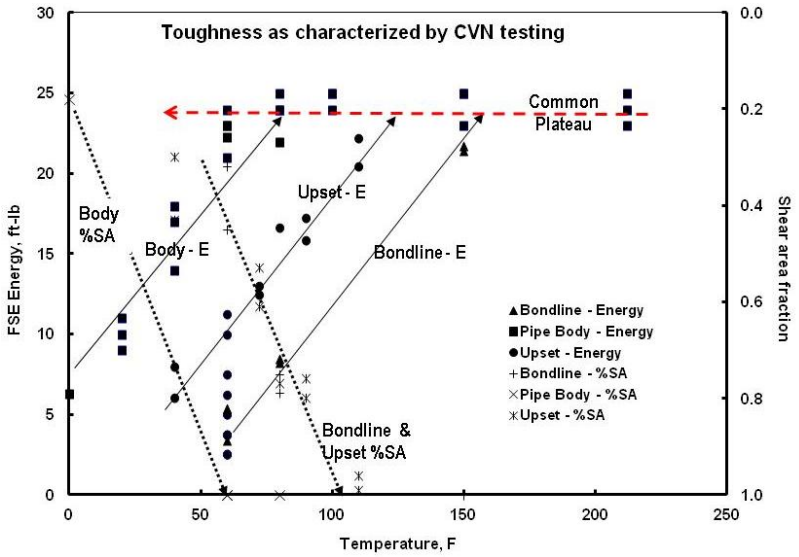

Figure 27. Differences in toughness depending on the location in the seam

Inspection of Figure 27 indicates that as quantified by the CVN test the fracture resistance in the bondline is roughly 50% of that in the upset/HAZ, and about 25% of that shown by the body of the pipe. These results indicate that the upset/HAZ has a fracture resistance that is roughly one-

half of that in the pipe body. It is evident from Figure 27 that values of the full-size equivalent energy in the bondline fall as low as a few foot-pounds. Comparable trends have been developed for this DC-ERW pipe in regard to two additional failure analysis archived at Battelle. Other less extensive studies demonstrate on a much broader basis that ERW/FW seams in general show limited fracture resistance relative to the body of the pipe. While not detailed herein, testing done to quantify the fracture initiation resistance and the stable tearing resistance based on J-Tearing fracture theory are correspondingly low. Figure 27 shows that, as quantified by the CVN test practice that typically shows some scatter, the fracture morphology of the bondline and upset/HAZ are comparable, with a much higher SATT than the body, such that these areas will show more brittle fracture response at in-service temperatures.

Others have explored the fatigue crack growth rate in an ERW seam[39]. While their results indicated that the seam response was comparable to that of the pipe body, records indicate that outcome was largely affected by the use of rather narrow test specimens, the blanks for which were cut adjacent to one another from pipe that contained a shallow hook crack, apparently located well out into the upset. Once coalescence occurred along and over the depth of the hook-crack, the continued propagation of the crack occurred in steel that experienced little influence of the upset and/or the presence of planes weakened by pancaked inclusions. This fatigue crack growth occurred through steel comparable to that of the pipe body, which precludes evidence of step-growth and/or influence of an upset microstructure, as would be expected for a cold weld or other hook crack origins.

In summary, the results of some exploratory work indicate that the fracture resistance in the seam is significantly reduced as compared to the pipe body, whereas cross-weld tensile properties run from the rated capacity of the pipe body down to quite low levels, depending on the defect type and its relative size. Such outcomes indicate the need to quantify these properties if viable predictions of integrity metrics, like failure pressure and remaining life or re-inspection interval, are anticipated, as required to close the critique in regard to P-09-1.

Defect Type and Trends Apparent with Pressure and Time

Consider now trending that quantifies differences in defect response as a function of failure pressure and the time in service, including the role of pressure testing – with such results distinguished by defect type for the four most prevalent types noted in Table 1. This trending makes use of a normalized cumulative frequency with a view to offset differences in the scope of the data available, which for stitched defects is sparse. Note in regard to the trends in Figure 15, which uses this same format, that this trending will produce much different outcomes as compared to the raw results as binned for increasing failure pressure in Figure 14b.

Figure 28 maps the failure response of the major defect types in Table 1 as function of pressure, where pressure is presented on the x-axis normalized by the pressure that corresponds to SMYS. Figure 28 also shows the cumulative frequency for this population in regard to the trend noted as Figure 15.

It is evident from the results shown in Figure 28 that for larger defects (all else being equal), the fabrication related defect origins fail at higher pressure relative to origins that trace to SSC. This

is a quite logical and expected outcome realizing that SSC often occurs in conjunction with OD corrosion. Not only does the OD corrosion reduce the net section and so increase the net-section stress above the nominal level for the full pipe wall, this reduced wall acts to magnify the stress (strain) concentration factor associated with the V-groove[(e.g., see41)]. About 23% of this SSC population fails at pressures less than 50% of SMYS, while almost 75% of this SSC population fails at pressures less than 72% of SMYS. Accordingly, SSC poses a significant threat to in-service pipelines relative to the population of pipe making defects in Battelle's database. This conclusion reflects the unique mix of failures characterized over the decades in Battelle's archives, which dates to the late 1950s. The entities that underlie the joint KAI/DNV database trace to the mid1980s, yet for this database the relative fraction of SSC failures is similar. On this basis it is reasonable to conclude that SSC poses a significant threat to in-service pipelines across a much broader population, and as such merits the same scope of effort in rationalizing defect shapes and sizes, and rates of growth relative to the defects due to pipe making.

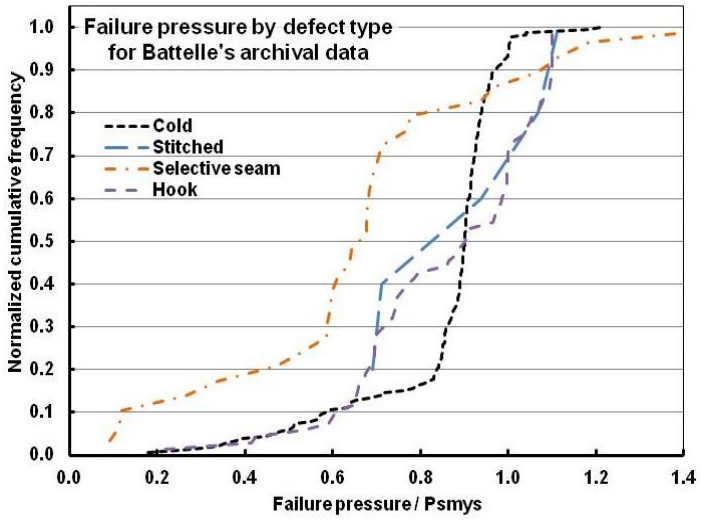

Figure 28. Effect of pressure level on failure at ERW/FW seam defects

In regard to the population of defects due to pipe making, which trace to inadequate heating and/or inadequate upset, and the role of lower quality steel, it is apparent that the largest of the defects (all else being equal) show similar response due to pressure up through about 68% of SMYS, which represents virtually all of the in-service failures – except for those that occurred in lines grandfathered for service at pressures up to 80% of SMYS (to the extent they still operate at such pressures). However, it is apparent that their response to hydrotests differs up to pressures at about 115% SMYS, beyond which the results associated with laboratory and other such studies converge.

The lower tails for hydrotesting that caused stitched and hook cracks to fail at relatively lower pressures apparently represents the longer, deeper features and/or weaker seam properties, whereas the upper tail of this population reflects shorter, shallower features and/or stronger seam properties. In contrast, the trend for cold defects is characteristic of failure populations that involve two mechanisms – with these data suggesting that one controls at pressures less than about 85% of SMYS, and the second controls at higher pressures.

Based on the trends developed for Battelle's database, effective control of the four types of defects requires hydrotesting to a minimum pressure the order of 110% SMYS. The data in Figure 28 indicate that this level exposes 98% of such defects, but is slightly less effective in regard to SSC – potentially because some of this defect-type does not involve OD corrosion, and involves a V-groove that can be quite shallow. In this context, prior hydrotesting to higher pressures on the order of 110% in a test section will remove most defects that pose a threat to integrity. However, as higher-pressure hydrotests open to the potential for pressure reversals, it is essential that the spike test[42], evolved in the early 1990s for the PRCI, be employed to minimize growth in the remnant defect population be used. In that context consideration also should be given to designing/optimizing the pressure-time sequence in regard to both the type(s) of defect known or anticipated to be present, and the steel's flow and fracture properties. One example of that practice can be found in Reference 38, in applications to less-tough seam.

Whereas Figure 28 indicates that hydrotesting to a minimum pressure the order of 110% SMYS exposes 98% of such defects, pressure testing to that level can be impractical where elevation changes and/or other factors are involved. Testing to lower levels can be beneficial, but in such cases a reduced test pressure raises the possibility that more defects remain in the line. While lower pressures can be coupled with longer holds at pressure, which could selectively expose a few more defects, this practice opens to stable tearing of the larger defects, which in turn opens to pressure reversals in the leading edge of that population. As such, care must be taken to broadly understand the cause of the defects likely present in the pipeline – and their response to prior pressure testing. Such information can be gleaned from past failure experience and like-similar analysis of the experience of others with pipe of comparable vintage from the same supplier. It also can come from mill test data, to the extent that such information remains available.

Consider now the trends that emerge in regard to the time dependence of Battelle's failure population, results for which are presented in Figure 29. The structure of this figure is comparable to that of Figure 28, except that it maps trends in time rather than failure pressure.

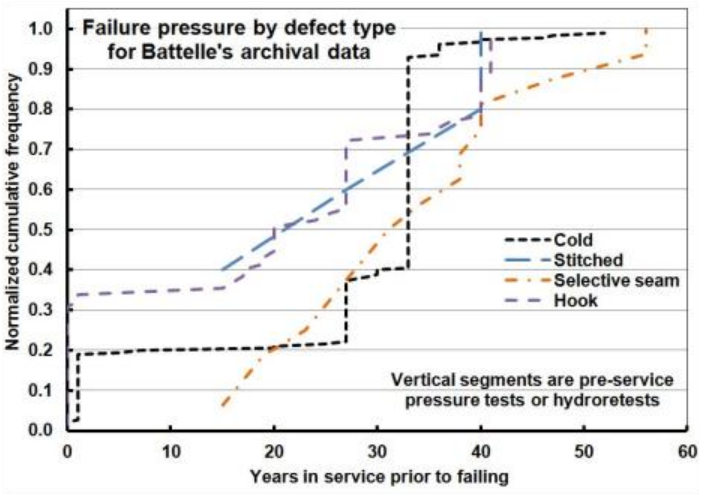

Figure 29. Time dependence of failure at ERW/FW seam defects

As was evident in Figure 28, the trend for SSC shown in Figure 29 is unique in comparison to those shown for defects due to inadequate upset and/or inadequate heating, and lower quality steel. The trend for SSC shows a gradual increase in cumulative frequency that is nearly linear on linear coordinates – beyond about 12 years. This trend indicates that there is an incubation period for this mechanism, which for the population in Battelle's archives required about 12 years before posing an integrity threat. This observation is in sharp contrast to another Battelle study of 68 SSC in-service failures that noted 70% of the failures occurred within the first four years of pipeline installation and 90% had failed within seven years[26]. The nearly linear trend of the SSC failures beyond 12 years indicates that relatively the same number of failures occurred on a yearly basis for that population. This too is rather opposed to the earlier Battelle study that showed the rate of failure dropped sharply in less than 10 years.

Clearly, coatings in use today are much improved over those used historically –both in their consistent application and in their durability. Also, today CP is mandated, whereas until the ASME code addressed CP, its use and maintenance was according to company policy/practice. On that basis, incubation in a practical setting today might involve decades, and would require the coupled failure of the coating in the vicinity of a longer term upset in the CP. Likewise, the development of SSC on pipelines built after the mid to late 1970s would be much slower as compared to the period when vintage systems were bare and unprotected. It follows that the threat posed by SSC noted in regard to Figure 28 tends to be focused in the earlier pipeline construction – particularly that which has a history of SSC.

Consider next trends for the defect types that represent inadequate upset and/or inadequate heating, and lower quality steel. These populations each show the phenomenon often termed infant mortality. This phenomenon is evident in the initial step increase in occurrences that reflect the large number of failures in pre-service hydrotesting, or which caused in-service failures within the first year. This trend is clear for the hook origins and the cold defects, with the trend for the stitched features consistent with the hook origins, as occurred for the pressure dependence. But, while consistent with the infant mortality trend for the hook origins, the data for clearly stitched features are too sparse to determine their response over this early window in time. It is significant to note that effective exposure of these features during pre-service testing involves higher pressure testing – consistent with Figure 28.

The populations for defect types that form due to inadequate upset and/or inadequate heating, and lower quality steel, also indicate the effectiveness of higher pressure retesting. In regard to Figure 29, exposing a large defect population during a hydro-retest is evident in the vertical segments shown in this figure at the same service life. In total, Figure 29 presents the results of six major retest campaigns, with one of these exposing significant numbers of both cold welds and hook origins. This testing involved target pressures for the test sections considered that were in the interval between 100% and 110% of SMYS, with some sections locally going above that level.

In summary, the results shown in Figure 28 indicate that for larger defects (all else being equal) the fabrication-related defect origins fail at higher pressure relative to origins that trace to SSC. On that basis SSC poses a significant threat to in-service pipelines across a broad population of

features, and as such merits the effort to quantify defect shapes and sizes, and rates of growth relative to the defects due to pipe making. However, because coatings in use today are much improved over those used historically and CP is mandated, the effort to manage SSC should be in balance with its diminishing likelihood over the life of the pipeline system.

In regard to the population of defects due to pipe making, it is apparent that the largest of the defects (all else being equal) show similar response due to pressure up through about 68% of SMYS, which represents virtually all of the in-service failures. Beyond the highest pressure for most transmission pipelines, the response to pressure shows a dependence on defect type up to pressures at about 115% SMYS, beyond which the results converge. But, regardless of these differences, the results show that effective control requires hydrotesting to a minimum pressure on the order of 110% SMYS – with 98% of such defects exposed by testing to this level.

It follows that higher pressure tests can be an effective component of pipeline condition assessment in the integrity management plan for operators with ERW/FW pipe in their systems. However, hydrotesting does open to the potential for pressure reversals, such that a spike test design[(42)] should be used to limit their development. Refinement of this practice is possible through use of a pressure-time history that has been optimized in regard to both the type(s) of defect known or anticipated to be present, and the steel's flow and fracture properties.

While higher pressure hydrotesting can be an effective component of pipeline condition assessment, this practice leads to 1) a snapshot in time, which 2) based on Figure 29 exposes most, but not all, of the ERW/FW-related seam defects, and 3) pressure reversals can occur, although their impact can be diminished by an optimized spike test.

Thus, it also follows that alternative detection schemes based on ILI will remain an important element of the condition assessment. The viability of ILI in this context remains an open question, as Battelle's archives involve occasional cases where ILI was done which for one case a seam-related failure occurred shortly after the inspection. The literature also points to concerns regarding the effectiveness of ILI, as outlined in the next major section, which follows discussion of pressure reversals as a function of defect type, the possible effects of aging, and the conclusions to this section dealing with the traits, trends, and observations relative to Battelle's archival database.

Defect Type and Trends in Pressure Reversals

While not discriminated in Figure 16, the larger reversals tended to occur in cases involving hook origins or SSC, as Figure 30 indicates. The hook origins that caused the largest of the reversals for this defect type occurred in pipelines in operation under Part 195 (liquid/products service), and produced ruptures. As noted in regard to Figure 9, the fracture features for such failures either showed clear evidence of in-service growth, which was confirmed via SEM, or there were indications of such a mechanism, but this could not be confirmed conclusively. Hook origins in pipelines in operation under Part 192 also showed large reversals, but did so much less frequently. Hook origins also gave rise to pressure-test leaks, which occurred for both types of service. Prior hydrotest history appeared to be a factor, with reversals being less frequent and often smaller for scenarios where a prior high-pressure test had been done. As for the hook

origins, in-service growth of the crack-like form of SSC also led to very large pressure reversals for SSC, although only three such scenarios exist in the database.

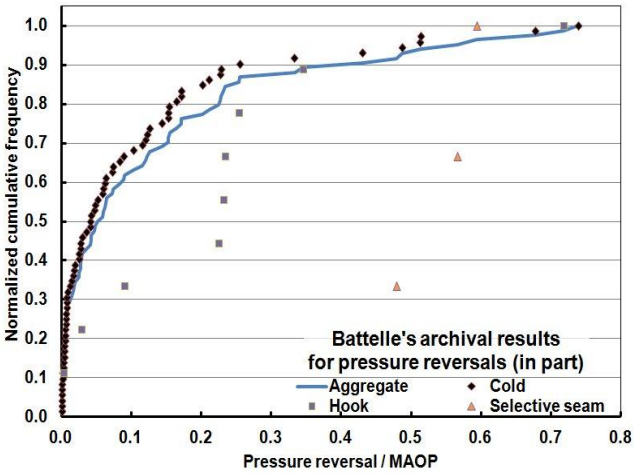

Figure 30. Trends in the size and frequency of pressure reversals by defect type

It is clear from Figure 30 that the sizes of a pressure reversal vary significantly, from very small up through levels approaching the order of MAOP in cross-country service. If, as noted earlier, smaller reversals of less than a few percent are discounted due to possible error in the measured pressure in field tests, it remains apparent that the size and frequency of reversals is unchanged. This trend develops for all types of defect illustrated, covering hook origins, SSC, and cold welds. This trend is anticipated, even for cold welds, because the magnitude of the reversal varies with the amount of growth in the size of the feature – which, in turn, is controlled by the mechanisms driving growth, the range of toughness local to the defect, the axial continuity of the defect leading to possible axial coalescence between adjacent tips, and the pressure that activated failure/instability. While stable growth in-service is easy to rationalize for hook origins and SSC due to the effects of fatigue and selective attack, respectively, cold welds in less tough seams can grow in a pressure test due to stable tearing. Analysis also indicates that such sharp features can grow stably at service pressures, provided the bondline is ductile. In this context, it is difficult to conclude as to what causes a given reversal or its magnitude – unless the circumstances local to the defect involved can be quantified.

Observations on Metallurgical Aging Issues

While the topic of age is often cited in opinions on the integrity of the US pipeline infrastructure, relatively little has been written on this topic that is quantitative. Recent work on this topic by Battelle, done for the Interstate Natural Gas Association of America (INGAA) circa 2004[(43)], developed a quantitative analysis of aging as part of a broader study on the integrity of vintage pipeline systems. While not conclusive, a recently completed web-crawl on the topic of aging in pipeline steels indicates that little quantitative work has been done since; thus the INGAA work remains timely until new quantitative work develops. While Battelle's reporting to INGAA was publically available, the discussion on aging was buried in an annex, such that key aspects of that work are addressed next, followed by commentary specific to ERW seams.

Background to Aging and Related Design Considerations

The following paragraphs evaluate the potential causes for aging relative to typical transmission pipelines operating in liquid/products and gas transmission service. Aspects that involve time-dependent degradation, due for example to corrosion, which could reduce pipeline integrity in the absence of usual maintenance and of from operational upsets are excluded, as these are assessed in other reporting, along with consideration of re-inspection intervals.[(e.g., see 9)] While time-temperature dependent reactions can occur within the steel at sufficiently high temperature, and/or over a sufficiently long time, the circumstances evaluated are specific to the service timeframe and usual operation of a pipeline system.

The working stress design (WSD) philosophy adopted as the basis for the US consensus pipeline design codes in the 1930s[(e.g.,44)] and used since[(e.g.,45)] assumes that design properties for the steel remain constant over the operational life of the pipeline. Reference 46 outlines how this design basis evolved over the years, and eventually was embedded in the regulatory structure. It follows that it is essential to establish the viability of the assumed constancy of these properties to assure system integrity. The WSD design philosophy also assumes that the cross section provided for through design is achieved in the as-built pipeline, and remains effective throughout the useful life of the pipeline. Thus, it is also essential that the pipeline system is adequately maintained. Regulatory mandates[(47,48)] address operations and maintenance (O&M) of pipelines to ensure the adequacy of the cross section provided in design, with industry guidance[(49,50)] developed in support of those mandates. As the O&M aspects are well documented elsewhere, this section considers the time-dependence of the line-pipe properties important from a design and integrity perspective under the assumption that the maintenance is adequate.

Reference 51 outlines WSD as applied to pipelines. WSD is based on elastic response under design conditions and is founded on the long-recognized theory of elasticity, which is elaborated in detail in many textbooks[(e.g.,52)]. According to the theory of elasticity, under simple uniaxial tension, the stress, denoted here S, and strain, denoted here e, are linearly related according to Hooke's law:

$$S = E \bullet e \qquad (1)$$

In this context, the elastic modulus, E, is a constant of proportionality between stress and strain, with Equation 1 representing is the slope of the typical stress-strain curve prior to the onset of yielding. The minimum stress achieved prior to yield is the SMYS[6]. To ensure the response remains elastic in service, and to embed a margin of safety, WSD makes use of a design factor, DF, whose value is less than one, which is applied to SMYS as outlined in Reference 53 in regard to pipelines. On this basis, the maximum design stress (MAS) is defined as:

$$MAS = DF \bullet SMYS \qquad (2)$$

[6] The term strength is typically used in lieu of stress as done here. The term strength in this context is a misnomer given that Equation 1 deals with stress. Yield stress is defined in reference to permanent deformation, and typically is evaluated at an offset plastic strain of 0.002 or a total strain of 0.005. See Reference 50 or related textbooks for further details.

It follows that E and SMYS are key parameters in the WSD basis for pipelines, which must not change with age. The design factor in WSD always has a code-specified value less than 1.0, to ensure that the maximum stress during operation remains safely within the elastic regime. Thus, the DF in Equation 2 provides a margin of safety against unexpected or unusual loading as well as the presence of anomalies. Early pipeline designs used a single design factor[51], while later designs governed by Parts 193 and 195 of the CFR make use of up to three, as follows:

- a longitudinal joint factor that accounts for seam welds that had a higher flaw frequency and ranges from 0.6 for early welding processes to 1.0;
- for gas transmission lines a class-location factor that accounts for population density near the line and ranges from 0.4 for pipelines in heavily populated areas to 0.72 for lines in less populated or rural areas, with an analogous approach adopted for liquid/products lines, which use a value of 0.5 in higher risk areas and 0.72 elsewhere; and
- a temperature de-rating factor, that applies for operating temperatures above 250 F (uncommon because gas and liquid/products transmission pipelines typically operate at temperatures below about 140).

Pipeline integrity can involve material properties other than those associated with WSD, which become important when the wall thickness specified in accordance with WSD is locally reduced due to corrosion or the presence of another anomaly. Potentially important parameters in such situations involve fracture resistance, which is needed for fracture control. As discussed earlier the CVN energy[30] has been used by the pipeline industry for decades to quantify the resistance to fracture initiation and propagation. With respect to fracture propagation resistance, the relationship of the ductile-brittle transition temperature (DBTT) to the pipeline operating temperature also is of interest.

Strain Aging Processes

While several types of metallurgical aging processes can occur, the form of aging that is relevant to pipelines occurs during or after application of a plastic strain – either in pipe making or during pipeline operation. Aging that occurs due to plastic straining is termed strain aging. When it occurs during straining is referred to as "dynamic strain aging"[54], whereas if it occurs after the straining it is referred to as "static strain aging"[55,56]. Both types of strain aging are possible in transmission pipeline steels. Dynamic strain aging favors lower strain rates and requires higher temperatures that facilitate high rates of diffusion that are the order of the strain rate; to be of consequence over the life of a pipeline it would require a temperature the order of several hundred degrees Fahrenheit[57]. Over most of a pipeline system the steel temperature depends on the temperature of the product transported, moderated by the ground temperature. However, locally warm sections exist downstream of compressor or pumping stations, with the discharge temperature typically bounded above by ~140° F. It follows that dynamic strain aging is not a concern, whereas static strain aging can occur in typical transmission pipeline systems.

Plastic strain necessary to promote static strain aging in line pipe steel can occur due to several sources. These include lower temperature steel rolling, pipe forming, and local flow associated with welding residual stress, which are part of steel making and pipe manufacture and pipeline construction. Considering the pipe diameters involved, the plastic strain level developed during

pipe forming is the order of 1 to 2%. Cold expansion that can be used to size the pipe would add plastic strain the order of 1%, depending on the grade and amount of expansion used. It follows that pipe forming could develop plastic strain levels up to few percent.

Plastic strain during construction can occur from welding (localized) and cold field bending. The plastic strain due to cold field bending depends on the angle, but can be taken at about 1.3%. During operation, the likely sources of plastic strain are deformation from outside forces and mechanical damage, which in cases where the strains are larger than that typical in construction usually leads to pipe replacement.

In assessing the strains resulting from pipe manufacturing and construction it is important to note that some develop circumferentially (around the pipe), while others develop axially (along the pipe). While these strains are not simply additive, they can lead to directionally different properties. Following strain aging, the response of steel to strain can be affected by the direction of the additional applied strain with respect to the pre-strain, as discussed in a following section.

General Effect of Strain Aging on Steels

Strain aging is a process that consists of plastic pre-strain and time period at an ambient or elevated temperature. Dislocations are the mechanism of plastic deformation, being generated during flow. They are relevant to aging because they are effective nucleation sites that promote solute precipitation at the dislocation, which occurs through diffusion that in turn leads to the dependence of this process on time and/or temperature. Diffusion leads to concentrations of interstitial solute atoms, such as carbon and/or nitrogen, which act to lock or pin the dislocations and thereby impede their movement. In turn, this leads to changes in properties. For example, because dislocations become locked, an increased applied stress is required to further deform the material.

Strain aging has been described as a four-step process[55,58-60]. Step 1 involves the migration of solute atoms to dislocations, effectively reducing their mobility or locking them. During Step 2, the quantity of solute atoms affecting dislocations increases and precipitates form on the dislocations. The size of these precipitates increases in Step 3, with over-aging occurring in Step 4. Material property changes relevant to integrity that can occur during the different steps of the strain aging process are summarized in Table 2.

Table 2. Aging effects

Mechanical or Fracture Property	Usual Effect	Aging Step Involved
Lower YP elongation (Luders)	Increase	1
Hardness	Increase	1,2
Yield Stress	Increase	1
UTS	Increase	2,3
E	None	–
DBTT	Increase	1
Elongation to fracture	Increase/Decrease	3

Table 2 indicates the stage during the strain aging process when the effect begins to develop. Typically, a yield strength increase, a ductile-to-brittle transition temperature (DBTT) shift to a higher temperature, and increased hardness are among the first detectable effects. Other changes including an increase in the ultimate tensile strength and a change in elongation to fracture occur during the later steps of the process. Unlike the increase for the just-noted properties evident in Table 2, the elongation to fracture results show the change due to strain aging as either an increase or a decrease[58-60], with the amount of change being small in either case. Other design related properties including the CVN energy absorption for a 100% shear fracture decreases during strain aging. None of the strain aging literature reviewed indicated any influence on the elastic modulus[55,56,58,61].

The two main solute atoms typically contained in steels that influence strain aging are carbon and nitrogen. Both carbon and nitrogen influence strain aging behavior since both have a high solubility in ferrite and a high diffusion coefficient, and can readily restrict or prevent dislocation movement. At lower temperatures (<212°F), free nitrogen is the primary solute atom contributing to strain aging. This is due to the fact that at lower temperatures, nitrogen has a greater solubility in the ferrite matrix than carbon. Because the operating temperature is bounded above typically at about 140 F, nitrogen is the primary solute affecting strain aging. Above 212°F, carbon starts to play a role. Carbon can induce strain aging in steels at temperatures above 212°F and may have an effect at lower temperatures depending on the prior thermal history of the material. Very low levels of free carbon or nitrogen are sufficient for strain aging to occur; higher levels result in an increased response[55,56,61,62].

Alloy additions that tend to form stable nitrides (of Al, Ti, and B) reduce the amount of free nitrogen within the matrix, thus reducing strain aging propensity at lower temperatures. Other alloying elements such as V and Nb form stable nitrides and carbides that reduce both the free carbon and nitrogen. If a sufficient quantity of these elements is present, the levels of free carbon and nitrogen are reduced to the point that the strain aging propensity becomes limited but is not totally eliminated[58,59]. Research has indicated that other typical steel alloying elements including silicon and manganese, under certain conditions, can retard strain aging[55,56].

Considering the impact of typical steel alloying elements, strain aging response can also be related to the steel manufacturing method. Steels that have been incompletely or partially deoxidized are more susceptible to strain aging; fully deoxidized and microalloyed steels tend to be less susceptible. Aging susceptibility can be related to the degree of deoxidation treatment and alloying additives in the steel being manufactured. The strain aging susceptibility of several steels used for pipe production is shown in Table 3below, listed in order of decreasing tendency for strain aging.[62-64]

Literature on strain aging research frequently includes data from evaluations of rimmed steels. For pipeline applications, rimmed steels are not of particular interest. Rimmed steels contain little soluble Al or other nitride formers, leaving most of the N in solid solution and thereby available for strain aging. Therefore, they tend to be most susceptible to strain aging.

The other steel types shown in Table 3have been frequently used for line pipe steel production. Historically, most Grade B through Grade X56 pipe was manufactured from semi-killed steels

that typically contained limited amounts of deoxidizers and other alloying elements with resultant higher levels of free solutes. Grade X60 and higher strength line pipe were typically manufactured from killed microalloyed steels that were deoxidized with either silicon, aluminum, or a combination of silicon and aluminum. Silicon killed steels are deoxidized with silicon that can also combine with nitrogen under certain conditions and retard strain aging. Aluminum is a commonly used deoxidizer and also a nitride former thus it reduces the level of free nitrogen[62].

Table 3. Steel strain aging tendency

Rank	Type of Steel
1	Rimmed steels
2	Semi-killed steels
3	Silicon killed steels
4	Aluminum killed steels
5	Silicon-Aluminum killed steels
6	Killed Microalloyed steels (HSLA)

HSLA steels are susceptible to strain aging and exhibit many of the same aging characteristics as plain carbon steels. These steels are typically produced by controlled rolling and cooling and contain additions of V, Nb, Ti, and other elements for development of higher strength through solution and precipitation hardening mechanisms. It has been found that strain aging activation energy for HSLA steels is higher than for killed or semi-killed steels so strain aging occurs at a slower rate. It should also be noted that in addition to HSLA steels, other steel types shown in Table 3including some semi-killed steels that were produced in the mid 1960s and later also may have contained Nb or V additions or both[58,61,65,66].

In addition to the effects of steel composition discussed above, other variables including the pre-strain direction and level, aging temperature, and prior material condition can influence strain aging response. The relationship of pre-strain direction prior to aging to the direction of any additional strain does affect material response. A material pre-strained, aged, and then loaded in the same direction will exhibit a comparatively rapid return of the lower yield stress. Where the same material is pre-strained in compression or in tension perpendicular to a subsequently applied strain, the lower yield stress return is delayed. However, other properties including ultimate tensile strength and elongation are not affected by this strain direction relationship. It has also been shown that amount of tensile pre-strain (on the order of 2 to 7%) does not have a significant effect on that amount of yield strength increase[55,59].

Data from strain aging evaluations have indicated that steel property modifications can result from straining and aging. Pre-strain prior to aging can cause a significant proportion of the total change. This includes a significant fraction of the DBTT shift to higher temperatures that occurs in plain carbon and HSLA steels[55,58].

Quantifying Strain Aging Effects on Steels

Different test procedures have been used to evaluate the extent to which strain aging affects a change in the property that involve impact (CVN and similar), hardness, and tensile results. Strain aging experiments often are conducted at elevated temperatures and high pre-strain levels to accelerate the process. Such temperatures are generally well above that experienced in-service, which means the results of such experiments must be transformed to quantify the response at lower aging temperatures and/or equivalent aging times. Methods based on the Arrhenius relationship have been developed as the means to assess the extent of strain aging under conditions that differ from that of the experiment.[(e.g.,55,67)]

Two of the methods that can be used to equate the results of strain aging evaluations to lower temperature equivalent aging times are shown as Equations 3 and 4. Equation 3 is only applicable to rimmed or plain carbon steels and should be used to predict the effect of aging temperature after application of a defined pre-strain. It is also based on the assumption that nitrogen is the major active solute and that the solute concentration does not change with temperature. In addition, Equation 3 does not account for the effects of carbon that can contribute to the aging effects at temperatures higher than 212°F. Strain aging response estimates from tests conducted at higher temperatures can be a combination of nitrogen and carbon diffusion and precipitation. Therefore, the strain aging response indicated by such data may represent a more extreme effect when compared to typical pipeline operating temperatures[(55,67)]:

$$\log\left(\frac{t_r}{t}\right) = 4000\left[\left(\frac{1}{T_r}\right) - \left(\frac{1}{T}\right)\right] - \log\left(\frac{T}{T_r}\right) \quad (3)$$

where:

t_r = equivalent aging time at lower temperature;
t = time at aging temperature;
T_r = lower or room temperature (K);
T = aging temperature (K).

For other steels with different strain aging activation energies, similar equations have been proposed to equate different temperatures and times required for aging following a pre-strain. For instance, Equation 4 has been proposed for application to HSLA steels as follows[(66)]:

$$\log\left(\frac{t_r}{t}\right) = 7500\left[\left(\frac{1}{T_r}\right) - \left(\frac{1}{T}\right)\right] \quad (4)$$

Equation 4 is valid up to 400 F aging temperatures and uses the same terminology described above for Equation 3.

Evaluation and Trending of Data on the Effects of Strain Aging

Strain aging data from the literature has been reviewed and trended to evaluate and illustrate its expected effects on pipeline integrity. The available data represent a wide variety of carbon steel materials subjected to various strain aging treatments. This review has focused on data illustrating the performance of carbon steels subjected to pre-strains less than 5% and lower

temperature aging conditions, as these are relevant to strain aging as it might occur in a transmission pipeline system.

An evaluation described in Reference 68 included data from a semi-killed, low carbon steel that was partially deoxidized with silicon the results for which are shown in Figure 31. The material was pre-strained between 2.3 and 18.5% followed by aging at 250°C for one hour. Although the aging temperature is high in reference to transmission pipeline systems, the lower end of the range of pre-strains evaluated is similar to that for line pipe.

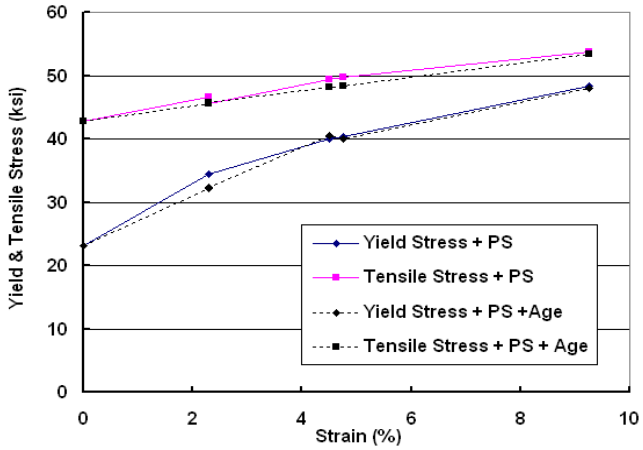

Figure 31. Strain aging data compiled from Reference 68

Figure 31 illustrates the variation in yield and tensile strengths due to a 2.3 to 9.25% pre-strain and pre-strain plus an aging treatment. The yield and tensile response shown at zero percent strain represents the initial material properties. The upper trend in this figure reflects circumstances where the pre-strain alone accounts for the apparent increase in yield and tensile strength. Where straining is coupled with subsequent aging, the benefit in increased mechanical properties is slightly decreased, as evident in the lower trend in Figure 31.

The effect of long-term aging (21 years) at room temperature on an aluminum killed steel following a 0.5% temper rolling treatment as described Reference 69 is illustrated in Figure 32. It is evident From Figure 32 that the results lie within the scatter-band typical of the test practice, with such data showing no change yield strength, tensile strength, or hardness variation over this 21-year interval. While for this set of experiments the percent elongation (not shown) did increase slightly during this period, other data reviewed indicate that percent elongation does not show this trend consistently, but rather indicate no significant differences[(e.g.,60)]. The observed independence over the 21-year test interval is not a surprise, as rated of diffusion that drive the underlying processes are inconsequential under these pipeline-like test conditions. While this means that the slight benefits that accrue under higher temperatures do not develop for pipeline systems, it also means that key properties do not degrade with the age of the system.

One of the more extensive evaluations of line pipe steel strain aging behavior[(59)] was conducted by United States Steel (USS). The objective of their evaluation was to determine the effects of heating cycles from application of fusion bonded epoxy coatings on line pipe. A 3% pre-strain was used to simulate the pipe manufacturing induced plastic strain in large diameter double submerged-arc welded (DSAW) line pipe formed by the U-O-E process[(60)].

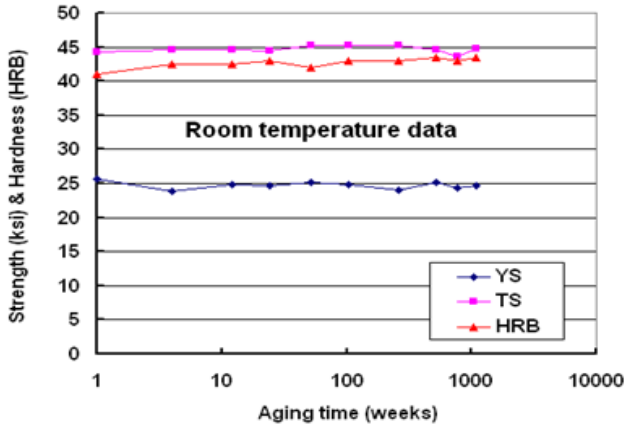

Figure 32. Room temperature strain aging data compiled from Reference 69

The USS evaluation was comprehensive, covering the different types of steel listed in Table 3, except for rimmed steel – with seven fully killed and semi-killed steels, including several containing microalloying elements Steels were finished in the hot rolled condition (1800F) using two controlled rolling schedules that involved 1550 or 1330 F as a finishing temperature. Aging was conducted at 250 F and 475 F (0.5 hr.) with the latter temperature included to simulate fusion bonded coating applications. Data collected included yield strength, tensile strength, elongation, reduction of area, CVN upper shelf energy (USE), and CVN 50% SATT.

Figures 33 and 34 present comparable dataset generated as part of the USS study that illustrate the extent of aging effects on steel, including those used in vintage pipelines. Figure 33 presents results for a semi-killed plain carbon steel, while Figure 34 deals with a Si-Al killed steel. In all cases results for the as-rolled (AR) condition are contrasted to the effects of pre-strain, whose effect on steel fracture resistance characterized by several different resistance measures is well known, as is the effect of pre-strain on integrity and integrity management of pipelines. Thereafter, the effects of aging are presented in contrast to un-aged, with results presented for aging at either 250 F or 475 F[7].

Figure 33a illustrates the dependence of yield and tensile strength for the semi-killed plain carbon steel finished by hot rolling at 1800 F, contrasting the as-rolled (AR) condition to pre-strain without aging, and then following aging at either 250 F or 450 F. The tensile stress was essentially unaffected by pre-strain or after aging. The yield stress can be seen to increase due to pre-strain and thereafter, to a lesser extent, due to the subsequent aging even for the higher temperature. The variation of CVN USE and 50% SATT for the same semi-killed steel are shown in Figure 33b. A reduction in CVN USE is evident due to the effects of pre-strain that accounts for more than half of the overall reduction when the effects of aging are included. This difference in energy is of the same order as the typical variability in this parameter within a joint of pipe; consequently, such differences are not of great practical significance. The CVN 50% SATT increased somewhat beyond that due to pre-straining, but again such differences are not of great practical significance in contrast to variability within a pipe joint.

[7] As noted earlier, aging at 250 F involves a temperature well above that encountered in transmission pipeline service.

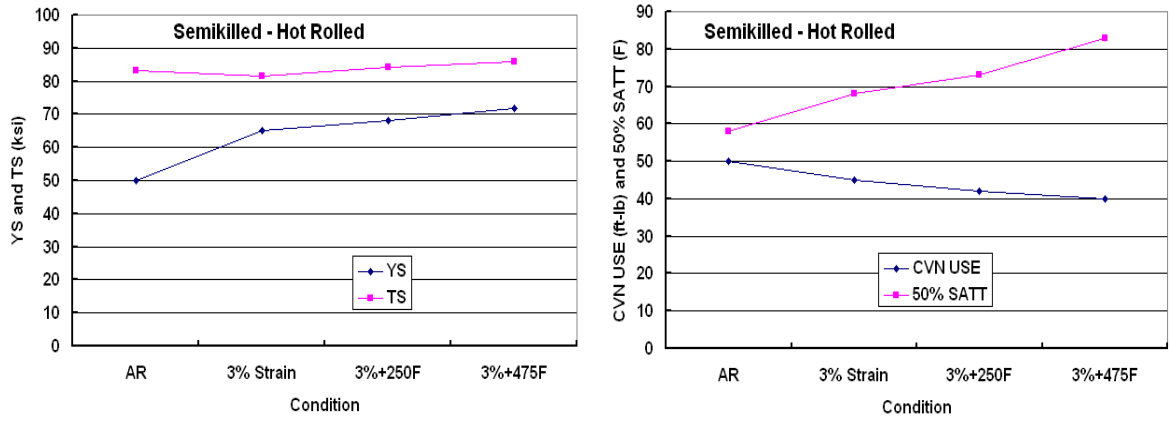

a) variation in yield and tensile stress **b) variation in CVN energy and SATT**

Figure 33. Effect of pre-strain and aging on a semi-killed hot-rolled steel

All steels evaluated that are typical of those available to vintage construction show trends in yield and ultimate stress comparable to those shown in Figure 33a. While similarities exist in stress response with pre-strain and aging, significant differences are evident in the fracture resistance in comparison to that in Figure 33b. This is evident in Figures 34a and 34b, which present results from a Si-Al fully killed steel included in the USS evaluation.

Comparing the trends in Figures 33a and 34a indicates that the tensile stress for both is largely independent of thermal or mechanical history. The yield stress for the controlled-roll steel shows the expected effects of strain hardening, as evident in the increase due to the pre-strain. Aging results in a further beneficial increase in the yield stress as compared to SMYS.

As shown in Figure 34b, CVN USE changes little in reference to typical scatter in a joint of line pipe, while the CVN 50% SATT shows an increase with pre-strain, and subsequent aging has less effect. But, regardless of the change in SATT, the temperature remains well below typical service temperatures for cross-country pipelines.

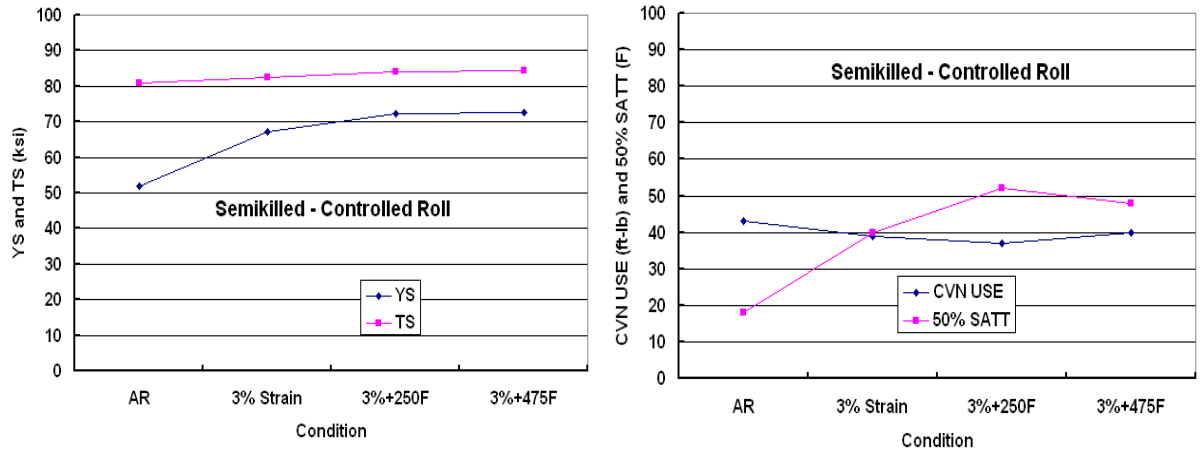

a) variation in yield and tensile stress **b) variation in CVN energy and SATT**

Figure 34. Effect of pre-strain and aging on a Si-Al killed controlled-roll steel

Figures 33 and 34 represent two of the seven steels included in the USS study and also reflect two of the six rolling schedules considered. This study included results for yield and tensile stress in addition to elongation, reduction in area, CVN USE, and CVN 50% SATT[8]. Of these parameters, yield stress is central to pipeline design, while elongation or reduction in area serve as measures of fracture initiation resistance in the same manner as CVN USE via correlation to parameters like J-integral, and CVN USE and CVN 50% SATT serve as measures of fracture propagation resistance.

The yield stress as well as the tensile stress for all cases behaved as the trends shown in Figures 33 and 34. In no case was the yield stress after pre-strain and aging less than the initial yield stress; in most cases the resulting yield stress after this history was significantly larger than the initial value. Results for elongation, reduction in area, CVN USE, and CVN 50% SATT are somewhat more complex in their behavior. Only the data for reduction in area are addressed, because the trends for elongation and reduction in area were similar, as anticipated. Figure 35 summarizes these results in terms of the cumulative distribution of percent reduction and CVN USE, in parts a and b, respectively, with that for the 50% SATT not shown because its trend parallels that evident for CVN energy. Each part of this figure presents the cumulative frequency on the y-axis and the corresponding parameter value on the x-axis. In each case the figure contrasts the result after the pre-strain to the corresponding result after the hold-time at 250°F, which represents an upper bound to the circumstances that might occur in pipelines relative to thermal aging. Results for the pre-strain condition prior to aging are shown as the open squares in each view, while the results after the hold at 250°F are shown as the + symbols.

Figure 35a shows the results for percent reduction in area, which here serves as a surrogate for total fracture resistance. In the format of this plot, values of area reduction that are less than that prior to the hold time indicate a reduction in fracture resistance. In many cases the result is unchanged by the aging, while in others it increased or decreased slightly. As the variation shows no clear trend and the scatter is the order of that typical in this parameter, the data do not indicate aging has a detrimental influence on fracture initiation resistance assessed in terms of this surrogate.

Consider now Figure 35b which presents results for CVN USE, which can serve as a surrogate for fracture initiation resistance, and is used a measure of fracture propagation resistance. In the format of this plot, values of CVN USE that are less than that prior to the hold time indicate a reduction in resistance to fracture initiation. The figure shows that in many cases the result is unchanged by aging, while in others it increased or decreased slightly, the extent to which is well within the scatter typical of this parameter. As the variation shows no clear trend and the scatter is the order of that typical in this parameter, the data do not indicate aging has a detrimental influence on fracture initiation resistance assessed in terms of this surrogate, or fracture propagation resistance. As the trend was the same in regard to results for 50% SATT, which is a measure of the transition ductile to brittle fracture, there was no apparent influence of aging on fracture mode.

[8] That modulus is not considered points to their awareness that it is independent of such effects over their range of interest

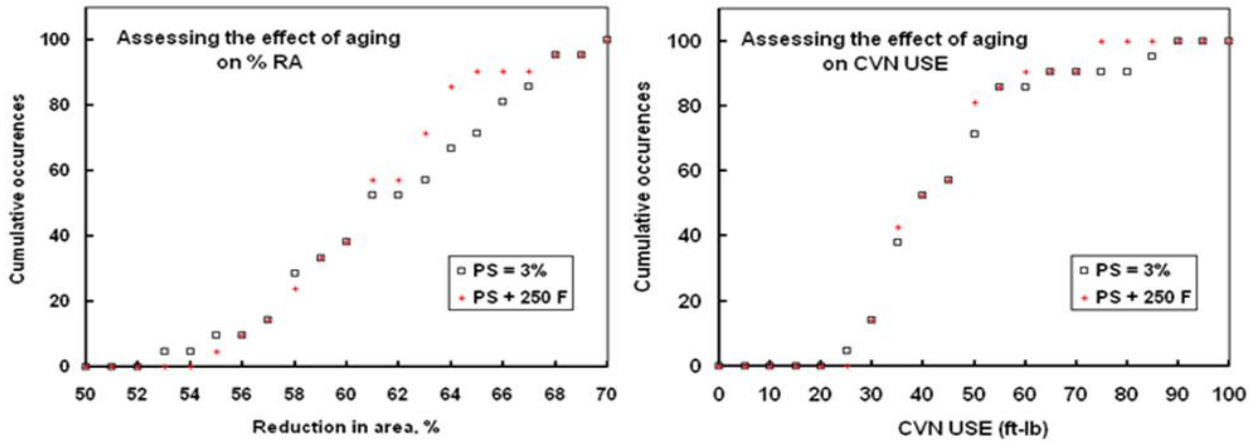

a) variation in reduction in area **b) variation in CVN USE**

Figure 35. Effect of aging for seven steels

In summary, the results for the comprehensive USS steel study of aging effects leads to similar trends across the full range of steels and rolling schedules considered, as follows:

- Yield strength increased with pre-strain
- Pre-strain alone accounted for the same incremental increase as due to aging, or more
- Tensile strength either remained essentially constant or increased slightly
- The CVN USE was largely invariant of aging at 250 F
- The CVN 85% SATT increased, but even then was below the operating temperatures experienced in cross-country pipelines
- Ductility was largely invariant of aging at 250 F.

Effect of Strain Aging on ERW Seam Integrity

The strain aging data reviewed in regard to WSD indicate that pre-strain and aging would not show an adverse effect on the properties of vintage or HSLA based line pipe steels when considered relative to the plastic strains developed in pipe making. Changes in three properties have a potential impact on fracture resistance also were evaluated, to assess the extent these important metrics for integrity assessments are influenced by aging. Data trends show increase in DBTT, with a modest decrease in both CVN USE and elongation to fracture – although that evident is within the scatter shown with these testing practices.

While the above conclusions are relevant to the pipe body, the upset that forms in making an ERW seam involves locally smaller curvature, which leads to correspondingly higher plastic strain as compared to that developed in cold-forming the pipe body. ERW seams also involve exposure to locally higher temperatures, although for a very short period (as evident by the rapid cooling leading to the untempered martensite evident in many of the cross sections). However, even though these upset strains are very high, they develop through hot-work, rather than cold-work, and so are not a driver for aging. Experience developed in viewing the microstructures in cross sections of vintage seams today supports this view, because such sections today show the same traits evident since such seams were first characterized at Battelle in the late 1950s.

It follows that aging constitutes a comparatively minor concern, with any change due strain aging being a second order effect on the flow and fracture properties relevant to pipeline integrity. Consistent with this, the authors are not aware of any pipeline failure attributable to strain aging effects on an in-service transmission pipeline.

Modulus of Elasticity

As noted earlier in reference to Equation 1, the elastic modulus is central to pipeline design. The value of the modulus of elasticity is determined by atomic binding forces and the crystalline structure of the material involved, which is steel for transmission pipeline systems. These binding forces and crystallography cannot be changed without modifying the basic nature of the steel. For this reason, within a given class of materials, such as steel, the elastic modulus is among the most microstructure invariant mechanical properties. It can be marginally affected by alloying additions, heat treatment, and cold work. Other factors including crystallographic defects such as vacancies, dislocations, or polycrystalline features like grain size also have a minimal effect on the elastic modulus[70-72].

Depending on their concentration, alloy additions in solid solution with alpha iron can either increase or decrease the elastic modulus. However, at the levels typically used in steels, such changes are minimal. For instance, heat treated alloy steel may have a higher elastic limit and yield strength but the elastic modulus is the same[57,73].

In summary, this review indicates that strain aging can affect material properties, but detrimental effects if any occur at aging temperatures well above that for transmission pipeline service. The trends noted above lead to the conclusion that aging is unlikely to be a factor in the performance of vintage pipelines. It was evident in regard to the design parameters that underlie WSD that E remains unchanged by aging and that the yield stress is not adversely affected.

Important Conclusions Regarding Traits, Trends, and Observations

As evident above, the results of that subsection section lead to several key conclusions, which like the prior subsection, were noted in summaries that followed each of the subsections. The more significant of these follow:

1. The available literature indicates that the age of a properly maintained pipeline system does not adversely affect key design parameters, such as the modulus of elasticity, the yield stress, the UTS, and toughness as quantified via the CVN test.
2. High-pressure hydrotesting to pressures the order of 110% of SMYS effectively expose most ERW/FW seam defects that are a threat to pipeline integrity; testing to lower pressures is marginally less effective down to about 100% of SMYS, below which the practice can be much less effective.
3. Defect response to increasing pressure for a given pipe geometry in a pressure test and its failure pressure then or in-service depends on five factors:
    a. the feature's overall size and its axial and out-of-plane continuity with adjacent feature(s),
    b. the mechanical (flow) and fracture properties local to the axial tips of the feature,

c. the pressure-induced hoop stress (which can in some service scenarios act in combination with other hoop-oriented stresses) relative to SMYS,
d. whether the feature is blunt as occurs for penetrators (and by analogy those termed pinholes as defined by API 5T1) or sharp as is typically the case for cold welds, weld-area cracks, and hook cracks, and some stitched welds and SSC, and
e. the mechanism(s) driving growth, including possible axial coalescence between the tips of axially adjacent features.

4. For the small percentage of historic seam defects not exposed by hydrotesting, analysis indicates they are short and typically shallow; these cannot be assumed to be benign without cause, such that condition assessment consistent with the stated gas-industry goal of zero incidents[74] requires an alternative/supplemental practice to pressure testing to fully quantify condition.
5. Higher-pressure hydrotesting opens to the threat of pressure reversals through the stable growth of the defect population not exposed by a given pressure test; like the small percentage of seam defects remaining as noted in the 4th conclusion, this requires an alternative to pressure testing for the goal of zero incidents to be achievable.
6. Any defect type whose size and local properties lead to growth due to the applied pressure or service conditions noted in the 4th conclusion can lead to a pressure reversal. Of the defect types that historically have been an integrity threat (listed in Table 1), only the feature termed a penetrator (and by analogy in shape and size that termed pinhole in API 5T1) are likely not to experience a pressure reversal.
7. Except for penetrators (and by the just-noted analogy, pinholes), which as defined in API 5T1 are physically small blunt features, all other defect types listed in Table 1 have failed at in-service pressure levels, and thus can pose an integrity threat to an operating pipeline.
8. Repeated hydrotesting can be effective in exposing ERW/FW seam defects that have grown in-service; however, as noted above, the possibility remains that even after a higher-pressure hydro-retest defects remain that pose a subsequent threat. Prior work[e.g.42] indicates that shorter (deeper) features as well as shallow features can remain.
9. Pressure reversals have occurred, which while minimized through a spike test whose concept and design dates to the early 1990s[42], opens to improvements based on the parameters determined then; thus, the optimum hydrotests that emerged then should be reassessed relative to the development of stable tearing from the types of defects relevant to ERW/FW seams.
10. In service growth was evident in the observation that hydro-retesting has caused failures at a pressure below that of a prior pressure test for the test section. The scope of the failures indicated such growth can occur due to fatigue, SSC, HSC, and SCC. Of these, growth rates been quantified only for SCC, with relatively less work done for SSC, HSC, and fatigue. Given that the threat due to HSC and SSC can be mitigated by maintenance and other controls, whereas managing fatigue impacts operations, further understanding of the fatigue failure process might open to management schemes not yet considered practical.

11. While too little information is available from the work Battelle has done to quantify conclusions regarding the utility and effectiveness of ILI in detecting or sizing ERW/FW seam features, one failure is known shortly after an inspection. Such events point to uncertainty in regard to effectiveness, and thus indicate that further related work is warranted.

While potentially useful guidance can be gleaned from the details, the interdependent complexity evident in the five factors noted above in Point 3 to control defect response to pressure in the fourth conclusion above suggests such generalizations might be dangerous. In succinct terms, these five factors are: 1) defect size and shape, 2) whether the defect is blunt or sharp, 3) the local mechanical and fracture properties, 4) the local stress, and 5) the mechanism(s) driving its growth. Suffice it to note that only the short and blunt nature of the oxide-filled penetrator makes it less a threat to integrity that the other features. However, the fact that API list of defects includes the pinhole, which can result from the breakdown of the oxide in a penetrator, warns against that specific generalization because a pinhole is a leak path. That observation coupled with the fact that all other defect types listed in Table 1 have failed at in-service pressure levels, and thus can pose an integrity threat to an operating pipeline, precludes a list of generalizations in regard to aspects such as the range of SMYS causing failure, the nature of pressure reversals, defect shapes and local properties, and predictive models. Even the trends noted in regard to frequency of occurrence in Table 1 cannot be considered general, as they reflect the unique mix of failures sent to Battelle over the decades.

The only clear factor that emerges from Battelle's database covering events over a period of more than 50 years is that the frequency of seam-related failures is generally decreasing since late in the 1960s, as Figure 13a indicates. Because this decrease appears to reflect improved controls in production and the use of better in-mill inspection technology, consistency in their use and diligence in applying this technology is critical. Otherwise problems will recur, such as emerged in regard to pipe expansion, which became an issue circa 2007. Of concern in this context is the modest upturn evident in Figure 13a.

IMPLICATIONS FOR ERW-SEAM INTEGRITY MANAGEMENT

Following analysis of the Carmichael incident and its IM Program[e.g., see 1,2], the NTSB[4] concluded in a letter to the PHMSA that (their) "current inspection and testing programs are not sufficiently reliable to identify features associated with longitudinal seam failures of ERW pipe prior to catastrophic failure" of an operating pipeline. Related commentary focused critically on ILI, stating that "accumulated data from the three in-line inspections … illustrate the limitations of current in-line inspection technology for detecting significant flaws". All upset autogenous electric-resistance longitudinal seams rely on a forged upset weld. Thus it is plausible that, while the above-noted conclusion is specific to the LFERW pipe in the subject pipeline, the underlying concerns of the NTSB for this LF pipe apply equally to the HFERW, HFI, and FW processes.

This section begins consideration of "actions that can be implemented by pipeline operators to eliminate catastrophic longitudinal seam failures in ERW pipe" in the context of this project. In view of the above, because HFERW, HFI, LFERW, and FW pipe all can be considered ERW

pipe, this project and report assesses ERW seams across this scope, but does not distinguish between the HF processes. Because operators use a process termed integrity management (IM) to identify and manage their integrity threats, the next subsection briefly outlines this IM process as backdrop for analysis that follows.

Overview of Integrity Management

According to industry guidance[e.g.,47,48], integrity management (IM) is a broad-based program built upon integrated component plans to manage/ensure aspects like: Integrity, Performance, (Continuous) Improvement, Communications, Change, and Quality. Regulatory mandates[49,50] detail the expectations of the IM program and direct its timeframes, including the operator's response, as a function of service and other parameters. This project is directed at improvements to the Integrity Management Plan (IMP).

An IMP involves a cyclical process of threats assessment and evaluation, inspection and condition monitoring, risk assessment, a systems-wide supporting database that is integrated and aligned in space and time, and finally, as needed, an integrity assessment with its supporting database and follow-up mitigation – with feedback into the other program-level plans. Of the elements involved in the IMP, this project as scoped by the PHMSA in concert with the NTSB guidance targets integrity assessment and the database that supports it. Specifically, this includes: 1) condition assessment, 2) the analysis of anomalies identified including their severity, and 3) prioritization of the defects and 4) the timeline to respond. Severity is quantified in regard to failure pressure, which is evaluated relative to the defect population, the line-pipe's properties, and the operational/service conditions and protection systems for the pipeline, leading to a prioritized response plan.

The ensuing discussion considers the experience and implications of the outcomes of the prior sections to better understand the threats that can develop specific to the several upset autogenous weld processes. The role of the upset and the heating essential to create a viable forged weld were outlined and discussed to identify common aspects versus critical differences and understand how inadequacies in the upset and heating processes cause defects in an otherwise viable forged weld. Thereafter, the consequences of these threats have been illustrated relative to full-scale failures, to better understand the potential pitfalls and issues in the use of hydrotesting and ILI as the basis to quantify the condition of such seams. The full-scale failures were evaluated to: 1) identify the defect types that lead to failures, 2) quantify and characterize the associated defect shapes and sizes; 3) assess variations in their flow and fracture properties; and 4) reflect on the necessary traits of viable predictive models used to quantify defect severity and re-inspection interval. The following subsections consider the implications of the related discussion and conclusions in regard to avoiding catastrophic and other failures in ERW seams.

Implications and Insights as Guidance Going Forward

As commentary to NTSB Recommendation P-09-1 has been critical of the PHMSA approach for ERW seam integrity assessment that relies on ILI and hydrotesting, the availability of practical alternatives is considered first. Thereafter the implications and insights that follow from the

analysis of the full-scale failure archive are presented in light of literature data and trends where useful, first for hydrotesting, then for predictive modeling, and finally for ILI.

Condition Assessment via Hydrotesting and/or ILI: Alternatives?

Industry guidance[e.g.,47,48] to quantify condition as an input to the IMP identifies inspection (ILI and ITDM), pressure testing, and direct assessment (DA) as acceptable practices, and also opens to the "other proven integrity assessment methods" – although possible alternatives remain unspecified in the current revisions of this guidance. Of the three noted above – that is inspection, pressure testing, and DA – by virtue of the tools and procedures it relies on, DA is likely impractical, and also ineffective. A web-search for recently developed or emerging tools and sensors did not identify candidates that might emerge as longer-term options to qualify as other proven integrity assessment methods, which obliges the use of the current practices, and given the critique of ILI necessitates their improvement.

It follows that work to understand the inadequacies of the current tools relative to the "significant flaws" missed in the context of the NTSB's commentary should have a scope that is adequate to offset these inadequacies. While the NTSB's commentary did not similarly single-out hydrotesting, as has been shown in regard to Figures 28, and 29, even higher pressure testing can fail to expose defects; furthermore, Figure 16 makes clear that other defects can grow significantly during the test, leading to pressure reversals. Thus, work should be initiated to develop pressure-time test protocols to maximize exposure of near-critical ERW features, while minimizing pressure reversals in the remnant defect population. Finally, the statement that "the limitations of current ILI technology for detecting significant flaws" noted by the NTSB can be in conflict with some industry expectations that "Longitudinal Seam Weld Imperfections" can be detected[48], with the caveat above a threshold size. Consideration should be given to clarifying the caveat to indicate that the threshold might exceed the critical defect size for some applications.

Implications for IM Plans and Concern for System Age

Figures 31 through 35 consider the effects of time, temperature, and plastic strain as they pertain to possible changes in the parameters that underlie pipeline system design, and system integrity due to the age of the line pipe. Because pipeline systems are designed for nominally elastic response with a safety margin of 1.39 up through 2.5 on pressure, the strain that drives usual in-service loading is elastic, and so not an issue in regard to strain aging. It follows that, so long as the cross section provided for in the as-built pipeline remains as specified via maintenance, the only plausible effects of pipeline age arise in the context of strain aging motivated by cold work introduced in pipe making and pipeline construction. As has been shown relative to experiments done on steels like those in pipelines, no change occurs in the elastic modulus, while changes in the mechanical properties tend to improve them, rather than degrade them. The same appears to nominally be the case in regard to other properties relevant to integrity. As such, age is not an issue in the context of a well maintained pipeline.

Implications for Hydrotesting and Predictive Modeling

As just noted, the results that underlie Figures 28 and 29 indicate that even higher pressure testing can fail to expose defects, while results for Figures 16 and 30 indicate that defects do grow during the pressure-test phase, leading to pressure reversals. Even when considering those drawbacks together with other issues like access and treatment for disposal, pressure testing has been shown to effectively expose up to 98% of the defects that have caused the failures that populate Battelle's archives. One possible reason that higher-pressure testing does not expose all such defects reflects the observation that some defects are much more resistant to failure than others. This resistance derives from the size of the defect relative to its critical size. Defects can be small relative to their critical size because of either locally high fracture resistance, or a physically smaller defect size, or a combination of both.

Penetrators and stitched welds are examples of defect types that can survive higher-pressure testing because the seam is relatively strong and the defects often are not sharp, as Figures 4a and 5a suggest. In contrast, other features that, because of their size coupled with the local properties, can survive a higher-pressure test do grow subsequently in-service due to cyclic operational loads or environmental effects. Figure 16 shows a portion of the population of reversals in Battelle's archives, which indicates this phenomenon was not uncommon (for various reasons). Of the many such reversals evident, a significant fraction occur as the first test break in a retesting campaign that failed to reach the pressure developed in a prior hydrotest, or in some cases a prior gas test. In this context, the first-break reversals that are larger than a few percent reflect in-service growth; for the most part, these involved liquid/products service that in several instances showed SEM evidence of fatigue, while for others step advance of the crack front over a period of time was evident macroscopically. Figure 9 illustrates one example of step advance due to fatigue, while Figure 21 shows an example of the advance of crack-like SCC.

It follows that predictive models are needed to quantify such behavior both during pressure testing, as well as in-service. Because the different defect types respond to different growth drivers, there is a need to develop defect-specific models, as well as the data needed to calibrate them based on laboratory testing. It is important to note that the same basic model underlies these developing features; the essential differences are in models used, reflecting the database needed to make them application-specific. While aspects of such modeling reflect growth due to pressure, it should be noted that these same models are also needed when condition is assessed via ILI, because defect severity must be quantified as a function of pressure, and a re-inspection interval must be determined regardless of how condition is quantified.

Figure 29 and others make clear that depending on the size of the defect, different types of defects respond quite differently to pressure. Figure 27 indicates that the resistance to failure also depends on the type of defect and its location in the seam, which means that properties to calibrate models based on collapse and fracture theory must be established for features in the bondline as well as in the upset/HAZ of the seam. Because such defects can be continuous or discontinuous through-wall and/or axially, as is evident in viewing most of the fracture surfaces, models must involve fundamental calibrations across the range of idealized shaped and sizes. It follows that the range of shapes and sizes must be characterized by defect type, and that a

scheme to represent discontinuous features must be developed for failure by collapse, as well as by fracture.

Finally, it is known that shorter, deeper features experience a reinforcing effect due to the proximity of sound weld at either end. Likewise, longer shallow features can be reinforced by the sound seam that remains in the net section. It follows that the mechanics models used to represent collapse and fracture theories must embed these aspects. As the industry requires tools that are flexible while still simple, which cannot be too conservative on pressure without being nonconservative on defect size, it follows that such models must be based on trending of results developed by viable numerical analysis, for example finite element analysis.

As discussed above, hydrotesting can lead to pressure reversals. Consequently, analysis to quantify the response of the various types of defects to spike pressure-time histories should be done as the basis to optimize defect exposure in balance to control of pressure reversals. Whereas the initial design of the spike test developed in regard to sharp PTW defects, with the resulting rules of thumb developed proving effective for SCC, similar parametric studies are needed to evolve spike histories relevant to cold welds versus hook origins, and so on.

Implications for ILI

In-line inspection methods for pipelines have been used for assessing pipeline anomalies since the 1960s. Each implementation of an inspection technology typically focuses on a subset of the pipeline anomalies that affect pipeline serviceability. Because corrosion was the first anomaly considered, many methods to detect and size corrosion are mature and broadly used by the pipeline industry. In contrast, the in-line inspection methods for seam weld anomalies that are commercially available came into development much later, and so have been evolving as they are used. As in all such developments, new technology and methods are introduced to overcome the limitations that have been identified, such as the incorrect identification of anomalies when none are present (false calls), failure to detect anomalies, and sizing discrepancies. This section evaluates the outcomes noted to this point and their implications for potential inspection technologies in applications to seam weld anomalies.

Anomaly Implications

The bulk of this document describes a number of weld anomalies that lie in or along the bondline and heat affected zones. Anomalies at the interface/bondline are the most challenging for nondestructive testing. Since these anomalies can be as thin as an oxide layer, not all inspection modalities are appropriate. The properties of the interface can affect the reflection and the transmission factors for the sound waves impinging the interface, thus affecting the signals used to detect and size these anomalies. A subset of the interface anomalies is selective seam weld corrosion. This can be considered a separate class of anomalies for the bond line anomalies because of the loss of metal. In addition to ultrasonic methods, because of this loss of metal, magnetic flux leakage techniques can be added to the list of potentially appropriate technologies. For cracks in the heat affected zones, ultrasonic methods can be appropriate technologies, although the through-thickness angle of the anomalies (evident for example in Figure 2) can be

an important factor, as discussed later. If the crack is open, as the case for many hook cracks, magnetic flux leakage methods can again be an appropriate technology.

The upset and trim associated with the fabrication of the weld is an important variable, because these typically produce signals. Signals from weld defects combine with the signals from the upset and trim to produce a signal pattern that is complicated and thus must be carefully analyzed. For welds with a consistent trim, the signal processing methods can be used to extract the signals from the anomalies. A typical weld signal can be generated by averaging recorded data from several axial measurement positions. To detect defects, the average weld signal is subtracted from the measured signals. This difference should reveal the anomaly signal only, but also shows natural variations in the welding process and potential defects. If there is a local variation in the trim, the change produced by this factory condition can be misconstrued as an injurious defect to some technologies.

The inspection tools are developed for ideal weld geometry with the interface between the two edges of the pipe essentially planar and vertical. While this is nominally the case, non-uniform heating and upset can cause a deviation in the interface. Based on the images for some of the examples shown earlier, interface angles of 20 degrees or more can develop. This variation is likely to adversely influence the ultrasonic methods that rely on the return of reflected energy. The deviation of the weld interface can direct the reflected sound in unexpected directions while mode conversion can cause the wave to arrive at unexpected times. Either case may cause signals from weld anomalies to go undetected.

When developing an inspection technology, knowing the dimensions and characteristics of a critical anomaly early in the development process can influence engineering decisions such as resolution and aperture. The size must be defined in terms of length along the axis of the pipe and depth or percentage of the wall thickness. One issue is the length relative to the aperture of the inspection technology. If the length of the anomaly is large compared the aperture of the sensor, then the depth of the anomaly is typically a simpler function than if the anomaly is shorter than the aperture. Unfortunately, the critical length of anomaly is a function of mechanical properties such as fracture toughness, one of the topics being addressed in the current research program. Therefore, certain technologies being deployed are based on parameters derived from pipe operators' intuition or rules of thumb. The converse implies that new definitions of critical anomaly dimensions may require modifications to existing tools.

Implications for Existing Inspection Technologies

Implementations of inspection technologies typically focus on a subset of the pipeline anomalies that affect pipeline serviceability. For the seam weld problem, three technologies are viable:

- Magnetic flux leakage inspection with the magnetization in the circumferential directions, transverse to the more typical axial field;
- Angle beam ultrasonic inspection with the energy generated by piezoelectric transducers; and
- Plate wave ultrasonic inspection with the energy generated by electromagnetic acoustic transducers (EMATs).

Each technology is discussed in turn below.

Magnetic Flux Leakage (MFL). MFL systems, regardless of configuration, can be designed to remain functional in an abusive pipeline environment for long distances at product flow speeds. The source of inspection energy (permanent magnets) requires no energy during an inspection and the sensors and data recorders require reasonably low power to operate. The magnetic flux naturally enters the pipe and distributes evenly to produce a full volumetric inspection. While the deficiencies of MFL systems are often highlighted, these attributes keep MFL at the forefront of pipeline inspection technologies.

MFL systems can detect cracks, as evidenced by magnetic particle inspection that is a MFL-based method that has been used for over a century. The strongest signals come from cracks that have broken to surface where the sensor is located. Also, the width of the crack opening plays an important role in detecting these anomalies[(75)]. To be effective in detecting axially aligned features, the magnetization direction must be such that the flux crosses the seam weld. The most common approach is circumferential MFL, which is transverse to the more typical axial field used in the earlier MFL systems. A new implementation of MFL uses an oblique magnetization direction; the output is a combination of the axial and circumferential response[(76)]. For the seam weld anomalies considered earlier, the non-axial MFL configurations are the most appropriate to detect selective seam corrosion at the interface and hook cracks in the heat affected zone. Sizing these anomalies can be challenging since the amplitude of the MFL signal used to perform this task is a function of three variables (axial length, radial depth and the circumferential opening width). Besides amplitude, the only other independent measure is the length for the three variables. Depth is more difficult to accurately assess because of the potential variation in crack opening. To overcome this limitation, calibration methods for the cracks on the specific pipeline are used to provide better estimates. A patented method for detection of cracks and performing such a depth assessment is available[(77)]. Variation in trim of the seam weld can produce signals that are affected by other implementation issues, and thus affect performance of these in-line inspection tools.[(78)]

Angle beam ultrasonic testing (UT). Angle beam ultrasonic inspection methods with the energy generated by piezoelectric transducers are commonly used in many industries for detecting cracks in metals. Implementations for in-line inspection became commercial in the mid 1990s[(79)]. These systems require the pipeline to contain liquid media for coupling the ultrasound from the transducer into the pipe; this complicates the utilization of this technology for natural gas pipelines.

All the seam weld anomalies presented in this document have the potential to be detected if sufficiently large; this includes interface anomalies such a cold welds, selective seam corrosion, and hook cracks in the heat affected zone. The UT systems are sensitive to upset and trim associated with the fabrication of the weld, as well as inclusion and laminations that are considered benign anomalies. Distinguishing the fabrication and material variation from potentially significant weld seam anomalies requires examination of signals from multiple pairs of sensors and detailed analysis. The depth of crack-like features is provided in bins that typically reach a quarter or eighth of the wall thickness[(80)]. Sizing axial length and radial depth

involves examining images of sensor output in both pulse echo and thru-transmission mode, from both sides of the weld. The sizing method can work well for planar radial cracks; however, misaligned skelp and the complex shapes of some hook cracks can make sizing less accurate because the angle and curvatures can cause mode conversions that redirect ultrasonic energy. This technology has an excellent potential for detecting significant seam anomalies, but both the process of filling gas pipelines with liquid and identification of false calls due to fabrication and materials variation can make this approach less desirable. For many pipelines, the extent of the modifications that must be made to run liquid coupled ILI tool can make a hydrotest a more cost-effective option.

Electromagnetic Acoustic Transducers (EMATs). EMATs ILI is an ultrasonic method that can work in natural gas pipelines (without liquid coupling) for detecting axial pipeline anomalies. This emerging technology was first prototyped for pipelines in the 1980's[(81)], and functional commercial systems arrived in the last decade. Ultrasonic waves are generated directly in the pipe by an electromagnetic pulse and can be configured to propagate in almost any direction including around the circumference of the pipe.

Compared to the angle beam ultrasonic systems, circumferentially guided ultrasonic waves that are generated by EMATs have significant differences, which lead to advantages and disadvantages. A primary difference is that the frequency of the EMAT generated ultrasonic waves is an order of magnitude lower. The EMAT generated sound waves tend to be less responsive to upset and trim associated with the fabrication of the weld, as well as inclusions and laminations in the base metal; however, EMATs can be sensitive to the exterior coating adherence.[(82)] EMAT systems have fewer larger sensors than angle beam ultrasonic systems[(83)]; each sensor interrogates a larger volume of material than UT systems and combines the anomaly response over the aperture of the transducer. EMAT tools also can operate in both pulse echo and thru-transmission mode. The depth sizing is based to the signal from both sensor configurations where the angle beam method often uses multiple sensors to assess an anomaly. The longer wavelength and size of EMAT transducers currently challenges implementations for pipe smaller than about 12 inches in diameter. It should also be noted that EMAT systems can be configured in many more ways than MFL or UT tools. This is due to the fact that there are many sensor configurations and the frequency of operation can be varied to control the wave type and mode of propagation[(81)]. Hence, EMAT inspection tools from different ILI vendors can have more unique performance attributes and constraints than MFL or UT systems from different ILI vendors.

In summary, these three classes of inspection technology have the capability to detect seam weld anomalies that can cause pipelines to fail. However, the nature of some of the critical anomalies, the variation within the manufacturing processes, and the pipeline operating conditions can potentially constrain the capability of these technologies to find all critical anomalies. Furthermore, the engineering considerations made during the design process of these tools, based on the current understanding of the inspection goal, also can potentially limit the capability of these technologies. Potential performances improvements can be expected as in-line inspection tools for seam weld issue evolve.

Assessment of Performance of ILI Tools

Pipeline owners and government regulators benefit from knowing the detection and sizing capability of in-line inspection tools. One source of information that relates in-line inspection tool performance to anomalies found in pipelines is available in papers written by pipeline owners or their contractors who discuss rehabilitation jobs that involve in-line inspection, in the ditch assessment, and hydrotesting. An assessment of use of circumferential MFL as a substitute for hydrotresting was investigated for a pipeline with a history of failure due to hook cracks[84]. It was concluded that while confidence in circumferential MFL method to detect seam-weld cracks was achieved, similar confidence in inspection tolerances relative to anomaly discrimination and sizing was not present. The repair methodology was based on anomalies detected by ILI and in the ditch sizing to determine sections for replacement.

The literature also contains papers illustrating the number of flaws that were detected by a specific ILI technology, including papers on angle beam ultrasonics[85], EMAT[86], and circumferential MFL[87]. These papers provide detailed data to illustrate the potential of ILI to detect, identify, and size anomalies in the seam weld. However, the information in these papers is typically limited to the anomalies that are detected by the ILI tool. A comprehensive assessment of probability of detection needs a large population of representative anomalies of sizes ranging from inconsequential to service limiting, which is typically not available in this type of survey.

Conclusions

This report is an initial step in meeting the objectives of the project initiated by the PHMSA to identify actions that can be implemented by pipeline operators to eliminate catastrophic longitudinal seam failures in such pipe. It serves to sharpen the focus of the remaining work scope for this project, the first to consider the many factors summarized above in an integrated effort to better understand the threats posed by anomalies/defects in ERW seams, with a view to identify and quantify actions that can be implemented by pipeline operators to eliminate catastrophic longitudinal seam failures in ERW pipe. Work in that context continues, as it integrates the outcomes of this reporting with that of the KAI/DNV database to best implement the proposed work scope.

SUMMARY AND CONCLUSIONS

This report describes Battelle's experience with ERW and flash weld seam failures and discusses their causes and implications for pipeline integrity management. Activities related to this effort included the development of a database on ERW/FW defects using data from Battelle's archives and the related literature; analysis and trending to determine the utility and effectiveness of hydrotesting and ILI to assess pipeline condition; and an evaluation of the results. The outcomes were used to assess the viability of the predictive tools that couple with defect sizes and the seams properties to implement an operator's IM Plan, noting the gaps and related implications as part of that assessment.

Several conclusions were drawn throughout this report, with many of the key ones noted at the end of the section on the failure database under the subhead Important Conclusions Regarding Traits, Trends, and Observations. The following list summarizes the higher-level conclusions from that section as they pertain to the integrity management process:

1. Higher-pressure hydrotesting coupled with ILI and related ITDM provide the only practical basis to assess pipeline condition, with a well designed hydrotest capable of exposing the pipeline condition during the course of the test.
2. In-line inspection tools can find seam weld anomalies, however some anomalies that lead to failure have gone undetected. With better definition the seam defect parameters that need to be quantified by inspection methods, objective data on the current state of the art of inspection technology, improvements in sensing technology, and the combination of inspection methodologies, an adequate in-line inspection approach to detect all critical seam weld anomalies appears possible.
3. While both hydrotesting and ILI are in need of refinement and development, respectively, the current uncertainty in regard to the effectiveness of ILI in contrast to the better understood circumstances for hydrotesting suggests a primary role for hydrotesting in condition assessment, serving as a short term stopgap while certainty builds in regard to ILI for detection and sizing, supported by ITDMs.
4. Seam properties vary greatly from the center of the bondline out into the upset/HAZ, which are direct metrics of the underlying microstructural differences and also indicative of seam quality. However, in general, the underlying details and their implications may not be broadly understood in the ILI and its supporting nondestructive inspection (NDI) community. It is plausible that sensor and signal conditioning/analysis algorithms have been developed in other applications that could enhance detection and sizing via ILI and ITDM.
5. Condition assessment is only one part of the IM Plan – which involves a range of decisions such as when to re-inspect and what to rehab and when, that depend on predictive models that in turn rely on defect sizes and related properties. Clear gaps have been identified in practices used to size features, which have a first-order effect on the utility of an IM Plan. Gaps in approaches to quantify the needed properties have been identified, as have first-order differences in such properties in or across the seam relative to the pipe body. Clearly, work is needed in regard to both quantifying inputs to the predictive models, with related errors forced by idealizations necessitated by fundamental gaps in those models.
6. While work remains as part of this project that begins to address some of the many gaps identified, because this is the first project to consider the integrity of ERW/FW seams in an integrated fashion one can anticipate such work will define the path forward, more so than close the issues along that path. Details are presented next in the Recommendations section of this report.

Finally, while potentially useful guidance might be gleaned from the details of the database and the trending reported in Figures 11 through 16, and in Figures 27 through 35, the interdependent complexity evident in the five factors found to control defect response to pressure suggests such

generalizations might be dangerous. Succinctly stated these five factors are: 1) defect size and shape, 2) whether the defect is blunt or sharp, 3) the local mechanical and fracture properties, 4) the local stress, and 5) the mechanism(s) driving its growth. For example, the nature of an isolated short and blunt oxide-filled penetrator suggests that it poses little threat to integrity. In contrast, inclusion of a pinhole in the API list of defects – which can result from the breakdown of the oxide in a penetrator – warns against that generalization, because a pinhole is a leak path. This coupled with fact that all other defect types considered have failed at in-service pressure levels, and so can pose an integrity threat to an operating pipeline, precludes listing generalizations regarding aspects like the range of SMYS causing failure, the nature of pressure reversals, defect shapes and local properties, and predictive models.

One factor that emerges conclusively from Battelle's database over the more than 50-year period it represents is that the frequency of seam-related failures began a sharp decline in the 1960s, and is generally decreasing since the 1970s – as the trending in Figure13 demonstrates. This decrease appears to reflect improved processes and controls in production, as for example sliding contact coupled with automated process controllers. It also appears to reflect the broader use of in-mill inspection technology, and improvements to that technology to achieve more consistent seam quality in the outbound product. In spite of these improvements, occasional issues emerge in regard to paste welds, which if large enough or weak enough can pose an integrity concern. Clearly where success reflects the role of QC during production and QA upon completion, consistency in these practices is essential, as it diligence in applying the technology. Otherwise problems can recur, such as emerged in regard to pipe expansion, which became an issue circa 2007 – and gave rise to the PHMSA Pipeline Safety Bulletin ADB-09-01involving potential low and variable yield and tensile strength properties in high strength line pipe. Other advisory bulletins that address areas once thought to be resolved convey the same message. Of concern in this context is the modest upturn evident in ERW seam issues that can be seen recently in the trending.

RECOMMENDATIONS

Consideration of the above conclusions and the related summaries presented throughout the report indicates that the integrity management issues evident for ERW seam defects, which underlie P-09-1, can be grouped into five separate categories. Approaches to resolve issues and questions associated with each category are recommended below:

1. Hydrotesting. Questions remain regarding its viability in regard to specific feature types and sizes of seam defect: whether it is a detriment, and, if so, under what circumstances for each type of seam feature. It is apparent that this practice can be made more effective and less detrimental by developing test histories adapted/optimized to the types of defect that, from a historic perspective, pose the greatest threats.
2. ILI. The NTSB's comments emphasize a concern that the viability of ILI remains open to question for detection and sizing of ERW seam defects. Run-specific tool tuning, and dig/document practices can be key to tool success, although related metrics and calibration remain a concern. In addition, third generation concepts appear to be

emerging with progress in understanding and relating the pressure and cycle dependence of magnetic properties and hysteresis to their analog evident in the flow response of steel, and progress in understanding cyclic plasticity effects on mechanical properties.

3. Defect Characterization: Types, Sizes, Shapes, and Idealizations. Because FW and ERW processes are shown to produce similar types of features, the seam defects from both can be grouped in reference to bondline defects, and upset/HAZ defects. Different properties develop in either case, for which viable test practices are limited/unproven. There is a parallel need to establish idealizations for the shapes of these features and adequately capture reality for purposes of sizing as an input to predictive modeling and analysis, which by definition requires different sizing schemes for fracture-controlled versus collapse-controlled failure.
4. Models and Mechanisms. The viability of models to quantify defect severity relative to plastic collapse and fracture is open to question for most defect types. Reasons for this include a) the limited idealizations available for sizing, b) the uncertain values for the properties required for such models (consistent with Category 3 above), referencing the absence of test practices and standards to quantify seam properties and the rates of mechanisms like SSC and fatigue, and c) the limited scope of relevant fracture and collapse solutions. Addressing these issues will resolve many questions of viability.
5. Defect-Specific Management Protocols and Tools. Integrity management of vintage seams is in part experience based, and relies on empirical protocols coupled with condition assessed primarily through ILI and hydrotests, supplemented by ITDM. The NTSB notes this area is inadequate, since vintage seam failures continue to occur. The existing tools/ protocols could be improved by reformulation based on the outcomes of this project; semi-empirical tools could benefit similarly, or be replaced in the context of work developed under the above four categories, with the outcomes packages as truly user friendly software. Updated protocols would provide a near-term response to P-09-1 as a stopgap, while the tools emerge over a longer-term as the basis for sound integrity management.

This hierarchy of five categories provides the structure needed to address the concerns as they are now understood. Priority for what needs to be done and the sequence follows from the primary objective of this project, which is to close out P-09-1.

Condition is the key to safety, and needs to be assessed before revalidation and re-inspection interval become concerns. This drives Category 1 (Hydrotesting) and Category 2 (ILI) to the top of the list. Since ILI, particularly for natural gas applications, is likely tied to electromagnetic acoustic transducers (EMATs), this suggests that ILI is likely most relevant for pipe diameters of 12 inches and above. In contrast, hydrotesting (in spite of its drawbacks) can be applied over a broader range of diameters. While both hydrotesting and ILI will struggle to identify and expose short features, it is reasonable to conclude that such features are exposed in combination with detection of relatively lower strength and toughness. On this basis, the top near-term priority is resolving the issues with hydrotesting for use as the near-term tool to assess condition; meanwhile, the more complex issues involved with ILI can be better quantified and plans developed for their resolution.

Category 3 (Defect Characterization) and Category 4 (Models and Mechanisms) rank equally as the next priority, being somewhat lower than the categories related to condition assessment. However, the fact remains that condition must be communicated in a format of the technology used to interpret condition and quantify safety threats and defect severity. Consequently, the gaps in these aspects must be resolved in almost the same time frame as the work on condition assessment. Fundamental models that quantify defect growth and failure pressure based on plastic-collapse and fracture theories must be adapted and proven viable. At the same time, understanding susceptibility to SSC and fatigue is essential, as these remain drivers for in-service growth and seam failure.

It follows that gaps and opportunities identified throughout the report should be addressed first in regard to hydrotesting and ILI, with a parallel made to develop practical tools to quantify defect severity and understand and quantify susceptibility to SSC and fatigue. Ultimately, for such work to translate into a safer infrastructure, it must be reduced to practice in the form of simple tools of direct utility to operators.

REFERENCES

1. Anon., "Rupture of Hazardous Liquid Pipeline With Release and Ignition of Propane, Carmichael, Mississippi, November 1, 2007," NTSB PAR-09/01, Adopted October 2009: see http://www.ntsb.gov/investigations/summary/par0901.htm for related documentation.
2. Dyck, R., NTSB Materials Laboratory Factual Report Draft Report No.07-122 dated 18 April 2008.
3. Kiefner, J. F., Haines, H., Rosenfeld, M, Beavers, J. A., Amend, W., Bruce, W. A., Leis, B. N., Zhu, H-K., Nestleroth, J. B., and Clark, E. B., "Gap Analysis and Review of NTSB Report Par 09-01," Final Report on Project PR-218-103706 / PRCI Task IM-1-1, Pipeline Research Council International, Inc., January, 2011.
4. Anon., NTSB Safety Recommendation P-09-1, Letter Commentary dated October 27, 2009 to the PHMSA
5. Kiefner, J. F. and Kolovitch, K. M., "ERW and Flash Weld Seam Failures," KAI Interim Report on Task 1.4, September, 2012
6. Kautny, T., *Autogenous Welding and Cutting*, (translated by Whiteford, J. F.,) M^{c}Graw-Hill (UK), 1915
7. Anon., A O Smith Corporate Documentation, including Bulletin 576 and www.aosmith.com
8. Patterson, B. R., "The Evolution and Development of ERW Pipe," presented at the API Committee on Standardization (Midyear Meeting), Pipe Symposium, Denver, 19 June 1989.
9. Messler, R. W., *Principles of Welding: Processes, Physics, Chemistry, and Metallurgy*, Wiley-VCH, 1999.
10. Koch, F. O. and Peters, P. A., "Distinguishing Characteristics of High-Frequency Induction-Welded Pipe," presented at API Standardization Conference, Pipe Symposium, New Orleans, 23 June 1986.
11. Baralla, E. and Tommasi, C., "Integrated System for Process Control of High Frequency Electric Resistance Welded Steel Pipe," Proceedings PAN NDT Meeting, Rio de Janeiro, 2003
12. Anon., "Complete Inspection Solutions for ERW Tubes (including Large Diameter Pipe)," Olympus Document, see http://www.olympus-ims.com/en/erw/, accessed July 2011.
13. Hong, H. U., Kim, C. M., and Lee, J. B., "Characteristics of Pressure Reversal Fracture in Electric Resistance Welded Seams of API-X70 Steel," Posco Technical Report, Vol. 10, No. 1, 2006.
14. Kim, D., Kim, T., Park, Y. W., Sung, K., Kang, M., Kim , C., Lee, C. and Rhee, S., "Estimation of Weld Quality in High-Frequency Electric Resistance Welding, with Image Processing," *Welding Journal*, Research Section, March 2007, pp 71-S to 79-S.
15. Nakata, H. I., Kami, C., and Mathou, N., "Development of API X80 Grade Electric Resistance Welding Line Pipe," JFE Technical Report No. 12, October, 2008
16. Roza, J. E., Fritz, M. C., and Tivelli, M. A., "API 5L X80 ERW Pipes: Tenaris-Confab and Usiminas Development," *International Pipeline Conference, IPC2006-10406*, pp. 497-502, Calgary, September 2006

17. Choi, J.-H., Chang, Y. S., Kim, C.-M. Oh, J.-S., and Kim, Y.-S., "Penetrator Formation Mechanisms during High-Frequency Electric Resistance Welding," *Welding Journal*, Research Section, January 2004, pp 27-S to 31-S.
18. Weimer, G., and Cagganello, R., "Electric Resistance Welding at a Glance: Process, Power Supply, and Weld-Roll Basics," 13 June 2002 see www.thefabricator.com for this and others on resistance welding, on-line access in July 2011.
19. Scott, P., "Choosing the Right HF Welding Process for API Large Pipe Mills," Thermatool Corp Paper, 29 November 2005.
20. Scott, P., "The Effects of Frequency in High Frequency Welding," Thermatool Corp Paper, 1996.
21. Pierson, J. and DiDonato, M., "High-Frequency Electric Resistance Welding: An Overview" June 1, 2010, see www.thefabricator.com for this and others on resistance welding, on-line access in July 2011.
22. Warren, L., "Skelp Edge Preparation for Manufacturing ERW Pipe," in thefabricator.com, dated May 30, 2001.
23. Anon., "API Bulletin on Imperfection Technology," API Bul. 5T1 (R2010), 2010
24. Brossia, S., "Selective Seam Weld Corrosion Literature Review," DNV Report to PHMSA, April, 2012.
25. Lukezich, S. J., "Susceptibility of Modern ERW Pipe to Selective Weld Seam Corrosion in Wet Environments," Project PR-15-9306, Cat #L51775, 1998
26. Groeneveld, T. P., Davis, G. O., and Williams, D. N., "Susceptibility of Resistance Welded, Flash Welded, and Induction Welded Pipe to Selective Seam-Weld Corrosion," NG-18 Report No. 199, Pipeline Research Council International (1991).
27. Nichols, R. K., "Common HF Welding Defects," Thermatool Corp., (www.thermatool.com/.../common-hf-welding-defects.pdf), undated
28. Wright, J., "Optimizing Efficiency in HF Tube Welding Processes," *Tube and Pipe Technology*, November/December, 1999 (www.eheimpeders.com/uploads/TB1011.pdf)
29. Joosten, M. W., Kolts, J., Kiefer, J., Humble, P. G., Marlow, J. A., "Aspects of Selective Weld and HAZ Attack in CO_2 Containing Production Environments," *Corrosion 96*, Paper 79, 1996: see also Duran, C., Treiss, E., and Herbsleb, G., "The Resistance of High Frequency Inductive Welded Pipe to Grooving Corrosion in Salt Water," *Materials Performance*, p. 41, September 1986.
30. Stonesifer, R. B., Brust, F. W., and Leis, B. N., "Mixed Mode Stress Intensity Factors for Interacting Semi-Elliptical Surface Cracks in a Plate", *Engineering Fracture Mechanics*, Vol. 45, No. 3, pp. 357-380, 1993.
31. Anon., "Specification for Line Pipe," API Specification 5L, American Petroleum Institute, Dallas, 2010.
32. Broek, D., *Engineering Fracture Mechanics*, Nordhoff, 1974.
33. Anon., "Standard Test Method for K-R Curve Determination, ASTM E561, Vol. 03.01, 2010.

34. Anon., "Standard Test Method for Measurement of Fracture Toughness," ASTM E1820, Vol. 03.01, 2011
35. Anon., ASTM Standard E23-98, Notched Bar Impact Testing of Metallic Materials, ASTM Vol. 03.01.
36. Williams, D. N., "Use of the Notched Tensile Test to Measure the Ductility of the Seam Weld in ERW Pipe," NG-18 Report No. 141, Battelle Final Report to American Gas Association, December 1983.
37. Leis, B. N., Clark, E. B., Zhu, X. K., and Galliher, R. D., "Guidelines for Assessing Corrosion Associated with Girth and Long-Seam Welds," Gas Research Institute Report GRI 04-0119, October 2004
38. Leis, B. N., Galliher, R. D., Sutherby, R. L., and Sahney, R., "Hydrotest Protocol for Applications Involving Lower-Toughness Steels," *International Pipeline Conference, IPC04-0665*, Calgary, October 2004, pp.
39. Mayfield, M. E., and W. A. Maxey, "ERW Weld Zone Characteristics," NG-18 Report No. 130, PRCI Catalog. No. L51427June 1982.
40. Masamura, K. and Matsushima, I., "Grooving Corrosion of Electric Resistance Welded Steel Pipe in Water - Case Histories and Effects of Alloying Elements", Paper No. 75, Corrosion 81, NACE International, 1981: see also Skvortsov, S.V. "A Calculation Method of Predicting the Corrosion Rate of Welded Joints in Hull Steels in Sea-Water," *Welding International*, Vol. 7, p. 569 , 1993
41. Peterson, R. E., *Stress Concentration Factors*, Wiley, 1974
42. Leis, B. N. and Brust, F. W. "Hydrotest Strategies for Gas Transmission Pipelines Based on Ductile Flaw Growth Considerations, NG-18 Report No. 194, PRCI Cat. No. L51665, July 1992: see also Leis, B. N., and Brust, F. W., "Ductile Crack Growth Model and Its Implications With Regard to Optimum Hydrotest Strategies", *Proceedings of the Pipeline Technology Conference*, Part B, Oostende, pp. 13.11-19, 1990
43. Clark, E. B., Leis, B. N., and Eiber, R. J., "Integrity of Vintage Pipelines," Battelle Final Report including seven annexes to INGAA Foundation, October 2004,
44. Anon., "American Tentative Standard Code for Pressure Piping," American Engineering Standards Committee, Sectional Committee B31, 1935.
45. Anon., *Gas Transmission and Distribution Piping Systems*, B31.8, American National Standards Institute/ American Society of Mechanical Engineers, 2011
46. Leis, B. N. and Bubenik, T. A., "Primer on Design to Avoid Failure in Steel Transmission Pipelines", Gas Research Institute Report, GRI 00/0229, January 2001.
47. Anon., ASME B31.8S Managing System Integrity of Gas Pipelines, American Society for Mechanical Engineers, June 2010.
48. Anon., API Standard 1160, Managing System Integrity for Hazardous Liquid Pipelines, American Petroleum Institute, November 2001
49. Anon., Subpart O of Part 192 (Transportation of Natural and other Gas by Pipeline) of Title 49 of the CFR.

50. Anon., Section 195.452 of Subpart F and Appendix C of Subpart H in Part 195 (Transportation of Hazardous Liquids by Pipeline) of Title 49 of the CFR.
51. Shires, T. M. and Harrison, M. R.; "Development of The B31.8 Code and Federal Pipeline Safety Regulations: Implications for Today's Natural-Gas Pipeline System", Gas Research Institute Report GRI-98/0367, 1998.
52. Timoshenko, S. P. and Goodier, J. N., *Theory of Elasticity*, McGraw-Hill, 1970
53. Michalopoulos, E. and Babka, S., "Evaluation of Pipeline Design Factors," Hartford Steam Boiler Inspection and Insurance Company Final Report to the Gas Research Institute, GRI 00/00076, February 2000.
54. Hahn, G. T. Reid, C. N., and Gilbert, A., "The Relation between Delay-Time, Strain-Rate, and Strain-Aging Phenomena in Mild Steel," NG-18 Report No 6, March 1962: see also Hooper, W. H. L., *J. Inst. Metals*, vol. 81, p. 563, 1952: see also Phillips ,V. A., Swain, A. J., and Eborall, R., *J. Inst. Metals*, vol. 81, p. 625, 1952.
55. Baird, J. D., "Strain Aging of Steel – a Critical Review: Parts I & II", *Iron & Steel*, May, 1963.
56. Baird, J. D., "The Effects of Strain Aging Due To Interstitial Solutes on te Mechanical Properties of Metals", *Metallurgical Reviews*, Review 149, pp 1-18.
57. Clark, D. S. and Varney, W. R., *Physical Metallurgy For Engineers*, 2nd Ed., Van Nostrand Company, 1962, pp 102-103, 198-199.
58. Herman, W. A., Erazo, M. A., Depatto, L. R., Sekizawa, M., Pense, A. W., "The Strain Aging Behavior of Microalloyed Steel", Welding Research Council Research Bulletin 322, Welding Research Council, April 1987.
59. Wilson, D. V. and Russell, B., "The Contribution of Precipitation to Strain Ageing in Low Carbon Steels", *Acta Metallurgica*, Vol. 8, July 1960, pp 468-479.
60. Wilson, D. V. and Russell, B., "The Contribution of Atmosphere Locking to the Strain-Ageing in Low Carbon Steels", *Acta Metallurgica*, Vol. 8, July 1960, pp 36-45.
61. Baldy, M. F. and Anney, F. W., "Strain Aging Plate for Large Diameter Line Pipe", *Pipe Line Industry*, November 1981, pp 118-123.
62. Rashid, M. S., "Strain Aging of Vanadium, Niobium, Titanium-Strengthened High-Strength Low-Alloy Steels", *Metallurgical Transactions A*, American Society for Metals, Vol. 6A, June 1975, pp. 1265-1268
63. Leslie, W. C. and Rickett, R. L., "Influence of Aluminum and Silicon Deoxidation on the Strain Aging of Low-Carbon Steels", *Journal of Metals*, August 1953.
64. Daniloff, B. N., Mehl, R. F., and Herty, C. H., "The Influence of Deoxidation on the Aging of Mild Steels", *Transactions, American Society for Metals*, Vol. 24, 1936, p 595.
65. Gawne, D. T., "Strain Aging and Carbide Precipitation in Aluminum-Killed Steels", *Materials Science and Technology*, Vol. 1, The Institute of Metals, August 1985, pp 583-592.
66. Tither, G. and Lavite, M., "Beneficial Stress-Strain Behavior of Moly-Columbium Steel Line Pipe", *Journal of Metals*, 1975, Vol 27, pp15-23.

67. Rashid, M. S., "Strain Aging Kinetics of Vanadium or Titanium-Strengthened High-Strength Low-Alloy Steels", *Metallurgical Transactions A*, American Society for Metals, Vol. 7A, April 1976, pp. 497-503.
68. Hundy, B. B., "The Strain Age Hardening of Mild Steel", *Metallurgia*, 53, 203, May 1956, pp 203-211: see also Hundy, B. B.; "Accelerated Strain Ageing of Mild Steel", *Journal of the Iron and Steel Institute*, September, 1954, pp 34-38
69. Edwards, C.A., Phillips, D. L., and Jones, H. N., "A Study of Strain Age Hardening of Mild Steel", *Journal Iron and Steel Institute*, Vol. 139, 1939, pp 341-385.
70. Shoenberger, L. R. and Paliwoda, E. J., "Accelerated Strain Aging of Commercial Sheet Steels", *ASM Transactions*, American Society for Metals, 45, pp 345.
71. Deiter, G. E., *Mechanical Metallurgy*, 3rd edition, McGraw-Hill, 1986, pp. 280-281.
72. Mack, D. J., "Young's Modulus-Its Metallurgical Aspects", *AIME Transactions*, Vol. 166, pp. 68-85, 1946.
73. Leslie, W. C., *The Physical Metallurgy of Steels*, McGraw-Hill, 1981, pp. 110-115.
74. Anon., "Goal is Zero Incidents," http://www.ingaa.org/6211/11460.aspx, accessed August 2011.
75. Dobman, G. "Physical Analysis Methods of Magnetic Flux Leakage," *Research Techniques in NDT*, Vol. IV, R. S. Sharp, Editor, 1980.
76. Simek, J., Ludlow, J., and Tisovec, P., "Oblique Field Magnetic Flux Leakage Inline Survey Tool: Implementation and Results," Proc. of the 8th Int. Pipeline Conference, IPC 2010, Calgary, September 2010.
77. Duckworth, N., and Sherstan, R., "System, Method and Program Product to Screen for Longitudinal Anomalies," US Patent 7,899,628, March 2011.
78. Nestleroth, J. B , Bubenik, T. A., and Davis, R. J., "Circumferential Magnetic Flux Leakage," GRI-00/0193, Gas Research Institute, 2003
79. Williams, H. H., Barbian, O. A., and Uzelac, N. I., "Internal Inspection Device for Detection of Longitudinal Cracks in Oil and Gas Pipelines," ASME International Pipeline Conference, Calgary, 1996.
80. Reber, K., Beller, M., Barbian, O.A., and Uzelac, N., "A New Generation of Ultrasonic Inspection Tools; How Defect Assessment Methods Influenced Design," The Pipeline Pigging, Integrity Assessment and Repair Conference, February 2002.
81. Alers, G., "A History of EMAT," 27th Review of Quantitative Nondestructive Evaluations," *Am. Inst. of Physics*, p 801, 2008.
82. Al-Qahtani, , Beuker, H, T., and Damaschke, J., "Crack Detection and Coating Disbondment," 20th International Pipeline Pigging, Integrity Assessment & Repair, Houston, February 2008.
83. Yasinko, E, Veith, P., et. al. "Platte Inspection Program Supports Alternative to Hydrostatic Testing," *Oil & Gas Journal*, March 26, 2001.
84. Mead, R. "Non-Destructive Evaluation of Low-frequency Electric Resistance Welded (ERW) Pipe Utilizing Ultrasonic In-Line Inspection Technology," *Proceeding of the*

European Conference on NDT, Berlin, 2006.

85. Klann, M. and Beuker, T., "Pipeline Inspection with the High Resolution EMAT ILI–Tool: Report on Full-Scale Testing and Field Trials," IPC2006-10156, 6th International Pipeline Conference, Calgary, September 2006.
86. Grimes, J., and Nunez de Alvarex, A., "Utilizing Circumferential MFL for the Detection of Linear and Axially Oriented Metal Loss Anomalies in Pipelines," IPC2008-64275, 7th International Pipeline Conference, Calgary, September 2008.

ANNEX A: TABULATED DATABASE

Line Pipe & Service Related									Failure Related								
OD	WT	Gr	SMYS	Seam	Mfgr	Vintage	MOP or MAOP	Service	Cause		Leak vs Rupture	Test vs Operate	Failure Pressure	Pf/Psmys	Max Prior Pressure	Date	Date Failed
inch	inch		psi						Primary	Other Factors			psig		psig		
8.625	0.219	42	42000	HFERW	/Copperw	2000		gas	cold	clear thumbnail crack advance	L	PSHT	640	0.300	2133	2001	2001
16	0.312	52	52000	LFERW	Republic	1959	1460	gas	cold weld	skewed-offset	R	Oprn	1300	0.641		none	1959
16	0.312	52	52000	LFERW	Republic	1959	1460	gas	cold weld	skewed-offset	R	HT	500	0.247		none	1959
10.75	0.188	42	42000	ERW-DC	YS&T			gas	hook origi	some ID overscarf	R	GT	650	0.442	1400	milltest	1964
16	0.375	B	35000	LFERW		1947		gas	SSC		R	Oprn	1049	0.639	1110	1947	1966
26	0.375	52	52000	FW	AOSmith	1952		gas	hoor origin		R	HT	1457	0.971			
16	0.438	B	35000	DC-ERW	YS&T	1943		products	cold weld		R	HT	1500	0.783	1280	1943	1970
16	0.312	B	35000	DC-ERW	YS&T	1943		products	cold weld		R	HT	1305	0.956	915	1943	1970
16	0.312	B	35000	DC-ERW	YS&T	1943		products	cold weld		R	HT	1310	0.960	1305	1970	1970
16	0.312	B	35000	DC-ERW	YS&T	1943		products	cold weld		R	HT	1367	1.001	1310	1970	1970
16	0.312	B	35000	DC-ERW	YS&T	1943		products	cold weld		R	HT	1367	1.001	1367	1970	1970
16	0.312	B	35000	DC-ERW	YS&T	1943		products	hook origi	w PWHT issues	L	HT	900	0.659	915	1943	1970
16	0.312	B	35000	DC-ERW	YS&T	1943		products	cold weld		R	HT	1085	0.795	915	1943	1970
16	0.312	B	35000	DC-ERW	YS&T	1943		products	cold weld		R	HT	1280	0.938	1085	1970	1970
16	0.312	B	35000	DC-ERW	YS&T	1943		products	cold weld		R	HT	1265	0.927	1280	1970	1970
16	0.312	B	35000	DC-ERW	YS&T	1943		products	cold weld		R	HT	1367	1.001	1280	1970	1970
16	0.312	B	35000	DC-ERW	YS&T	1943		products	cold weld		R	HT	1105	0.810	915	1943	1970
16	0.312	B	35000	DC-ERW	YS&T	1943		products	cold weld		R	HT	1275	0.934	1105	1970	1970
16	0.312	B	35000	DC-ERW	YS&T	1943		products	cold weld		R	HT	1315	0.963	1275	1970	1970
16	0.312	B	35000	DC-ERW	YS&T	1943		products	hook origin		R	HT	1365	1.000	1315	1970	1970
16	0.312	B	35000	DC-ERW	YS&T	1943		products	hook origin		R	HT	1365	1.000	1365	1970	1970
16	0.312	B	35000	DC-ERW	YS&T	1943		products	cold weld		R	HT	1345	0.985	915	1943	1970
16	0.312	B	35000	DC-ERW	YS&T	1943		products	cold weld		R	HT	1260	0.923	915	1943	1970
16	0.312	B	35000	DC-ERW	YS&T	1943		products	cold weld		R	HT	1240	0.908	1260	1970	1970
16	0.312	B	35000	DC-ERW	YS&T	1943		products	stitched		R	HT	1280	0.938	1260	1970	1970
16	0.312	B	35000	DC-ERW	YS&T	1943		products	cold weld		R	HT	1364	0.999	1280	1970	1970
16	0.312	B	35000	DC-ERW	YS&T	1943		products	hook origin		R	HT	1367	1.001	1364	1970	1970
16	0.312	B	35000	DC-ERW	YS&T	1943		products	hook origin		R	HT	1205	0.883	915	1943	1970
26	0.250	52	52000	FW	AOSmith	1957		gas	SSC		R	Oprn	703	0.703	702	1970	1972
14	0.375	60	60000	HFERW?		1973		products	hook origi	badly ovalized w tension at seam ori	R	Oprn	700	0.218	2160	1973	1974
34	0.281	52	52000	LFERW	dnPhoeni	1967		liquid	hook origin	with fatigue	R	HT	895	1.041			1991
26	0.281	52	52000	FW	AOSmith	1954	eat image	liquid	hoor origi	LCF inferred	R	Oprn	838	0.746	836	1954	1973
26	0.281	52	52000	FW	AOSmith	1954		liquid	hoor origi	LCF inferred	R	Oprn	852	0.758	836	1954	1973
26	0.281	52	52000	FW	AOSmith	1956		liquid	hook origi	severe misalignment	R	Oprn	734	0.653	1015	1965	1981
20	0.250	B	35000	DC-ERW	YS&T	1943		gas	SSC	MIC inferred as driver	R	HT	680	0.777	900	1943	1990
24	0.250	52	52000	FW	AOSmith	1960s		gas	cold weld	inadequate upset	R	HT	1126	1.039		ns	1994
12.75	0.250	52	52000	ERW		1974	liquid but preserv		hoor origin		R	PSHT	1753	0.860			1974
12.75	0.250	52	52000	ERW		1974	liquid but preserv		hoor origi	ID overscarf	R	HT	1837	0.901			
20	0.250	46	46000	DC-ERW	YS&T			gas	ID seam gi	brittle poor/absent PWHT	R	Oprn	675	0.587	1100	i977	1984
26	0.281	52	52000	FW	AOSmith	1951	800	gas	hoor origin		R	GT	877	0.675	880	66gastest	1966
18	0.250	B	35000	LFERW	YS&T	1941		gas	cold weld	brittle poor/absent PWHT	R	Oprn	330	0.339			1966
16	0.312	B	35000	LFERW		1942		gas	SSC		R	Oprn	125	0.092	300	1963	1969
20	0.250	52	52000	DC-ERW	YS&T	1958		sour gas	SSC in ID	slot & hydrogen stress cracking	R	Oprn	880	0.677			1968
20	0.250	52	52000	DC-ERW	YS&T	1958		sour gas	SSC in ID	slot & hydrogen stress cracking	R	Oprn	880	0.677			1970
20	0.250	52	52000	DC-ERW	YS&T	1958		sour gas	SSC in ID s	brittle no PWHT	R	Oprn	888	0.683			1971
16	0.250	52	52000	LFERW				gas	cold weld	hook cracks also evident	R	HBT	1965	1.209			1973
16	0.250	52	52000	LFERW				gas	stitched	cold weld also evident	R	HBT	1735	1.068			1973
16	0.250	52	52000	LFERW				gas	cold weld		R	HBT	1925	1.185			1973
16	0.250	52	52000	LFERW				gas	stitched		R	HBT	1810	1.114			1973
22	0.312	B	35000	FW	AOSmith	1928		gas	Cold Welc	SSC also evident	L	Oprn	40	0.040	425	ghestservi	1974
22	0.312	B	35000	FW	AOSmith	1928		gas	Cold Welc	SSC also evident	L	Oprn	80	0.081			1975
8.625	0.375	B	35000	LFERW				gas	SSC	extensive corrosion	L	Oprn	800	0.263			1957
8.625	0.250	42	42000	LFERW	J&L	1957		products	SSC		R	HT	1434	0.589			1986
20	0.375	B	35000	DC-ERW	YS&T	1943	945	gas	cold weld		R	HRT	1136	0.866	750	1950	10-12-67
20	0.375	B	35000	DC-ERW	YS&T	1943	945	gas	cold weld		R	HRT	1197	0.912	750	1950	10-16-67
20	0.375	B	35000	DC-ERW	YS&T	1943	945	gas	cold weld		R	HRT	1188	0.905	750	1950	10-5-67
20	0.375	B	35000	DC-ERW	YS&T	1943	945	gas	cold weld		R	HRT	1076	0.820	750	1950	9-27-67
20	0.375	B	35000	DC-ERW	YS&T	1943	945	gas	cold weld		R	HRT	1159	0.883	750	1950	9-30-67
20	0.375	B	35000	DC-ERW	YS&T	1943	945	gas	cold weld		R	HRT	1182	0.901	750	1950	10-2-67
20	0.375	B	35000	DC-ERW	YS&T	1943	945	gas	cold weld		R	HRT	1156	0.881	750	1950	9-13-67
20	0.375	B	35000	DC-ERW	YS&T	1943	945	gas	cold weld		R	HRT	1161	0.885	750	1950	9-18-67
20	0.375	B	35000	DC-ERW	YS&T	1943	945	gas	cold weld		R	HRT	1205	0.918	750	1950	9-21-67
20	0.375	B	35000	DC-ERW	YS&T	1943	945	gas	cold weld		R	HRT	1100	0.838	750	1950	9-12-67
20	0.375	B	35000	DC-ERW	YS&T	1943	945	gas	cold weld		R	HRT	1104	0.841	1105	1967	9-18-67
20	0.375	B	35000	DC-ERW	YS&T	1943	945	gas	cold weld		R	HRT	1094	0.834	750	1950	9-20-67
20	0.375	B	35000	DC-ERW	YS&T	1943	945	gas	cold weld		R	HRT	1158	0.882	750	1950	9-21-67
20	0.375	B	35000	DC-ERW	YS&T	1943	945	gas	cold weld		R	HRT	1147	0.874	1156	1967	9-23-67
20	0.375	B	35000	DC-ERW	YS&T	1943	945	gas	cold weld		R	HRT	1180	0.899	750	1950	9-26-67
20	0.375	B	35000	DC-ERW	YS&T	1943	945	gas	cold weld		R	HRT	1114	0.849	1184	1967	9-27-67
20	0.375	B	35000	DC-ERW	YS&T	1943	945	gas	cold weld		R	HRT	1183	0.901	750	1950	9-30-67
20	0.375	B	35000	DC-ERW	YS&T	1943	945	gas	cold weld		R	HRT	1187	0.904	750	1950	10-2-67
20	0.375	B	35000	DC-ERW	YS&T	1943	945	gas	cold weld		R	HRT	1184	0.902	1198	1967	10-4-67
20	0.375	B	35000	DC-ERW	YS&T	1943	945	gas	cold weld		R	HRT	1186	0.904	750	1950	10-5-67
20	0.375	B	35000	DC-ERW	YS&T	1943	945	gas	cold weld		R	HRT	1185	0.903	750	1950	10-7-67
20	0.375	B	35000	DC-ERW	YS&T	1943	945	gas	cold weld		R	HRT	1189	0.906	750	1950	10-10-67
20	0.375	B	35000	DC-ERW	YS&T	1943	945	gas	cold weld		R	HRT	1184	0.902	1185	1967	10-16-67
20	0.375	B	35000	DC-ERW	YS&T	1943	945	gas	cold weld		R	HRT	1127	0.859	750	1950	9-5-67
20	0.375	B	35000	DC-ERW	YS&T	1943	945	gas	cold weld		R	HRT	1236	0.942	750	1950	9-6-67
20	0.375	B	35000	DC-ERW	YS&T	1943	945	gas	cold weld		R	HRT	1247	0.950	750	1950	9-11-67
20	0.375	B	35000	DC-ERW	YS&T	1943	945	gas	cold weld		R	HRT	1217	0.927	1245	1967	9-12-67
20	0.375	B	35000	DC-ERW	YS&T	1943	945	gas	cold weld		R	HRT	1263	0.962	750	1950	9-14-67
20	0.375	B	35000	DC-ERW	YS&T	1943	945	gas	cold weld		R	HRT	1265	0.964	750	1950	8-18-67
20	0.375	B	35000	DC-ERW	YS&T	1943	945	gas	cold weld		R	HRT	1110	0.846	750	1950	8-29-67
20	0.375	B	35000	DC-ERW	YS&T	1943	945	gas	cold weld		R	HRT	1090	0.830	1136	1967	24717

Line Pipe & Service Related									Failure Related								
OD	WT	Gr	SMYS	Seam	Mfgr	Vintage	MOP or MAOP	Service	Cause		Leak vs Rupture	Test vs Operate	Failure Pressure	Pf/Psmys	Max Prior Pressure	Date	Date Failed
inch	inch		psi						Primary	Other Factors			psig		psig		
20	0.375	B	35000	DC-ERW	YS&T	1943	945	gas	cold weld		R	HRT	1168	0.890	750	1950	9-12-67
20	0.375	B	35000	DC-ERW	YS&T	1943	945	gas	cold weld		R	HRT	1178	0.898	750	1950	9-13-67
20	0.375	B	35000	DC-ERW	YS&T	1943	945	gas	cold weld		R	HRT	1178	0.898	750	1950	9-14-67
20	0.375	B	35000	DC-ERW	YS&T	1943	945	gas	cold weld		R	HRT	1183	0.901	1187	1967	9-18-67
20	0.375	B	35000	DC-ERW	YS&T	1943	945	gas	cold weld		R	HRT	1143	0.871	1200	1967	9-19-67
20	0.375	B	35000	DC-ERW	YS&T	1943	945	gas	cold weld		R	HRT	1206	0.919	750	1950	9-20-67
20	0.375	B	35000	DC-ERW	YS&T	1943	945	gas	cold weld		R	HRT	1186	0.904	750	1950	9-22-67
20	0.375	B	35000	DC-ERW	YS&T	1943	945	gas	cold weld		R	HRT	1124	0.856	1208	1967	9-25-67
20	0.375	B	35000	DC-ERW	YS&T	1943	945	gas	cold weld		R	HRT	1179	0.898	750	1950	9-26-67
20	0.375	B	35000	DC-ERW	YS&T	1943	945	gas	cold weld		R	HRT	1200	0.914	1206	1967	9-28-67
20	0.375	B	35000	DC-ERW	YS&T	1943	945	gas	cold weld		R	HRT	1193	0.909	1201	1967	10-2-67
20	0.375	B	35000	DC-ERW	YS&T	1943	945	gas	cold weld		R	HRT	1189	0.906	1190	1967	10-3--67
20	0.375	B	35000	DC-ERW	YS&T	1943	945	gas	cold weld		R	HRT	1192	0.908	750	1950	10-5-67
20	0.375	B	35000	DC-ERW	YS&T	1943	945	gas	cold weld		R	HRT	1175	0.895	1178	1967	10-6-67
20	0.375	B	35000	DC-ERW	YS&T	1943	945	gas	Cold Weld PenLikely		L	HRT	1210	0.922	750	1950	10-11-67
20	0.375	B	35000	DC-ERW	YS&T	1943	945	gas	Cold Weld PenLikely		L	HRT	1190	0.907	750	1950	10-26-67
20	0.375	B	35000	DC-ERW	YS&T	1943	945	gas	cold weld		R	HRT	1200	0.914	750	1950	8-15-67'
20	0.375	B	35000	DC-ERW	YS&T	1943	945	gas	cold weld		R	HRT	1180	0.899	750	1950	8-22-67
20	0.375	B	35000	DC-ERW	YS&T	1943	945	gas	cold weld		R	HRT	1140	0.869	1141	1967	8-24-61
20	0.375	B	35000	DC-ERW	YS&T	1943	945	gas	cold weld		R	HRT	1168	0.890	750	1950	8-28-67
20	0.375	B	35000	DC-ERW	YS&T	1943	945	gas	cold weld		R	HRT	1178	0.898	750	1950	8-30-67
20	0.375	B	35000	DC-ERW	YS&T	1943	945	gas	cold weld		R	HRT	1171	0.892	750	1950	8-31-67
20	0.375	B	35000	DC-ERW	YS&T	1943	945	gas	cold weld		R	HRT	1174	0.894	1198	1967	9-2-67
20	0.375	B	35000	DC-ERW	YS&T	1943	945	gas	cold weld		R	HRT	1126	0.858	1144	1967	9-6-67
20	0.375	B	35000	DC-ERW	YS&T	1943	945	gas	cold weld		R	HRT	1104	0.841	1144	1967	9-7-67
20	0.375	B	35000	DC-ERW	YS&T	1943	945	gas	cold weld		R	HRT	1117	0.851	1177	1967	9-11-67
20	0.375	B	35000	DC-ERW	YS&T	1943	945	gas	cold weld		R	HRT	1169	0.891	750	1950	9-12-67
20	0.375	B	35000	DC-ERW	YS&T	1943	945	gas	cold weld		R	HRT	1139	0.868	1218	1967	9-13-67
20	0.375	B	35000	DC-ERW	YS&T	1943	945	gas	cold weld		R	HRT	1124	0.856	1193	1967	9-14-67
20	0.375	B	35000	DC-ERW	YS&T	1943	945	gas	cold weld		R	HRT	1167	0.889	1212	1967	9-18-67
20	0.375	B	35000	DC-ERW	YS&T	1943	945	gas	cold weld		R	HRT	1228	0.936	750	1950	9-19-67
20	0.375	B	35000	DC-ERW	YS&T	1943	945	gas	cold weld		R	HRT	1228	0.936	1232	1967	9-21-67
20	0.375	B	35000	DC-ERW	YS&T	1943	945	gas	cold weld		R	HRT	1225	0.933	1228	1967	9-22-67
20	0.375	B	35000	DC-ERW	YS&T	1943	945	gas	cold weld		R	HRT	1197	0.912	1199	1967	9-25-67
20	0.375	B	35000	DC-ERW	YS&T	1943	945	gas	cold weld		R	HRT	1199	0.914	750	1950	9-26-67
20	0.375	B	35000	DC-ERW	YS&T	1943	945	gas	cold weld		R	HRT	1165	0.888	1199	1967	9-28-67
20	0.375	B	35000	DC-ERW	YS&T	1943	945	gas	cold weld		R	HRT	1173	0.894	1199	1967	9-30-67
20	0.375	B	35000	DC-ERW	YS&T	1943	945	gas	cold weld		R	HRT	1163	0.886	1187	1967	10-3-67
20	0.375	B	35000	DC-ERW	YS&T	1943	945	gas	cold weld		R	HRT	1214	0.925	1220	1967	10-4-67
20	0.375	B	35000	DC-ERW	YS&T	1943	945	gas	cold weld		R	HRT	1233	0.939	750	1950	10-5-67
20	0.375	B	35000	DC-ERW	YS&T	1943	945	gas	cold weld		R	HRT	1187	0.904	1199	1967	10-6-67
20	0.375	B	35000	DC-ERW	YS&T	1943	945	gas	cold weld		R	HRT	1200	0.914	1201	1967	10-9-61
20	0.375	B	35000	DC-ERW	YS&T	1943	945	gas	cold weld		R	HRT	1212	0.923	1219	1967	10-11-67
20	0.375	B	35000	DC-ERW	YS&T	1943	945	gas	cold weld		R	HRT	1202	0.916	1218	1967	10-14-67
20	0.375	B	35000	DC-ERW	YS&T	1943	945	gas	cold weld		R	HRT	1200	0.914	750	1950	9-19-67
20	0.375	B	35000	DC-ERW	YS&T	1943	945	gas	Cold Weld PenLikely		L	HRT	1203	0.917	750	1950	9-21-67
20	0.375	B	35000	DC-ERW	YS&T	1943	945	gas	cold weld		R	HRT	1205	0.918	1210	1967	9-23-67
20	0.375	B	35000	DC-ERW	YS&T	1943	945	gas	Cold Weld PenLikely		R	HRT	1122	0.855	1123	1967	9-26-67
20	0.375	B	35000	DC-ERW	YS&T	1943	945	gas	cold weld		L	HRT	1188	0.905	750	1950	10-26-67
20	0.375	B	35000	DC-ERW	YS&T	1943	945	gas	cold weld		R	HRT	1227	0.935	750	1950	8-22-67
20	0.375	B	35000	DC-ERW	YS&T	1943	945	gas	cold weld		R	HRT	1240	0.945	1245	1967	8-25-67
20	0.375	B	35000	DC-ERW	YS&T	1943	945	gas	cold weld		R	HRT	1186	0.904	1242	1967	8-28-67
20	0.375	B	35000	DC-ERW	YS&T	1943	945	gas	cold weld		R	HRT	1225	0.933	1231	1967	8-29-67
20	0.375	B	35000	DC-ERW	YS&T	1943	945	gas	cold weld		R	HRT	1145	0.872	750	1950	8-18-67
20	0.375	B	35000	DC-ERW	YS&T	1943	945	gas	cold weld		R	HRT	1122	0.855	750	1950	8-29-67
20	0.375	B	35000	DC-ERW	YS&T	1943	945	gas	cold weld		R	HRT	1220	0.930	750	1950	8-31-67
20	0.375	B	35000	DC-ERW	YS&T	1943	945	gas	cold weld		R	HRT	1243	0.947	750	1950	9-2-67
20	0.375	B	35000	DC-ERW	YS&T	1943	945	gas	cold weld		R	HRT	1255	0.956	1263	1967	9-11-67
20	0.375	B	35000	DC-ERW	YS&T	1943	945	gas	cold weld		R	HRT	1235	0.941	750	1950	8-23-67
20	0.375	B	35000	DC-ERW	YS&T	1943	945	gas	cold weld		R	HRT	1113	0.848	1172	1967	8-28-67
20	0.375	B	35000	DC-ERW	YS&T	1943	945	gas	cold weld		R	HRT	1183	0.901	1222	1967	8-30-67
20	0.375	B	35000	DC-ERW	YS&T	1943	945	gas	cold weld		R	HRT	1207	0.920	1224	1967	9-1-67
6.625	0.188	B	35000	ERW		1969	1410	products	cold weld		L	HRT	1700	0.856	1985	1969	1970
6.625	0.188	B	35000	ERW		1969	1410	products	cold weld		L	HRT	1767	0.890	1985	1969	1970
6.625	0.188	B	35000	ERW		1969	1410	products	cold weld		R	HRT	885	0.446	1985	1969	1970
6.625	0.188	B	35000	ERW		1969	1410	products	cold weld		R	HRT	1996	1.005	1985	1969	1970
6.625	0.188	B	35000	ERW		1969	1410	products	cold weld		R	HRT	1960	0.987	1985	1969	1970
6.625	0.188	B	35000	ERW		1969	1410	products	cold weld		R	HRT	1996	1.005	1985	1969	1970
6.625	0.188	B	35000	ERW		1969	1410	products	cold weld		L	HRT	1782	0.897	1985	1969	1970
6.625	0.188	B	35000	ERW		1969	1410	products	cold weld		R	HRT	1840	0.926	1985	1969	1970
6.625	0.188	B	35000	ERW		1969	1410	products	cold weld		R	HRT	1769	0.891	1985	1969	1970
8.625	0.203	42	42000	ERW		1969	1425	products	cold weld		R	HRT	922	0.466	1975	1969	1970
8.625	0.203	42	42000	ERW		1969	1425	products	cold weld		R	HRT	1990	1.007	1975	1969	1970
8.625	0.203	42	42000	ERW		1969	1425	products	cold weld		R	HRT	770	0.389	1975	1969	1970
8.625	0.203	42	42000	ERW		1969	1425	products	cold weld		R	HRT	1810	0.916	1975	1969	1970
8.625	0.203	42	42000	ERW		1969	1425	products	cold weld		R	HRT	1975	0.999	1975	1969	1970
8.625	0.203	42	42000	ERW		1969	1425	products	cold weld		R	HRT	1730	0.875	1975	1969	1970
8.625	0.203	42	42000	ERW		1969	1425	products	cold weld		R	HRT	1915	0.969	1975	1969	1970
8.625	0.203	42	42000	ERW		1969	1425	products	cold weld		R	HRT	1650	0.835	1975	1969	1970
8.625	0.203	42	42000	ERW		1969	1425	products	cold weld		R	HRT	1009	0.510	1975	1969	1970
8.625	0.203	42	42000	ERW		1969	1425	products	cold weld		R	HRT	1968	0.995	1975	1969	1970
8.625	0.203	42	42000	ERW		1969	1425	products	cold weld		R	HRT	1500	0.759	1975	1969	1970
10.75	0.250	42	42000	ERW		1969	1430	products	cold weld		R	HRT	1620	0.829	1985	1969	1970
10.75	0.250	42	42000	ERW		1969	1430	products	cold weld		R	HRT	1740	0.891	1985	1969	1970

Line Pipe & Service Related									Failure Related								
OD	WT	Gr	SMYS	Seam	Mfgr	Vintage	MOP or MAOP	Service	Cause		Leak vs Rupture	Test vs Operate	Failure Pressure	Pf/Psmys	Max Prior Pressure	Date	Date Failed
inch	inch		psi						Primary	Other Factors			psig		psig		
8.625	0.277	B	35000	LFERW		1940s	1124	gas	hook origi	brittle inadequate PWHT	R	Oprn	960	0.427			early 60s
26	0.406	52	52000	FW	AOSmith	late 1940s	1169	gas	cold		L	HT	1515	0.933	1140	early60s	7 yr post cons
16	0.250	42	42000	LFERW		late 1940s	945	gas	hook origin		R	HT	1290	0.983		late60s	requal mid70s
16	0.250	42	42000	LFERW		late 1940s	945	gas	cold weld		R	HT	1312	1.000		late60s	requal mid70s
16	0.250	42	42000	LFERW		late 1940s	945	gas	hook origin		R	HT	1309	0.997		late60s	requal mid70s
16	0.250	42	42000	LFERW		late 1940s	945	gas	mill-seam repair		R	HT	1312	1.000		late60s	requal mid70s
16	0.250	42	42000	LFERW		late 1940s	945	gas	cold weld		R	HT	500	0.381		late60s	requal mid70s
16	0.250	42	42000	LFERW		late 1940s	945	gas	hook origin		R	HT	1135	0.865		late60s	requal mid70s
20	0.250	46	46000	DC-ERW	YS&T	1950s	828	gas	cold weld	(underupset) w ID notch(unscaf/mis	R	Oprn	675	0.587	1100	1977	1984
20	0.312	B	35000	LFERW		late 1940s	786	gas	SSC	corrosion	R	Oprn	650	0.595	1095	1957	1969
8.625	0.219	42	42000	LFERW		1963	1536	products	cold weld		R	Oprn	1030	0.483	1690	1963	1968
16	0.250	60	60000	LooksFW	LooksAOS	1967	1350	sour gas	Hook - small	defect + hard + sour + inadeq PWH	L	Oprn	1000	0.533	1969	1967	1968
24	0.312	60	60000	HFERW	Stelco	1967	1123	sour gas	cold weld	misaligned	R	PSGT	1000	0.641		1967	1967
24	0.312	60	60000	HFERW	Stelco	1967	1123	sour gas	cold weld	misaligned	R	PSGT	925	0.593		1967	1967
34	0.281	52	52000	FW	AOSmith	1967	619	liquid	hoor origi	fatigue	L	Oprn	596	0.693	741	1975	1984
16	0.250	42	42000	LFERW				gas	hook origin								1996
34	0.281	52	52000	FW	AOSmith	1963	640	liquid	hook origin		R	Oprn	600	0.698	744	1975	1980
34	0.281	52	52000	FW	AOSmith	1963	630	liquid	hook origin		R	Oprn	598	0.696	744	1975	1979
20	0.250	46	46000	DC-ERW	YS&T	1950	828	gas	hook origin		R	Oprn	700	0.609			1977
20	0.250	46	46000	DC-ERW	YS&T	1950	828	gas	cold weld		R	Oprn	590	0.513			1977
20	0.250	46	46000	DC-ERW	YS&T	1950	828	gas	hook origin		R	Oprn	755	0.657			1977
20	0.250	46	46000	DC-ERW	YS&T	1950	828	gas	cold weld		R	Oprn	650	0.565			1977
20	0.250	46	46000	DC-ERW	YS&T	1950	828	gas	hook origin		R	Oprn	690	0.600			1977
20	0.250	46	46000	DC-ERW	YS&T	1950	828	gas	cold		L	Oprn	660	0.574			1977
20	0.250	46	46000	DC-ERW	YS&T	1950	828	gas	cold		L	Oprn	580	0.504			1977
20	0.250	46	46000	DC-ERW	YS&T	1950	828	gas	cold weld		R	Oprn	650	0.565			1977
20	0.250	46	46000	DC-ERW	YS&T	1950	828	gas	cold weld		R	Oprn	675	0.587			1977
20	0.250	46	46000	DC-ERW	YS&T	1950	828	gas	hook origin		R	Oprn	680	0.591			1977
20	0.250	46	46000	DC-ERW	YS&T	1950	828	gas	cold weld		R	Oprn	750	0.652			1977
20	0.250	46	46000	DC-ERW	YS&T	1950	828	gas	hook origin		R	HT	1042	0.906			1977
20	0.250	46	46000	DC-ERW	YS&T	1950	828	gas	hook origin		R	HT	1022	0.889			1977
20	0.250	46	46000	DC-ERW	YS&T	1950	828	gas	hook origin		R	HT	1048	0.911			1977
20	0.250	46	46000	DC-ERW	YS&T	1950	828	gas	cold weld		R	HT	1070	0.930			1977
20	0.250	46	46000	DC-ERW	YS&T	1950	828	gas	cold weld		R	HT	1085	0.943			1977
20	0.250	46	46000	DC-ERW	YS&T	1950	828	gas	cold weld		R	HT	1065	0.926			1977
20	0.250	46	46000	DC-ERW	YS&T	1950	828	gas	cold weld		R	HT	1060	0.922			1977
20	0.250	46	46000	DC-ERW	YS&T	1950	828	gas	cold weld		R	HT	1100	0.957			1977
20	0.250	46	46000	DC-ERW	YS&T	1950	828	gas	cold weld		R	HT	1052	0.915			1977
20	0.250	46	46000	DC-ERW	YS&T	1950	828	gas	cold weld		R	HT	1121	0.975		1977	1986
20	0.250	46	46000	DC-ERW	YS&T	1950	828	gas	hook origin		R	HT	1114	0.969		1977	1986
20	0.250	46	46000	DC-ERW	YS&T	1950	828	gas	cold weld		R	HT	1084	0.943		1977	1986
20	0.250	46	46000	DC-ERW	YS&T	1950	828	gas	cold weld		R	HT	1090	0.948		1977	1986
20	0.250	46	46000	DC-ERW	YS&T	1950	828	gas	hook origin		R	HT	1146	0.997		1986	1991
20	0.250	46	46000	DC-ERW	YS&T	1950	828	gas	hook origin		R	HT	1208	1.050		1986	1991
20	0.250	46	46000	DC-ERW	YS&T	1950	828	gas	hook origin		R	HT	1110	0.965		1986	1991
20	0.250	46	46000	DC-ERW	YS&T	1950	828	gas	hook origin		R	HT	1148	0.998		1986	1991
20	0.250	46	46000	DC-ERW	YS&T	1950	828	gas	hook origin		R	HT	1134	0.986		1986	1991
20	0.250	46	46000	DC-ERW	YS&T	1950	828	gas	hook origin		R	HT	1194	1.038		1986	1991
20	0.250	46	46000	DC-ERW	YS&T	1950	828	gas	hook origin		R	HT	1167	1.015		1986	1991
20	0.250	46	46000	DC-ERW	YS&T	1950	828	gas	hook origin		R	HT	1142	0.993		1986	1991
20	0.312	B	35000	DC-ERW	YS&T	1942	786	gas	SSC	misalignment	R	Oprn	668	0.612			1976
20	0.312	B	35000	DC-ERW	YS&T	1942	786	gas	SSC	corrosion thinned	R	HT	743	0.680			1980
20	0.312	B	35000	DC-ERW	YS&T	1942	786	gas	SSC	corrosion thinned	R	HT	1057	0.968			1980
8.625	0.203	42	42000	LFERW	Bethlehem	1963	1423	products	SSC	pluscorrosion	R	Oprn	1044	0.528	1726	1964	1980
6.625	0.188	52	52000	LFERW?	Stupp	1962	2125	preservice	hook origin	+ inclusion stringers	R	PSHT	2150	0.729			1962
6.625	0.188	52	52000	LFERW?	Stupp	1962	2125	preservice	hook origin	+ inclusion stringers	R	PSHT	2200	0.745			1962
6.625	0.188	52	52000	LFERW?	Stupp	1962	2125	preservice	hook origin	+ misaligned +inclusion stringers	R	PSHT	2175	0.737			1962
6.625	0.188	52	52000	LFERW?	Stupp	1962	2125	preservice	hook origin	+ misaligned +inclusion stringers	R	PSHT	2350	0.796			1962
20	0.250	46	46000	LFERW	YS&T	1949	828	gas	cold weld		R	Oprn	785	0.683		none	1977
12.75	0.250	46	46000	LFERW	Republic	1958	1300	liquid	hook origin	+ fatigue	R	Oprn	1210	0.671	1660	1987	1993
22	0.344	46	46000	LFERW		1948		liquid	hook origin		R	Oprn	1000	0.695			1988
16	0.250	52	52000	LFERW	Kaiser	1955	1170	liquid	Cold / Lack (	stitched adjacent weld	R	Oprn	1160	0.714	1308	1955	1991
16	0.375	B	35000	LFERW		1959	1181	gas	SSC	corrosion	R	Oprn	190	0.116			1990
16	0.281	60	60000	HFERW		1976	1517	liquid	skelp defects	near & remote to seam	R	HBT ILI/R	3212	1.524	1897	1976	1987
10.75	0.344	42	42000	LFERW		1953	1935	gas	SSC	corrosion thinned	R	Oprn	1730	0.644		1976	1976
22	0.344	46	46000	LFERW		1949	1036	liquid	hook origin	fatigue cited	R	HT	1128	0.784			1989
22	0.344	46	46000	LFERW		1949	1036	liquid	hook origin	misaligned	R	HT	1065	0.740			1989
22	0.344	46	46000	LFERW		1949	1036	liquid	hook origin		R	HT	1105	0.768	1135	1989	1989
22	0.344	46	46000	LFERW		1949	1036	liquid	hook origin	+ brittle haz	R	HT	1001	0.696	1095	1989	1989
22	0.344	46	46000	LFERW		1949	1036	liquid	SSC	corrosion	R	HT	860	0.598		1989	1989
22	0.344	46	46000	LFERW		1949	1036	liquid	hook origin	+ brittle haz	R	HT	984	0.684		1989	1989
22	0.344	46	46000	LFERW		1949	1036	liquid	hook origin	brittle haz	R	HT	1022	0.710	975	1989	1989
22	0.344	46	46000	LFERW		1949	1036	liquid	stitched in draft - lack of bond in final (looks stitc		R	HT	1024	0.712	975	1989	1989
22	0.344	46	46000	LFERW		1949	1036	liquid	stitched in draft - cold in final (looks stitched)		L	HT	995	0.692	975	1989	1989
6.625	0.125	42	42000	LFERW			1141	gas	cold weld -	dent noted w fatigue inferred	R	Oprn	1130	0.713	1268	1966	1986
18	0.250	42	42000	DC-ERW	YS&T	1940s	840	gas	cold - poor bond	- shows hints of stitching	R	Oprn	416	0.357			1986
20	0.250	46	46000	DC-ERW	YS&T	1949	828	gas	hook gives sm	notch + locally hard + HSC env	R	Oprn	750	0.652	960	1977	1986
8.625	0.322	46	46000	LFERW		1956	840	gas	SSC		R	HBT	2643	0.770			2012
8.625	0.322	46	46000	LFERW		1956	840	gas	SSC		R	HBT	4069	1.185			2012
24	0.281	52	52000	LFERW	Tubacero	1976	877	liquid	cold weld	PTW + fatigue	R	Oprn	669	0.549	1096	1976	2006
20	0.250	52	52000	ERW-DC	YS&T	1961		gas	hook origin	brittle haz	R	Oprn	540	0.415	600	1962	1981
8.625	0.250	A	30000	LFERW		1929		gas	SSC		R	Oprn	200	0.115	ns		1984
16	0.203	60	60000	DC-ERW	YS&T	1965		gas	mech dama	MD-Const	R	Oprn	826	0.543	1275	1965	1981
24	0.250	52	52000	FW	AOSmith	1960s		gas	cold weld		R	HT	1128	1.041			1994
12.75	0.188	52	52000	DC-ERW	YS&T	1963	800	gas	SSC	flank corrosion too	R	Oprn	725	0.473	1200	1963	2003
8.625	0.188	A	30000	LFERW		1959	500	liquid	ILI located	steel-related seam defects: DNF@1.6	R	HBT	2100	>1.605			2007

Line Pipe & Service Related									Failure Related								
OD	WT	Gr	SMYS	Seam	Mfgr	Vintage	MOP or MAOP	Service	Cause		Leak vs Rupture	Test vs Operate	Failure Pressure	Pf/Psmys	Max Prior Pressure	Date	Date Failed
inch	inch		psi						Primary	Other Factors			psig		psig		
10.75	0.250	42	42000	ERW		1969	1430	products	cold weld		R	HRT	1910	0.978	1985	1969	1970
10.75	0.250	42	42000	ERW		1969	1430	products	cold weld		R	HRT	350	0.179	1985	1969	1970
10.75	0.250	42	42000	ERW		1969	1430	products	cold weld		R	HRT	1810	0.927	1985	1969	1970
10.75	0.250	42	42000	ERW		1969	1430	products	cold weld		R	HRT	1660	0.850	1985	1969	1970
10.75	0.250	42	42000	ERW		1969	1430	products	cold weld		R	HRT	1750	0.896	1985	1969	1970
10.75	0.250	42	42000	ERW		1969	1430	products	cold weld		R	HRT	1684	0.862	1985	1969	1970
30	0.323	65	65000	FW	AOSmith	1965	1008	gas	hoor origin		R	PSHT	1397	0.998	1260	1965	1965
30	0.323	65	65000	FW	AOSmith	1965	1008	gas	hoor origin		R	PSHT	1474	1.053	1260	1965	1965
30	0.323	65	65000	FW	AOSmith	1965	1008	gas	hoor origin		R	PSHT	1529	1.092	1260	1965	1965
30	0.323	65	65000	FW	AOSmith	1965	1008	gas	hoor origin		R	PSHT	1539	1.100	1260	1965	1965
30	0.323	65	65000	FW	AOSmith	1965	1008	gas	hoor origin		R	PSHT	1540	1.100	1260	1965	1965
30	0.323	65	65000	FW	AOSmith	1965	1008	gas	hoor origin		R	PSHT	1513	1.081	1260	1965	1965
30	0.323	65	65000	FW	AOSmith	1965	1008	gas	hoor origin		R	PSHT	1499	1.071	1260	1965	1965
30	0.323	65	65000	FW	AOSmith	1965	1008	gas	hoor origin		R	PSHT	1540	1.100	1260	1965	1965
30	0.323	65	65000	FW	AOSmith	1965	1008	gas	hoor origin		R	PSHT	1540	1.100	1260	1965	1965
30	0.323	65	65000	FW	AOSmith	1965	1008	gas	hoor origin		R	PSHT	1539	1.100	1260	1965	1965
30	0.323	65	65000	FW	AOSmith	1965	1008	gas	hoor origin		R	PSHT	1509	1.078	1260	1965	1965
30	0.323	65	65000	FW	AOSmith	1965	1008	gas	hoor origin		R	PSHT	1537	1.098	1260	1965	1965
30	0.323	65	65000	FW	AOSmith	1965	1008	gas	hoor origin		R	PSHT	1534	1.096	1260	1965	1965
30	0.323	65	65000	FW	AOSmith	1965	1008	gas	hoor origin		R	PSHT	1540	1.100	1260	1965	1965
30	0.323	65	65000	FW	AOSmith	1965	1008	gas	hoor origin		R	PSHT	1540	1.100	1260	1965	1965
30	0.323	65	65000	FW	AOSmith	1965	1008	gas	hoor origin		R	PSHT	1540	1.100	1260	1965	1965
24	0.312	52	52000	FW	AOSmith	1952	973	gas conv fr	cold weld		R	HRT	1032	0.943	930	??	2004
20	0.250	52	52000	DC-ERW	YS&T	1957	936	gas	cold weld		R	HRT	1425	1.096	1364	1988	1993
20	0.250	52	52000	DC-ERW	YS&T	1957	936	gas	cold weld		R	HRT	1425	1.096	1364	1988	1993
20	0.250	52	52000	DC-ERW	YS&T	1957	936	gas	hook - SCC driven		R	HRT	1425	1.096	1364	1988	2003
20	0.250	52	52000	DC-ERW	YS&T	1957	936	gas	hook - SCC driven		R	HRT	806	0.620			1973
20	0.375	B	35000	DC-ERW	YS&T	1943	945	gas	cold weld		R	HRT	1116	0.850	1118	1967	9-6-67
20	0.375	B	35000	DC-ERW	YS&T	1943	945	gas	cold weld		R	HRT	1110	0.846	1136	1967	9-6-67
20	0.375	B	35000	DC-ERW	YS&T	1943	945	gas	cold weld		R	HRT	1117	0.851	750	1950	9-11-67